NUREG/CR–4563
SAND86–0576
RG
Printed September 1986

Analysis of Station Blackout Accidents for the Bellefonte Pressurized Water Reactor

R. D. Gasser, P. P. Bieniarz, J. L. Tills

Prepared by
Sandia National Laboratories
Albuquerque, New Mexico 87185 and Livermore, California 94550
for the United States Department of Energy
under Contract DE-AC04-76DP00789

Prepared for
U. S. NUCLEAR REGULATORY COMMISSION

SF2900Q(8-81)

Available from

Superintendent of Documents
U.S. Government Printing Office
Post Office Box 37082
Washington, D.C. 20013-7982

and

National Technical Information Service
Springfield, VA 22161

NUREG/CR-4563
SAND86-0576
RG

ANALYSIS OF STATION BLACKOUT ACCIDENTS FOR THE BELLEFONTE PRESSURIZED WATER REACTOR

R. D. Gasser
P. P. Bieniarz*
J. L. Tills**

Printed: September 1986

Sandia National Laboratories
Albuquerque, New Mexico 87185
Operated by
Sandia Corporation
for the
U. S. Department of Energy

Prepared for
Division of Accident Evaluation
Office of Nuclear Regulatory Research
U. S. Nuclear Regulatory Commission
Washington, DC 20555
Under Memorandum of Understanding DOE 40-550-75
NRC FIN No. A-1258

* Risk Management Associates, Albuquerque, NM
** Tills and Associates, Albuquerque, NM

ABSTRACT

An analysis has been performed for the Bellefonte PWR Unit 1 to determine the containment loading and the radiological releases into the environment from a station blackout accident. A number of issues have been addressed in this analysis which include the effects of direct heating on containment loading, and the effects of fission product heating and natural convection on releases from the primary system. The results indicate that direct heating which involves more than about 50% of the core can fail the Bellefonte containment, but natural convection in the RCS may lead to overheating and failure of the primary system piping before core slump, thus, eliminating or mitigating direct heating. Releases from the primary system are significantly increased before vessel breach due to natural circulation and after vessel breach due to reevolution of retained fission products by fission product heating of RCS structures.

CONTENTS

TABLES

FIGURES

Page

Figures (Cont.)

ACKNOWLEDGEMENTS

Special thanks must go to Dave Williams who offered much useful advice regarding the presentation of the analytical results and who also performed some of the direct containment heating calculations using the DHEAT Code. We would also like to express our gratitude to Thomas Walker of the NRC Containment Systems Research Branch for his careful editing of this document and his cogent editorial comments.

1.0 EXECUTIVE SUMMARY

An early attempt at an integrated "best estimate" of containment loading and radiological releases for specific accident sequences was carried out at Battelle Columbus Laboratories and disseminated in the BMI-2104 report. In that study five reactors were selected in order to characterize different major reactor types, and analyses were performed for a few of the accident sequences that were thought to dominate the risk or present unique challenges to the containment. The BMI-2104 analysis employed computer codes that were run independently and in large part were in an early stage of development. A number of issues have been raised in the interim, some of which are related to phenomenology not modeled in the BMI-2104 suite of codes. It is the objective of this study to address some of these issues with a view to improving the calculated estimate of containment loading and fission product releases to the environment. The present study has been limited to large, dry containments in general and to the TVA Bellefonte Unit 1 Pressurized Water Reactor (PWR) in particular.

Since it is currently thought that transient accident sequences tend to dominate the risk for large, dry PWRs in general, this analysis has been concentrated on two variations of the TMLB' accident sequences. The TMLB' sequence consists of the situation in which there has been a complete loss of offsite and onsite AC power together with a loss of auxiliary feedwater and a failure to recover power before a core-damaged state has evolved. The two variations involve, in one case, an intact primary system boundary until the core slumps and melts through the lower vessel head, and in the other case, an induced LOCA due to the failure of primary coolant pump seals.

It is the specific purpose of this analysis to estimate the primary system fission product transport and releases into containment, the containment pressure/temperature response, and the transport of fission products through the containment and ultimate radiological releases to the environment. The calculations have been performed for a number of cases and configurations in which several important issues have been specifically addressed. These issues are discussed below.

1.1 CURRENT ISSUES

An issue of considerable importance for PWRs, since it supplies a mechanism for early containment failure, is that of direct containment heating due to the high pressure ejection of molten core debris into the upper containment atmosphere. The ejected core debris, consisting of molten fuel, cladding, and structural materials, can form a dispersed aerosol capable of rapidly transferring its heat to the containment atmosphere. Because the calculated loads on the containment structure due to direct heating may challenge its integrity simultaneously with near maximum concentrations of radiological sources in the containment atmosphere, this scenario has the potential for large releases and severe effects on public health.

There are, however, a number of uncertainties attached to the direct heating question which range from the magnitude of its effect to whether it will, in fact, occur. Large uncertainties in the core meltdown phase of the accident, for example, yield a wide range of possible initial conditions for core debris at the time of vessel breach. Much of this uncertainty may be removed when the more advanced melt-progression codes such as MELPROG become available. In view of the current lack of knowledge regarding direct heating phenomenology, the present study has taken a parametric approach to direct heating.

The BMI-2104 calculations for primary system fission product transport employed a set of codes (MARCH, CORSOR, MERGE, and TRAP/MELT) which were run successively (without feedback) and which did not contain models for fission product heatup of the primary system, nor did they contain models for treatment of natural convective processes. Transport of volatile fission products through the primary system and releases of these materials into the containment are extremely sensitive to the temperature history of the primary system, so that these two processes should not be neglected. As a consequence of the absence of models for the aforementioned processes, the BMI-2104 calculations for the TMLB' sequence may underestimate primary system releases during the meltdown phase of the accident. Further, in that study it was not possible to calculate long term reevolution (revaporization) subsequent to vessel failure of those volatile fission products that had been retained on primary system surfaces during the meltdown phase. Certain containment conditions, such as a gradual depressurization due to leakage over the time period in which the volatiles are being reevolved, can supply a mechanism for moving these sources out of the primary system and ultimately into the environment.

In the present study an attempt has been made to treat fission product heating and natural convection in the primary system heat and mass transport calculations. An additional benefit of this modeling capability has been a somewhat improved characterization of the primary system temperature history, and as a result, the ability to gain some insight into another important issue: that of potential temperature induced failure of the hot-leg piping. Enhanced heat transfer due to natural circulation processes could generate high enough temperatures at the hot-leg nozzles or in downstream piping to weaken the structure and cause a breach. This may be particularly likely for the TMLB' station blackout sequence due to the high system pressure (2000-2400 psia). If primary system failure in the hot-leg occurred before core slump, direct heating might be effectively precluded. The magnitude and characteristics of the countercurrent flow regime in the pipes leading from the vessel to the pressurizer and steam generators have not been established, and the present analysis probably yields heat transfer rates that are somewhat high. Multidimensional codes may be required to achieve a definitive answer regarding natural convection in the complicated geometry of the primary system.

1.2 CODES AND METHODOLOGY

The primary strategy in this analysis was to use the best calculational tools available to treat each phase of the accident. The RELAP5 code was used to calculate the thermohydraulic sources during the pre-core-damage phase, and the MARCON code was employed during the period from incipient core meltdown out to and including the core/concrete interaction phase (the CORCON code which treats the core/concrete interaction has been combined with the MARCH code in the MARCON code). A interactive version of the CORSOR, MERGE, and TRAP/MELT code package was utilized to calculate primary system fission product releases. This code, called the MCT code, contains new models for fission product heating and natural circulation. It must be noted that these models were developed by P. P. Bieniarz and have not been extensively evaluated. The natural circulation flows are one-dimensional and driven by temperature differences between connecting volumes. Radiological releases from core/concrete interactions were calculated using the VANESA code. The thermohydraulic sources due to direct heating were calculated using a small stand-alone code backed up by hand calculations. Both the code and the hand calculations used an adiabatic model in which the core debris was brought into thermal equilibrium with the atmosphere. The aerosol sources for direct heating were obtained from results of the SPITS experiments conducted at Sandia National Laboratories. Heatup and degassing of the concrete floors in the containment after deposition of the debris from direct heating were also calculated using a stand-alone code. The various sources, both thermohydraulic and radiological, were supplied to the CONTAIN code which calculated the containment loading, the transport and deposition of fission products in containment, and the release of radiological sources to the environment.

1.3 ACCIDENT SEQUENCES

Two basic scenarios were examined in the study. The first scenario consisted of a TMLB' sequence in which temperature induced failure of the primary system did not occur prior to core slump. The primary system eventually failed at instrumentation penetrations in the lower vessel head due to the thermal attack of molten core debris. Since a previous breach in the primary system boundary did not occur (except for normal operation of the pressure operated relief valves, PORVs), the system was at high pressure (PORV set point, about 2400 psia) and the potential existed for direct heating. For this scenario a matrix of cases was analyzed in which selected direct heating parameters were varied. The primary system radiological releases were also varied by using MCT code predicted releases and selected combinations of the models in that code (i.e. fission product heating, natural circulation, reevolution of volatiles). Some cases were also analyzed using the RCS releases calculated in the BMI-2104 study of the Zion plant. The Zion releases were adjusted for differences in core power between the Zion and Bellefonte plants.

The second scenario assumed a TMLB' with failure of the seals in the primary system coolant pumps (pump seal loss of coolant accident, LOCA). In this scenario all four pump seals were assumed to fail at the outset of the accident, so that the system was at a somewhat lower pressure at the time of vessel breach. Thus, the direct heating scenario, if it occurred, would be of a smaller magnitude. For this analysis it was assumed that direct heating did not occur in the pump seal LOCA scenario.

1.4 RESULTS AND CONCLUSIONS

1.4.1 DIRECT HEATING

For the direct heating calculations a number of parameters were varied including the fraction of core injected into the containment, the quantities of hydrogen and molten steel burned during the event (all the injected zirconium was assumed to be oxidized), and the amount of reactor cavity water involved in the process.

For the case in which 90% of the core debris was involved, the peak containment pressures were in excess of the estimated failure pressure range for the Bellefonte containment (144.7 to 153.7 psia). With 50% core debris involvement the peak pressures were marginally close to the estimated containment failure criterion. Without the involvement of hydrogen and steel oxidation, pressures were somewhat below the failure criterion while inclusion of hydrogen and steel oxidation resulted in pressures at or slightly above the failure criterion. However, for the more probable scenarios in which cavity water was involved (primarily additional effective heat capacity), complete oxidation of the steel and the hydrogen (from the in-vessel oxidation of the cladding) was required to yield a peak pressure high enough to challenge the containment.

The results of the direct heating calculations were used to postulate the containment failure mode for the radiological source calculations. The 90% injection case was assumed to fail containment (a 7 ft^2 hole) at the time of direct heating. The 50% injection case, since it was marginally close to failure, was assumed to stress the containment sufficiently to induce a relatively small leakage pathway.

1.4.2 PRIMARY SYSTEM RADIOLOGICAL SOURCES

Three release "types" have been calculated in the present study. The release types correspond to MCT code calculations that were performed exercising combinations of the two major modeling changes that were added to the code. Type "A" releases are the RCS (Reactor Coolant System) releases obtained for the meltdown phase of the accident employing only the fission product heatup model. Releases from the RCS during the meltdown phase which utilize both the fission product heatup and the natural circulation models are referred to as type "B" releases. Finally, releases from the RCS during the reevolution phase, that is the period subsequent to vessel breach, are calculated using only the MCT fission product heating model and are referred to as type "C" releases.

The primary system releases for Bellefonte as calculated by the MCT code package are presented here in juxtaposition with the BMI-2104 Zion plant calculations. As discussed below the MCT type "A" calculations for Bellefonte produce releases that are comparable to those calculated for the Zion plant. However, the BMI-2104 study also analyzed the Surry and Sequoyah reactors and for those plants calculated relatively higher releases when compared to Zion results. The reason for the differences in the releases between the Zion, Surry and Sequoyah plants in the BMI-2104 study is not clear. There may be sensitivities in these calculations to different modeling assumptions in the code package or to actual differences in the primary system configurations. In any case, the comparison between the present results and the BMI-2104 Zion calculations should not be interpreted as being particularly significant. Rather, the selection of the Zion results for purposes of comparison should be viewed as an arbitrary one, and the Zion releases merely a "data base" against which the present results were compared. The important conclusion regarding primary system releases is to be derived from comparisons between the three types of releases (A, B and C in Tables 8 and 14).

For the high pressure cases using only the fission product heating model the meltdown phase releases from the primary system (up to and including the releases at vessel failure, Table 8, type 'A' releases) of CsI and CsOH were slightly higher (by a factor of 1.5) than those predicted by BMI-2104 for the Zion plant. The Te releases were higher by a factor of 6, partly due to differences in the MARCH code options that affected the oxidation of zirconium in the meltdown phase and resulted in higher Te releases from the core. Although the fission product heatup model did not produce significant changes in predicted releases during the meltdown phase, the long term heatup effects subsequent to vessel failure produced significant late reevolution of volatile fission products (Table 8, type 'C' releases). For the leakage cases involving a gradual containment depressurization, a mechanism existed for moving revolatilized fission products out of the breached vessel, and with these additional releases included, the total releases of CsI and CsOH from the RCS exceeded the BMI-2104 estimates by a factor of 10. Implementation of the natural convection model for the meltdown phase releases (without reevolution, type 'B' releases) produced RCS releases higher than BMI-2104 Zion releases by a factor of 15 for CsI and CsOH and a factor of 4.5 for Te (approx. 30% for CsI and CsOH and 17% for Te of the original inventories of these species). Although performance of the rather expensive computer calculations for long term reevolution using the natural circulation models after vessel breach was beyond the scope of this analysis, the releases could be still higher than those quoted above.

There were no comparable Zion BMI-2104 calculations against which to compare the pump seal LOCA calculated releases. Without natural convection the primary system volatile releases for this scenario were on the order of 10% of the original inventories (Table 14, type 'A' releases). With natural convection the predicted RCS releases of CsI and CsOH were very high, on the order of 80% or 90% and Te was about 13% (type 'B' releases). However, since direct heating was not involved in this sequence, there was no early containment failure and very small containment releases.

Also of significance was the predicted primary system temperature history. Hot-leg piping temperatures on the order of 1700^{O}F were calculated prior to core slump when the natural circulation model was used. It should be emphasized that the natural circulation calculations employed a rather simplistic one-dimensional model which represents a first cut at qualitatively accounting for this phenomenon. The complicated geometry of the primary system may not be amenable to so simplistic a treatment, and it seems likely that the primary system temperatures predicted by this model are somewhat high. However, the calculated temperature at the outlet nozzle would be within the regime in which failure could be induced, even if the actual temperatures were several hundred degrees lower. If the hot-leg piping failed in this mode soon enough to depressurize the primary system prior to vessel breach, the direct heating scenario could be precluded.

1.4.3 CONTAINMENT RELEASES

A general description of the containment release calculations is given in Tables 2 and 13 and the releases for these cases are summarized in Tables 10 and 15. Radiological releases from the containment are heavily dependent on the containment failure mode. Direct heating calculations indicate that for core debris involvement greater than about 50%, gross containment failure is likely in the Bellefonte containment. The 90% injection direct heating cases were, therefore, assumed to rupture the containment (7 ft^2 hole), and the releases of the volatiles, CsI and

CsOH were on the order of 1.5% of the initial inventories (Table 10, Cases-001 to 011A). Since the primary system releases of these materials were a factor of 10 higher when natural convection was modeled, the releases of these materials from the containment were also proportionally higher for this case, about 15% (Case-011B). Releases of Te were on the order of 20% to 30% while Ru was about 40%. Releases for the latter two fission product groups (Te, Ru) were strongly enhanced by an oxidation reaction that was assumed to occur during direct heating. Specifically, the species Te, Ru, and Mo were assumed to form volatile oxides during direct heating which were condensed as aerosols. The oxidation fraction (the fraction of the species that was converted to the oxide) applied to these species were taken from the Reactor Safety Study (WASH-1400). The WASH-1400 oxidation fractions were estimated and did not represent actual experimentally determined values. Containment failure at the precise point of maximum fission product concentration made these cases the most severe in terms of releases to the environment.

For the 50% direct heating cases (Table 10, Cases 002 to 112A), it was assumed that containment leakage pathways open at the time of vessel failure. Areas of 5 in^2 and 12 in^2 were used to estimate releases for these scenarios. The 5 in^2 leakage area was obtained from the Containment Performance Working Groups estimate of pressure induced leak area for the Zion plant. Estimated leakage characteristics are not presently available for the Bellefonte plant. For both of the leak areas used, the containment was gradually depressurized and, since much more time was available for aerosol removal, the releases were significantly lower. For the worst case (Case-112A), in which reevolution of volatiles was calculated and a 12 in^2 leak area was used, releases of the volatiles and Ru were on the order of 2% of inventory. These releases were about a factor of 12 higher than those calculated by assuming BMI-2104 Zion releases from the primary system (Case-102A). The assumed mechanism responsible for driving reevolved fission products out of the RCS was the depressurization of the containment.

For the TMLB' scenarios without direct heating (Cases 000,100) the induced leakage area was varied between 1 in^2 and 2.4 in^2, and the releases for these cases were very small, on the order of 1.0E-4 of the original inventories of CsI and CsOH.

The pump seal LOCA scenarios, since they are assumed not to involve direct heating, also yielded relatively small releases, on the order of 1.0E-4 for CsI and CsOH (Table 15, Cases 030,130). Primary system releases calculated with natural convection, however, increased the containment releases to about 0.2% for CsI and CsOH and to about 0.8% for Te (Table 15, Cases 031,131).

There are several conclusions that can be drawn from this study. One of the most significant is that, if direct heating occurs in which more than about 50% of the core debris is involved, containment failure is likely. In addition, this scenario fails the containment at a time when the fission product concentration in the containment atmosphere is maximized and leads to high releases outside the containment. Introducing simple modeling for natural convection and decay heating in the primary system fission product transport codes has significantly increased the predicted releases into the containment due to the added releases from reevolved volatiles and to natural convection heating of the primary system. However, the same modeling changes have lead to an indication that primary system structural temperatures may be high enough to induce failure and depressurization of the primary system before core slump, thus eliminating direct heating and with it the primary mechanism for early containment failure for this accident sequence.

1.4.4 MODELING ASSUMPTIONS AND LIMITATIONS

There are a number of modeling assumptions and limitations inherent in the analysis. Some of the limitations are related to the capabilities of the code package and others are related to engineering assumptions necessary to perform the analysis within budget. The major assumptions will merely be identified here while the more significant ones will be discussed in some detail in the appropriate sections of the report.

Due to the prohibitive expense associated with multi-volume containment code calculations, the bulk of the present analysis was performed using a single volume to model the containment. One multi-volume calculation was performed to baseline the single volume analysis. The new models that have been supplied to the primary system fission product transport code package have not been rigorously evaluated. The primary system natural convection model has two limitations that have been identified. The model appears to somewhat overpredict heat transfer between control volumes, and the heat that is transferred from the core by natural convection does not cool the core. To remove the latter limitation it would be necessary to link the meltdown progression code with the RCS fission product transport code package. Parallel or multiple flow pathways have not been modeled in the MCT code calculations. The radioactive decay of fission product species to their daughter species has not been treated. Due to a lack of phenomenological models for direct heating at the inception of the analysis, it was necessary to employ a number of limiting assumptions and a highly parameterized approach to the direct heating calculations. The decomposition of CsI due to high temperature and a high radiation field has not been treated. Lumped parameter models are employed in the MCT code package to estimate heat structure thermal response. Lumped parameter models can significantly underpredict structure surface temperatures and, thus, overpredict fission product retention on RCS surfaces. Finally, the assumption has been made that core/concrete interactions do not commence until all the water has been vaporized in the reactor cavity.

2.0 INTRODUCTION

The Severe Accident Sequence Analysis program at Sandia National Laboratories (SNL SASA) has as part of its objectives the task of performing detailed best-estimate analysis of reactor systems behavior during severe accidents. The analysis presented here is a study of the TMLB' (WASH-1400 nomenclature) station blackout accident sequence for the TVA Bellefonte (PWR) reactor. The TMLB' accident sequence involves a complete loss of offsite and onsite AC power together with a loss of auxiliary feedwater and a failure to recover power before core damage is sustained.

This report addresses in some detail two major scenarios of the TMLB' type accident sequence; namely, the low pressure and high pressure primary system failure scenarios. The high pressure scenario occurs when the primary coolant system boundary remains intact until vessel melt-through. Breach of the RCS boundary due to temperature-induced pump seal failure or piping failure which results in complete or partial depressurization of the RCS before vessel melt-through results in a low pressure TMLB' scenario.

A probabilistic risk assessments is not currently available for B&W plants with the Bellefonte configuration. It is thought[1], however, that the TMLB' sequence represents a dominant sequence for large dry PWR's in general. Based on that observation, together with the fact that many of the scenarios developing out of external events closely resemble the TMLB' accident sequence, the present analysis has been concentrated in that area.

To approach as closely as possible a best-estimate analysis, an attempt has been made to incorporate the most recent thinking in terms of the type of phenomenology deemed to be important and appropriate for the sequences under examination. In particular, for the present study, this includes calculating the effects of direct heating of the containment atmosphere due to the high pressure ejection of core material at the time of vessel breach. In addition, recent information[2,3,4] emerging from Sandia's experimental programs currently being conducted to assess the effects of high pressure ejection have also been utilized in this study. This information includes estimates of the fraction of the ejected debris that is injected into the containment atmosphere, the fraction of the injected debris that remains in the atmosphere as aerosols, and the particle size distribution of the aerosols generated by direct heating.

The primary thrust of the Bellefonte analysis is to determine both the thermal-hydraulic loadings on the containment system and radiological releases to the environment. The methodology employed in the analysis will be discussed in detail in Section 3. In general the most recent versions of the containment phenomenological codes were employed where appropriate, while stand-alone codes or hand calculations were used for phenomenology not contained in the major codes. Examples of the latter include the direct heating calculations and the calculation for the dehydration of the containment concrete floor subsequent to the deposit on it of core debris from direct heating.

Large uncertainties continue to limit the degree of accuracy that can be obtained in terms of arriving at best-estimate numbers for containment loading. It is generally agreed that in the event of vessel failure at elevated pressure, direct heating may pose a threat to containment integrity at precisely the time that radiological sources are exacerbated by the same phenomenon. Experiments [(3)] have indicated that large fractions of molten core debris may be ejected out of the cavity at high velocity. Intervening structures and surfaces may not offer sufficient holdup to prevent most of this material from being injected into the upper containment atmosphere where it may deposit both its sensible energy and the chemical energy that will be evolved upon interaction with the atmosphere. The experiments, it must be noted, have been performed using molten ejecta. It is by no means certain that all or most of the core debris will be molten at the time of vessel breach. One of the sources of uncertainty relates to the in-vessel meltdown progression. It is not known with any certainty what will be the composition and state of the core debris at the time of vessel breach. Large chunks of core debris, for example, would certainly affect the dynamics of the high pressure ejection scenario, and perhaps inhibit it to some degree. It is hoped that the meltdown progression codes currently under development (i.e. MELPROG) will help reduce the uncertainty and better quantify the physical state of the core debris.

Similarly, the timing and location of primary system failure is uncertain. It has been postulated that, for the TMLB' sequence, the transport and deposition of fission products along the flow path leading to the relief valves, together with energy transport by natural convective processes, will heat these structures and perhaps result in primary system failure at a higher elevation and at a time prior to lower vessel head meltthrough. The result would be that the primary system pressure may be relieved in advance of vessel melt-through, thus eliminating the threat of high pressure ejection. A more recent version of the TRAP/MELT code[(5)] which models both fission product heatup and natural convection has been used in this analysis and predicts significantly higher primary system temperatures than have heretofore been reported. With a better estimate of primary system temperatures it should be feasible to perform creep/failure calculations to estimate the time-to-failure for hot primary system structures at pressure.

Since there exists considerable uncertainty in the parameters that affect the high pressure ejection phenomenon, and arguments can be given to justify core debris ejections ranging anywhere from no ejection to nearly complete ejection, the fraction of the core participating in direct heating has been treated parametrically. The range of direct heating participation has been covered by including cases with no injection, 50% injection, and 90% injection. The term "injection" as apposed to "ejection" is used here to differentiate between ejection from the vessel and injection into the containment atmosphere. The latter case, 90% injection, is the case suggested by recent experiment [3,4] using molten materials. It should be noted, however, that the experiments were designed to model the flow paths and obstructions in the Zion plant reactor cavity region and do not necessarily characterize the Bellefonte configuration. In the present study it has been assumed that the ejected core debris is entirely molten at the time of vessel failure and that failure occurs due to the thermal attack of the molten debris on the lower reactor vessel head.

Radiological releases from containment have been estimated based on two sources for primary system releases. The primary system releases from the BMI-2104 [6] Zion plant analysis were adjusted up on the basis of reactor fuel inventory and used for the primary system releases. As stated in the executive summary, the releases for the Surry or Sequoyah plants could also have been used. The Zion releases were used because they were comparable to the Type "A" releases (Section 4.3) and were convenient for purposes of comparison. In addition a composite (hard-linked) version of the CORSOR, MERGE and TRAP/MELT codes, called the MCT code, was also employed to calculate the primary system fission product releases.

The overall methodology employed in this study together with a discussion of the codes used and the method of linkage is detailed in Section 3. A discussion of the TMLB' high pressure failure scenario and results are given in Section 4., while the low pressure case (TMLB' with induced pump seal LOCA) is treated in Section 5. The conclusions are given in Section 6.

3.0 CODES AND METHODOLOGY

The treatment of phenomena that are not modeled in any of the currently available codes has somewhat complicated the present analysis. Mechanistic models for direct heating and concrete degassing due to fission product heating are not presently available in containment codes, for example. Small stand-alone codes together with hand calculations have been used in conjunction with a suite of codes which treat various aspects of severe accident phenomenology. This section will discuss the phenomenology and the analytical tools employed.

A diagram outlining the flow of information between codes for the high pressure ejection scenario is given in Figure 1. The early phase of the reactor blowdown was calculated with the RELAP5 code and this calculation was run to incipient core degradation when the RELAP calculations became suspect. The criterion for terminating the RELAP calculations was a 1000°K temperature in any RELAP core node. The RELAP5 analyses for both the TMLB' high pressure and pump seal LOCA cases were performed and the results supplied to Sandia by EG&G[7,8]. The thermohydraulic sources thus obtained were input to the MARCON code as source tables. Figure 1 shows a direct link between RELAP and CONTAIN, but in fact, the effective linkage is between MARCON and CONTAIN. The MARCON code was modified to write an output tape that contains all the thermohydraulic sources from the primary system including those from RELAP.

The phase of the accident that commenced with the start of core degradation and, for some situations included ex-vessel core/concrete interactions, has been analyzed using the MARCON[9] computer code. The MARCON code consists of a hard link of the MARCH 2.0 containment code and the CORCON/MOD2 core/concrete interaction code. As indicated in Figure 1 linkages have been established between the MARCON code and both the CONTAIN and the MCT codes. MARCON supplies primary system conditions and thermohydraulic sources to the MCT code.

The primary system radiological sources are calculated with the MCT (MERGE,CORSOR,TRAP/MELT) code[5]. Information regarding the core and primary system conditions were supplied to the MCT code which calculated fission product releases from the degraded core, transport of fission products through the system, plateout and settling of fission products within the system, and estimated fission product releases into the containment building. The MCT component codes, especially TRAP/MELT, have been modified and improved to treat phenomenology not modeled in the original codes. These include the heatup of primary system structures due to the presence of fission products and due to heat transported from the core region by natural circulation. The code numerics have also been improved as have the linkage interfaces.

The MCT code has been supplied with an output/input linkage with the CONTAIN code which is similar to the MARCON/CONTAIN interface. This interface passes information regarding fission product species source rates (including vapors and aerosols) into the containment atmosphere.

Currently available containment codes do not presently contain models for direct heating phenomenology. A small computer code[10] that calculates end conditions after direct heating was used in this analysis to determine the peak temperature and pressure in the containment as well as the energy delivered to the atmosphere. The code performed an adiabatic calculation and assumed that the ejected debris came into thermal equilibrium with the atmosphere. Chemical energy from the oxidation of zirconium, steel, and hydrogen was also accounted for in the code. Hand calculations were performed for several of the direct heating cases and good agreement with the code was observed. The net energy delivered to the atmosphere as calculated by the direct heating code was input into the CONTAIN code as a mass source with an artificial specific enthalpy which yielded the correct integrated energy source. The core debris which was injected into the containment during high pressure vessel failure was not available on the reactor cavity floor to participate in a core/concrete interaction. It was, however, distributed on the containment floor in a rather shallow (perhaps 1/2 to 2 inches, if evenly distributed) debris bed. The initial temperature of the debris was the temperature at which thermal equilibrium between the debris and the atmosphere was calculated to occur. A small finite difference computer code(11) was employed and modified to calculate transient thermal conduction in the containment concrete floor and to estimate the quantity of steam evolved from concrete dehydration due to the layer of hot core debris deposited in containment by the high pressure ejection process. The degassing model was similar to the one used in the PWR version of MARCON(9) except that the free and bound water were assumed to come out of the concrete over two separate temperature ranges. The free water was evolved over a 20°K temperature range centered at 370°K and the bound water emerges over a 20°K range centered at 510°K. Although the debris layer on the containment floor, even for 90% injection was not sufficiently deep to melt the underlying concrete, it was found that considerable dehydration of the concrete occurred in this situation. In fact, the rate of heat transfer from the debris to the atmosphere (ranging from 800 MW at the time of DCH to about 6 MW 25 minutes after DCH for the 90% injection case) was dominated by the flow of steam out of the concrete surface rather than by radiation. The steam sources due to concrete dehydration, as obtained from these calculations, were input to the CONTAIN code in the form of source tables.

It has already been mentioned that the CORCON code, which is included as a subroutine of the MARCON code, has been utilized to calculate the thermohydraulic sources from the core/concrete interaction. The CORCON code was also used to supply the required information to the VANESA code to estimate the radiological releases from core/concrete interactions. The VANESA code (12) was designed to detail the chemical reactions in the molten pool and to estimate the releases of vapors and aerosols from the surface of the molten pool into the containment atmosphere. The releases, both thermohydraulic and radiological, as calculated by CORCON/VANESA were used as source terms to the CONTAIN code.

Containment conditions, including temperature and pressure, and the transport of gases and aerosol into and out of the containment atmosphere have been calculated for this analysis using the CONTAIN code. A detailed description of the CONTAIN code can be found in Reference (13). The thermohydraulic and radiological sources obtained from the other codes used in the analysis were all input to CONTAIN which then calculated the response and estimated the aerosol concentrations in the containment atmosphere as well as radiological releases to the environment.

4.0 TMLB' with High Pressure Ejection

The TMLB' accident sequence involves a loss of both offsite and onsite power together with a loss of auxiliary feedwater. Table 1 shows the sequence of events that occurred in the high pressure TMLB' case that was studied in this analysis. The steam generator dried out at about 5.8 minutes and incipient core melting occurred at 53.4 minutes. The lower reactor vessel head was calculated to fail at about 82 minutes at which time direct heating took place. Containment failure or leakage was assumed to occur concurrently with direct heating .

Table 2 gives a description of the case matrix for the TMLB' high pressure ejection sequences. The primary parameter in this matrix is the fraction of core debris injected into the upper containment during direct heating. This fraction was assigned values of 0, 0.5, and 0.9. The second parameter indicated in Table 2 is the participation of cavity water in the direct heating event. The MARCH code predicts that about 75,000 lbs of coolant will be residing in the cavity at the time of vessel breach. If this water is present in that location it will almost certainly be swept out with or ahead of the core debris during core ejection. To determine the effects of cavity water, cases were run both with and without the involvement of cavity water. For the cases in which cavity water was involved, it was assumed that the injected debris and the water were in good thermal contact so that the water was completely vaporized. In a real direct heating situation it is not clear what fraction of the debris and the water would be in intimate contact.

In order to keep the number of cases tractable, the estimated containment failure criterion (14) was employed as a bifurcation point. The direct heating calculations were used to estimate the peak pressure and this, compared to the ultimate loading estimates, determined which branch the analysis followed for each case. Thus, if the direct heating calculation seemed to indicate a high likelihood of exceeding the ultimate loading capacity of the containment structure, the containment was assumed to fail by opening a large hole in the boundary at a time coincident with direct heating. If the pressure did not equal or exceed the failure criterion, a leakage commensurate with the magnitude of the peak pressure was employed. For those cases in which the direct heating loads failed containment (all the 90% injection sequences) a break area of 7 ft^2 was assumed to open in the containment boundary at the time of direct heating. For those cases which were marginally close to the estimated ultimate loading capacity of the containment (all the 50% ejection sequences) a leakage pathway was assumed to open coincident with direct heating. The leak area for these cases was treated parametrically, two values being used, 5 in^2 and 12 in^2.

The "best estimate" leakage of 5 in^2 was obtained from the estimated leak area suggested in the Containment Performance Working Group final report for the Zion plant [15]. This value was selected in the absence of corresponding estimates for the Bellefonte plant. A 12 in^2 leak area was also used to determine the sensitivity of containment releases to the assumed leakage parameter. It should be noted that the 5 in^2 leakage area estimated for the Zion containment was obtained assuming a gradual pressurization of the containment. There are no estimates for containment leak areas induced by rapid transient events such as direct heating, steam spikes, or hydrogen burns.

The remaining parameters in Table 2 are related to the treatment of fission product releases and transport. The primary system releases were estimated in two different ways. The first method involved using the primary system releases calculated in the BMI-2104 study for the same accident sequence in the Zion plant. These releases were merely adjusted up according to the operating power of the two plants. The second method involved actually running the suite of codes that Battelle used to calculate primary system releases. An interactively run version of these codes, called the MCT code (for MERGE, CORSOR, TRAP/MELT) was employed for that purpose. Combinations of the modeling capabilities in MCT were treated parametrically as indicated in Table 2. Finally, for two cases (Cases-012A, and 112A) a core/concrete interaction occurred late in the sequence (at about 20 hours) and the VANESA code was used to estimate the radiological releases into containment due to this interaction.

4.1 Containment loading

For the accident sequences that include high pressure ejection of core debris, direct heating imposes more severe loads on the containment than occur at any other time during the course of the accident. A detailed examination of direct heating, therefore, will yield the peak loading conditions.

Uncertainties in many aspects of the direct heating phenomenology required that it be treated parametrically. Table 3 outlines the basic assumptions for the direct heating calculations. These assumptions include ejection from the vessel of 100% of the fuel and cladding materials and about 50% (100,000 lb) of the potentially available steel. This quantity of steel is about twice the amount of steel available in the core region and accounts for partial melting of steel in the core support structures and lower plenum. The initial temperature of the debris as it exits from the vessel was taken to be the corium eutectic temperature (approx. 2550°K).

The quantity of Zircaloy reacted in-vessel during the core meltdown phase was forced to be 50% by adjusting the core slump parameters in the MARCH code. Selection of a 50% metal/water reaction reflects the uncertainty in the extent of in-vessel clad reaction. This fraction of in-vessel oxidation was achieved by slumping the core when 65% of the core was molten. The hydrogen generated by in-vessel oxidation of zircaloy resulted in an average hydrogen concentration in containment at vessel failure of about 3 volume percent. The fraction of the remaining zircaloy that was injected into the containment was assumed to be completely oxidized during direct heating.

The direct heating calculations were performed with a stand alone code (DHEAT[10]) that calculated the end conditions of the event assuming that it was so rapid that it occurred essentially adiabatically and that the injected debris was, nevertheless, in contact with the atmosphere long enough for thermal equilibrium to be achieved. There were, at the time that this analysis was being performed, no phenomenological codes available that treated the direct heating process mechanistically. Holdup of debris on surfaces due to impact, heat transfer to surfaces, changes in particle size distribution as debris passes through lower containment volumes on its way to the upper containment, interaction with water in the cavity, heat transfer and chemical reactions between the ejected debris and the atmosphere and radiation between the hot debris, water droplets in the atmosphere, and the passive heat structures could not then be quantified. In the interim, work has been proceeding in this area and at least one computer code has been developed that can treat some of these phenomena [16,17]. Experiments done at Sandia[2,3] seem to indicate that minimal holdup will occur and about 90% of the ejected core debris could be transported into the upper levels of the containment. However, the experiments were performed for a cavity configuration similar to that in the Zion plant and may not be completely characteristic of the Bellefonte configuration. Heat transfer and the combustion processes as well as the aerodynamics of direct heating are involved and have not yet been studied in detail analytically.

Potentially, the most important parameters that affect the magnitude of the direct heating loads on containment include: the fraction of the core debris injected into containment, the degree of completion of the combustion process for the various combustible components in the debris, and the heat absorbing capacity of the containment atmosphere. Table 4 shows the matrix of parameters selected and the calculated containment conditions for each case. The fraction of core injected into the atmosphere was varied from 0% to 90% of original core inventory. The 0% case is not shown since it contributed no additional loading. The significant combustibles include zirconium, steel and hydrogen. At the temperatures involved it is likely that the injected zirconium will be completely oxidized. The steel oxidation was varied by assuming no involvement or 100% involvement. Although hydrogen at a concentration of 3% is not within the normal combustion limit, it is believed that much of it may be consumed in a catalytic process at debris particle surfaces. The hydrogen combustion contribution was assessed by calculating cases with no hydrogen combustion and complete hydrogen combustion. With regard to the heat absorbing capacity of the atmosphere, although the mass of non-condensible gases in the containment does not change significantly in the time frame of the direct heating process, the quantity of steam and water contained in the atmosphere depends largely on the accident sequence and on the timing of direct heating. MARCH code calculations predicted that about 75,000 lbs of water were present in the reactor cavity at vessel breach. This represents water that was condensed in the containment building during the blowdown phase, filled the containment sump, and overflowed back into the reactor cavity. This quantity of water, when its heat of vaporization is included, represents a large effective heat capacity. If this water is actually located in the reactor cavity, it is probable that most or all of it would be swept out with the debris and should be included in the direct heating calculation. The effect of this additional heat capacity was considered by performing the calculation both with and without the cavity water in the atmosphere. For the cases in which the cavity water was assumed to be swept into the containment together with the core debris it was also assumed that the water and the debris were in good thermal contact resulting in complete vaporization of the water.

The results of the direct heating calculations indicate (see Table 4) that all the cases involving 90% injection resulted in containment pressure loadings that were either in or above the estimated containment failure range (144.7 to 153.7 psia). The peak pressure, for example, in the case of 90% debris injection with hydrogen combustion, no steel oxidation, and complete injection of the cavity water resulted in a peak pressure of 169 psia. Since the optimistic assumptions for the 90% ejection cases resulted in loadings that exceeded the estimated failure pressure, it was not necessary to perform the cases with more conservative combinations of parameters.

The 50% injection cases were marginally close to the containment failure criterion and quite sensitive to the assumptions regarding the oxidation of hydrogen and steel. For the cases in which cavity water was not involved (Cases-002), it required the complete combustion of the steel to exceed the failure pressure. Direct heating with hydrogen combustion alone produced a pressure of 139 psia while direct heating with neither H_2 nor steel combustion yielded a peak pressure of only 117 psia, well below the estimated failure range. With the involvement of cavity water (Cases-002A) only the most pessimistic assumptions regarding combustion put the peak pressures into the containment failure range.

Although there are clearly a number of uncertainties regarding the direct heating scenario, it can generally be concluded from these parametric calculations that for core debris injection of 90%, containment failure is essentially certain, and that for injections much in excess of about 50% containment failure is likely. The contribution due to steel combustion appears to be the largest single factor increasing the pressure by about 40 psi. Cavity water and hydrogen combustion have about equal but opposing effects, the cavity water decreasing the pressure by about 20 psi and the hydrogen combustion increasing the pressure by about the same amount.

The energies transferred to the atmosphere during direct heating as calculated by the DHEAT code were input to the CONTAIN code over an assumed event duration of 30 seconds. The last column in Table 4 gives the net energy transferred to the atmosphere during direct heating. Although the modeling assumptions in the DHEAT code (and in the hand calculations) assumed adiabatic conditions (i.e. no heat transfer to structures), the CONTAIN code calculated the heat transfer processes during the direct heating transient. A comparison of the peak pressures for the adiabatic calculations and the CONTAIN code calculations revealed no significant differences. However, the version of the CONTAIN code that was used in this analysis did not have a model for radiation from the atmosphere to the walls and heat structures (The most recent version of the code now has a radiation model). Recent calculations performed by the University of Wisconsin for the Surry reactor plant [17] utilizing newly developed mechanistic direct heating models have suggested that radiation to the walls during the direct heating transient can somewhat reduce containment pressure and temperature. For example, a case calculated without water droplets in the atmosphere showed a reduction in the peak pressure from 103 psia to about 85 psia when radiation was modeled. The effect, however, may be overstated in the University of Wisconsin analysis. In those calculations the duration of the direct heating event was taken to be 20 seconds. Experiments [2,3], however, seem to indicate a much shorter duration, on the order of 5 to 10 seconds. A shorter event duration would, of course, reduce the quantity of heat that could be transferred to the walls.

The conclusions derived from the direct heating calculations have been used in the remainder of this study to define the containment failure modes. Thus, for cases involving 90% ejection the containment was assumed to fail in a gross manner blowing down to atmospheric pressure within minutes. Those scenarios which involved 50% core ejection or less were assumed to develop containment leakage pathways.

As already mentioned the peak loading conditions for the sequences that involve direct heating were in each case achieved at the time of direct heating, and those conditions are detailed in Table 4. Two 0% ejection cases were also calculated (Cases-000 and 100) with the assumption that, although the system was at pressure at the time of vessel breach, no debris was ejected out of the cavity region. In the absence of an energetic ejection of debris into containment, the loading on containment at the time of vessel breach consisted entirely of the "steam spike" that results from core slump, vessel blowdown at failure, and the interaction of core debris with coolant in the reactor cavity. The peak pressure at vessel breach for these cases (see Figure 2) was about 62 psia while the containment temperature was about 260°F (Figure 3).

Because the core debris was not ejected out of the reactor cavity for the non direct heating cases, the reactor cavity water was completely boiled off at about 450 minutes and a core/concrete interaction ensued which began generating hydrogen. At about 17.5 hours, a flammable mixture occurred in containment and a hydrogen burn resulted which raised the containment pressure to about 100 psia and the temperature to about 1000°F (Figures 2 and 3).

Hydrogen burns were not predicted to occur within the first 20 hours for any of the direct heating scenarios.

4.2 RADIOLOGICAL RELEASES FROM HIGH PRESSURE EJECTION

Direct heating, besides its apparent capacity for initiating early containment failure, also represents a serious threat in terms of its potential for generating large quantities of radioactive aerosols and depositing them directly in the containment atmosphere. Although most of the ejected core debris will fall out onto the containment floor and horizontal surfaces immediately after direct heating, experiments(2,3) have indicated that perhaps 2 or 3% of the ejected debris will subsequently remain in the atmosphere as aerosols for an extended period. In addition, several of the important radiological materials such as ruthenium may be heavily concentrated in this aerosolized component due to their possible involvement in oxidation reactions during the direct heating sequence.

Currently, the basis for a best estimate of the aerosol source term coming from the high pressure injection sequence is the SPIT-19 test(3). In this test, 10.3 kgs of thermitically generated melt was involved, 9.8 kgs of which were ejected at high pressure. Based on measurements at various locations in the experimental chamber, the total aerosolized fraction of particles less than 10 microns in diameter was in the range of 1% to 3% of the injected mass, and the component believed to be generated from the condensation of vapor was in the range of .6 to 1.8%. Thus, a bimodal particle size distribution was apparent with one mode centered at a mean aerodynamic equivalent diameter of 0.7 microns and the other at about 30 microns. The very small particle size mode appears to have been generated from the condensation of vapor components evolved from combustion reactions. The larger size distribution was generated mechanically (i.e. atomization during the ejection,etc.).

For the purpose of this analysis a total aerosol mass of 2% of the ejected debris mass was used, 1% consisting of the 0.7 micron size distribution and the other 1% consisting of the 30 micron distribution group. The fission product components for the 30 micron size aerosol were calculated by taking 1% of each of the fission product group masses that were present in the injection. The fission product groups were the same as those used in BMI-2104 (see Table 5). One percent of the inert materials in the core debris were also included in the large size aerosol component. The small size (.7 micron) component, since it consisted mostly of re-condensed combustion products, was made up of only those fission products that undergo a significant oxidation reaction together with the inert oxides (oxides of iron, zirconium, etc.) formed in the direct heating event. Thus the 0.7 micron aerosol distribution component was heavily enriched in the three fission products that may undergo an oxidation reaction, namely tellurium, ruthenium and molybdenum. The mass of each of these three aerosol components was calculated according to the following equation:

$$M_i = f_e f_i f_{ox} M_{oi}, \qquad (1)$$

where M_{oi} is the original inventory of species i, f_e is the fraction of the core debris ejected, f_i is the fraction of the species present in the core debris at the time of ejection, and f_{ox} is the oxidation release fraction (i.e., the fraction of species i present in the atmosphere that actually becomes oxidized). The estimates for the oxidation release fraction are taken from WASH-1400[18], 0.6 for tellurium, and 0.9 for ruthenium and molybdenum. There is some controversy regarding what values should be used for the oxidation release fractions and some indication that 0.9 may be too high for the ruthenium release. Tables 6 and 7 show the direct heating fission product releases for cases in which BMI-2104 primary system releases were used and for the cases in which the MCT code was used to calculate primary system releases, respectively.

The direct heating fission product releases were supplied to the CONTAIN code along with the primary system releases for calculating the transport and retention in the containment system and for estimating releases to the environment.

4.3 PRIMARY SYSTEM RADIOLOGICAL RELEASES

Fission product transport in the primary system and releases into the containment system have been estimated using the Battelle suite of codes, CORSOR, MERGE and TRAP/MELT. These three codes have been combined into a single code package called MCT (MERGE, CORSOR, TRAP/MELT). A description of the code together with the modeling and numerical modifications can be found in Ref. 5.

Three configurations were run for the TMLB' high pressure scenario employing the MCT code package. The first case (Type A) consisted of the configuration in which fission product decay heat was allowed to heat up the passive heat structures in each control volume of the primary system, but natural convection between control volumes was not accounted for. In the second case (Type B) a model which estimates the heat transfer between connected control volumes due to natural convective processes was activated. In the third case (Type C) the same modeling options used in the first case were utilized (i.e. fission product heating with no natural convection) and the case was run out to about 10 hours after vessel failure in order to calculate the late reevolution of fission products in the primary system.

Figure 4 shows the transport pathway for gas flow and fission product relocation through the primary system. This diagram also specifies the control volume sizes, flow areas, heat transfer areas and the heat capacities for passive heat structures in each control volume. The flowrate of gases and vapors from the top of the core together with the exit gas temperature was supplied to MCT by the MARCH 2.0 code. Gases exiting from the core region entered the upper plenum, passed through the outlet plenum, hot-leg piping, surge line and pressurizer and exited through the PORVs into the containment. This pathway was the same for the first two cases. For the third case, however, the vessel has failed and the flow path was somewhat reversed. For that configuration the PORVs were assumed to be closed and the flow that exited from the vessel had to do so from the breach in the bottom head of the vessel.

There are several limiting assumptions that are inherent in the MCT code modeling and that may introduce some inaccuracies in the results. The TRAP/MELT fission product modeling does not incorporate chemistry for the decomposition of CsI due to a high temperature and radiation environment and does not account for radioactive decay of fission products into daughter isotopes such as ^{132}Te into ^{132}I. There is considerable evidence that CsI decomposition is an important aspect and may lead to higher releases into containment. For those cases in which natural circulation has been modeled there is a pathway for natural circulation from the core region into the upper plenum. However, there is no provision for the cooler downflow from the upper plenum to cool the core region. This is an artifact of the non-interactive interface between the thermohydraulic code (MARCH 2.0) that calculates the core condition and the primary system fission product transport code (MCT). The heat absorbing structures have been treated using a lumped parameter model. Although the heat structures are composed of steel which has a fairly high heat transfer coefficient, the Biot number can be in excess of 0.5 for the thicker walled structures (up to about 7 inches thick). This Biot number indicates that there will be a significant temperature gradient in the heat structures and the surface temperatures will be somewhat higher than those calculated by the lumped parameter model. The higher surface temperatures will primarily affect the timing of fission product relocation tending to move the volatiles through the system somewhat faster than has been estimated here.

The MCT code modeling for natural convection has already been identified as a rather simplistic one-dimensional approximation. The lumped parameter modeling that is characteristic of the MCT code package in general makes this type of approach necessary in order to evaluate the effects of natural convection on the RCS releases. The question remains, however, as to the accuracy of the model used to calculate natural circulation in view of the rather complex geometry in the primary system. Figure 5 describes the model that is currently in the MCT code. The model assumes that the Bernoulli equation ,

$$v = [2\Delta P/\rho_0]^{.5}, \tag{2}$$

can be applied to describe the flow field between two control volumes located one above the other. The driving mechanism that sustains flow is the buoyancy resulting from the lower control volume being at a higher temperature than the upper volume,

$$P = (\rho_1 - \rho_0)gH. \tag{3}$$

The Bernoulli equation (Eqn 2) together with the buoyancy term (Eqn 3) and the ideal gas law yields the natural convection velocity,

$$v = [2gH(T_0/T_1 - 1)]^{.5}. \tag{4}$$

The further assumption is made that there is no pressure difference between the two volumes so that the upward flow of gases must be balanced by an approximately equal downward flow. To implement this requirement the flow opening is divided in half with half of the area devoted to upward flow and the other half to downward flow, thus, forming a single-roll flow cell.

A search of the literature has revealed a very limited treatment of this type of heat transfer problem. The approach that has been used in the MCT code was described in the literature [19]. However, the approach as described in the literature was applied to the case in which the control volumes were located side by side with an opening of height, H, in the vertical separating partition. In this configuration, H, can be thought of as the vertical length of the flow path between the control volumes. For this configuration a steady flow field is expected and the Bernoulli equation can be employed to approximate the flow velocities. The configuration in which the control volumes are one above the other with the lower cell having the higher temperature is basically unstable and a steady flow field cannot be assumed. Thus, the Bernoulli equation cannot be used to describe the flow for this situation. An experimental correlation [20] does, however, exist for this configuration and in terms of the Nusselt number the expression is as follows:

$$Nu = 0.0546Gr^{.55}Pr(L/H)^{.33}, \qquad (5)$$

where L is the characteristic dimension of the opening and H is the vertical length of the opening, while Gr and Pr are the Grashof and Prandtl numbers, respectively.

In order to estimate the accuracy of the model used in the MCT code a comparison was made between the MCT model and the above correlation. The velocity equation (Eqn 2) used in the MCT model can easily be cast into a heat transfer correlation of the type shown above and when this is done an expression for the Nusselt number in terms of the Grashof and Prandtl numbers is obtained:

$$Nu = 0.33C\ Gr^{.5}Pr. \qquad (6)$$

Here C is the flow discharge coefficient. Choosing two control volumes such that L/H is about 1.0 and setting the discharge coefficient equal to 1.0 (as is assumed in the MCT model), calculations of the Nusselt number using the two correlations were made. Figure 6 shows the Nusselt number as a function of the temperature difference between control volumes for the two correlations. In figure 6 the curve labeled Nu(1) is the correlation in Equation 6 which is the one used in the MCT code. The curve labeled Nu(2) is the one expressed by Equation 5. For this geometry the MCT code overpredicts the heat transfer between control volumes by a factor of about 4 at low temperature differences and a factor of 3 at higher temperature differences. Clearly, for the configuration in which control volumes are one over the other, the MCT code overpredicts natural convection heat transfer. However, for volumes that are connected in a horizontal arrangement such as between the outlet plenum and the hot-leg piping, assuming that H is defined as the height of the opening and not the differential elevation between the two volumes, the heat transfer rates between volumes may be a fair approximation.

Lumped parameter treatment of heat structure thermal response represents yet another source for error in the calculations. Calculations show that for steel structures with thicknesses on the order of 4 inches, the surface temperature of the structure as calculated by one-dimensional transient finite difference methods can be as much as 30% higher, and on the average 15% higher than the temperatures calculated using a lumped parameter treatment. Since lumped parameter calculations predict that surface temperatures are lower than they actually are, the effect is to hold up fission products on structures and move them through the system more slowly than they would actually move.

The errors associated with overpredicting natural circulation heat transfer and underpredicting heat structure temperatures are competing and tend to reduce the net error in terms of fission product transport. Multi-dimensional code calculations and experiments [21] have verified the importance of natural convection in the primary system with regard to primary system heatup and the associated cooling effects on the core.

Turning to the results of the primary system fission product transport calculations for the TMLB' high pressure scenario, Figures 7 to 10 show the conditions in the primary system as calculated by the MARCH code. The blowdown phase of the accident (until incipient core meltdown) was calculated by the RELAP5-MOD1.6 code and does not appear on these plots. Figure 7 shows the primary system pressure increasing up to the PORV set point and remaining at that level until vessel breach. The average core temperature is given in Figure 8 indicating a gradual temperature increase until core slump when the temperature was about 4700°F. As indicated in Figure 9, the core slumped at 65% meltdown and the fraction of clad oxidized in-vessel was about 50%. The in-vessel hydrogen production, Figure 10, for 50% clad reaction was about 1150 lbs and produced a hydrogen concentration at vessel failure of about 3 vol % in containment.

4.3.1 TMLB'(HPE) WITHOUT NATURAL CONVECTION (TYPE A)

The core outlet gas flow and outlet gas temperature for the high pressure ejection cases are shown in Figure 11 and 12. The sudden increase in flow at about 4600 seconds results from core slump which produces large steaming rates as the core debris quenches in the coolant on the lower vessel head. The outlet gas temperature follows the same trend as the core temperature increasing to a peak of about 3800°F at vessel failure. The thermal response of the primary system is shown in Figures 13 and 14. As expected the gas temperatures decrease with distance from the core region, but very large temperature differentials exist between adjacent control volumes which under the relatively quiescent conditions in this accident sequence would result in buoyancy driven flows. The upper plenum, as expected, is the hottest volume in the reactor system because it is nearest to the hot core exit gases and it also receives radiation heat transferred from the top of the core. The surge line is calculated to heat up quickly because of the relatively low thermal mass of the structure. The outlet plenum, the hot-leg and the pressurizer heat up somewhat more slowly, because of their large thermal masses.

Figure 15 shows the fission product heat deposited in each control volume. Clearly, the upper plenum region of the reactor system contains the largest portion of the fission products. At approximately 4600 seconds into the accident, the core collapsed and produced a relatively large flow of steam out of the core region which swept the vaporized volatile fission products out of the upper plenum region. This accounts for the observed decrease in the fission product heat at that time. Corresponding to this decrease, there is an increase in the fission product heat in the pressurizer and the surge line. This is due to the retention of the volatile vapors by those cooler volumes.

Figure 16 shows the retention factor of cesium iodide. The retention factor as used in this report is defined as the fraction of the total fission product species released out of the fuel matrix which is retained by either vapor condensation on structures, vapor condensation on aerosols with subsequent settling of the aerosols, or chemisorption. The sudden increase in gas flow out of the core at the time of core collapse drives the gas-borne volatiles away from the upper plenum region to the cooler volumes which include the hot-leg up to the surge line, the surge line and the pressurizer. There the vapors condense on the structures as well as the aerosols. This accounts for the increase in the overall retention factor for both cesium iodide and cesium hydroxide, at approximately 4600 seconds.

The behavior of tellurium, shown in Figure 17, is similar to that of cesium iodide and cesium hydroxide. The only difference of interest occurs at the time of revolatilization of the condensed tellurium in the upper plenum. This revolatilization is shown as a decrease in the upper plenum tellurium retention factor at approximately 4600 seconds. At that time, tellurium revolatilizes and is entrained in the gas flow. The residence time of the revolatilized tellurium in the upper plenum region is insufficient to result in significant chemisorption and therefore, the tellurium vapors continue flowing to the downstream volumes where the vapors are readily removed by chemisorption and condensation on structures and aerosols.

It is of interest to note that the principle removal means for both cesium iodide and cesium hydroxide is by vapor condensation on aerosols and their subsequent deposition. This is illustrated in Figure 18 which shows the mass of retained CsI. For both CsI and CsOH vapor condensation on structures plays only a minor role. In the case of cesium hydroxide, chemisorption did not play a significant role in its removal. Tellurium, however, shows significant removal by chemisorption (Figure 19). As indicated in Figure 20 the total CsI released to containment was about 0.8 Kg primarily in the form of particulate.

The results of this analysis indicate that for all fission product species, greater than 90% of the fission products released from the fuel during the core melt process remained in the primary system. The majority of the fission products remaining in the primary system were located in the upper plenum region of the reactor vessel with small quantities distributed throughout the remainder of the primary system. As will be seen in a subsequent section, following reactor vessel failure the fission products deposited on structures in the primary system will slowly heatup the structures and be revolatilized. The revolatilized fission products under certain conditions can be readily released through the opening in the lower reactor vessel head.

4.3.2 TMLB' (HPE) WITH NATURAL CONVECTION (TYPE B)

Figures 21 and 22 show the thermal response of the primary system during the TMLB' sequence when the effects of natural convection are included in the analysis. It is readily observed from the gas temperatures that the gases in the upper plenum and the hot-leg up to the surge line are quite well mixed because of the recirculating flows between volumes. Similarly the gases in the surge line and the pressurizer are also well mixed. When compared to Type A (Figure 13) discussed previously, it is seen that the gas temperatures in the primary system volumes are significantly higher than in the case where natural convection was neglected. This is due to the presence of recirculating flow between the upper plenum volume and the core itself, resulting in a continuous exchange of gases between the top of the core and the upper plenum region.

The heat structure temperatures calculated in this analysis are shown in Figure 22. These results indicate that the hot-leg temperature increases to a level at which loss of strength of the hot-leg piping would be expected. This level is approximately 1300^{o}F and it occurs at about 4400-4500 seconds, before the calculated time of lower reactor vessel head failure. The effect of a failure in the RCS before core slump could be to negate the high pressure ejection of core debris and the dispersal of significant fractions of the core into the upper containment regions.

Figure 23 shows the fission product energy in each primary system volume. It is seen that the fission products are somewhat more spread out through the primary system than in the case without natural convection. Figure 24 shows the cesium iodide retention factor. The retention factors for the volatile species are considerably lower than those calculated for the case without natural convection. The reason for this is that the natural convective flows increase the gas temperatures in the RCS, so that the primary means of removal of the volatile species is no longer through condensation on aerosols and subsequent deposition, but rather condensation on the structural walls, as seen in Figure 25. This is due to the inherent assumption in the MCT2 code that the aerosols exist at the carrier gas temperature. Because the temperatures are much higher in this case than in the case without natural convection, the volatiles no longer condense on the aerosols, but rather, condense on the heat structure walls since the structure walls are cooler than the gas. Due to the existing inter-volume flows, the residence time in a given volume is insufficient to allow significant condensation on heat structures. Eventually the heat structure temperatures increase sufficiently to completely terminate further vapor condensation. At the time of core slump, starting at approximately 4600 seconds, the majority of the volatile material that has not been deposited on the heat structures in the primary system is in vapor form rather than condensed onto gas-borne aerosol surfaces. The increased flow at core slump sweeps out the vapors from the primary system into the containment with a small portion of the vapors being trapped in the surge line and pressurizer regions. This small trapping accounts for the increase in the overall retention factor observed in Figure 24 at approximately 4700 seconds.

Figure 26 shows the accumulated mass of cesium iodide which was released to the containment during the TMLB sequence. During the early stages of the sequence up to approximately 4400 seconds, the primary form of the volatiles released to the containment was particulate, i.e. vapors condensed on aerosols. When compared to the corresponding figure in the previous case (Case A), the amounts released to the containment in particulate form appear to be considerably larger. This is due to the effect of the recirculating flows between the surge line and pressurizer which have the effect of reducing the deposition rate of the suspended aerosols which carry the condensed volatiles. At approximately 4400 seconds the flow rate of gases out of the core begins to increase significantly moving the vapors from the reactor vessel volumes through the surge line and pressurizer and out into the containment. This gas flow also sweeps the existing gas-borne aerosols out of the surge line and pressurizer. Therefore the arriving volatile vapors are primarily removed by the structural walls, as there are no gas-borne cool aerosols to provide large condensation surfaces. The removal process by condensation on the walls is slower than that by condensation onto aerosols and therefore a substantial portion of the vapors continue on through the pressurizer and out to the containment. It is only after the gas temperature in the pressurizer region falls at about 4700 seconds that condensation onto the aerosols takes place and an increase in the retention of volatiles by the pressurizer is observed.

The behavior of tellurium shown in Figure 27 does not differ significantly from the other volatiles. Once again, the high gas temperatures in the primary system result in tellurium existing as a vapor rather than condensed onto aerosol surfaces. Consequently the primary means of removal of tellurium is through chemisorption and the rate of removal depends on the residence times of tellurium in each primary system volume. At the time of increased gas flows out of the core, i.e. approximately 4400 seconds, the vaporized tellurium in the primary system is swept out into the containment as shown in Figure 28.

4.3.3 TMLB'(HPE) WITH LATE FISSION PRODUCT REEVOLUTION (TYPE C)

The results of the TMLB' analysis with no natural convection indicate that a great majority of the fission products released from the fuel matrix during the meltdown are retained in the primary system. Moreover, most of the retained material remains in the upper plenum region. Following the reactor vessel failure, these retained materials will heat up the structures on which they are deposited to a level at which revolatilization back into the gas phase will take place. The pressure rise due to heatup will induce a small flow out of the reactor vessel, but the primary mechanisms for removing reevolved fission products from the RCS are a gradual containment depressurization due to leakage, or a late containment failure. In order to estimate the amount of fission products that would be carried out during the long-term heatup of the reactor system, a simplified analysis was performed, one which examined the heatup rate of the gases and structures and calculated the revolatilization of the deposited fission products. A more detailed analysis, although possible with MCT2, was not performed due to resource constraints. The actual releases of reevolved volatiles was estimated from the reevolution rate calculated by MCT together with the leakage induced containment depressurization rate calculated by the CONTAIN code. Late reevolution was calculated only for the cases with containment leakage. Early gross containment failure depressurizes the containment before significant reevolution can occur. Primary system releases after containment failure are thought to be small because no effective mechanism exists for getting the reevolved fission products out of the primary system.

The thermal response of the primary system for Type "C" is shown in Figures 29 and 30. Vessel failure occurs at approximately 5000 seconds. After vessel failure, the heat structure temperatures begin to increase which causes the deposited materials to revolatilize. The upper plenum region contained the largest quantity of deposited material at the time of vessel failure, and therefore, that region is observed to heat up most rapidly. Figure 31 shows the cesium iodide retention factor and it is observed that at approximately 6000 seconds, the revolatilization of cesium iodide commences and by 8000 seconds, all of the deposited cesium iodide in the upper plenum has revolatilized. Because of the simplifying assumption of the long-term analysis, (that specified that the post vessel failure flow of gases continued in the same manner as the pre-vessel-failure flow, i.e. from upper plenum to the pressurizer), the revolatilized material is carried into the downstream volumes. In reality, this would not be the case and, in fact, the revolatilized material would be carried from the upper plenum back through the core region, out the breach in the lower vessel head and into the containment. Moreover, any revolatilized materials from the remainder of the primary system would not flow into the pressurizer but would flow out through the ruptured lower head of the reactor vessel. Therefore, for the purposes of estimating the release rate of volatiles from the primary system in the long-term following vessel failure, the rate of revolatilization was assumed to be the rate of the loss of retained mass, as extrapolated down to zero retention, as shown in Figure 32. Thus, since the majority of the retained material was located in the upper plenum region and the total mass retained is shown by the peak in Figures 32, the revolatilization rate can be obtained from these figures by calculating the rate at which the retained mass decreases. At the time the extrapolated curves intersect the abscissa, the volatiles initially present in the reactor system are completely in vapor form and available for release to containment. The rates of release of the revolatilized fission products from the RCS to the containment were based on the depressurization rate of the containment system.

The analysis of the revolatilization case did not account for natural convective flows because of resource constraints. Qualitatively, however, it is expected that convective flows would exist in the RCS because of the existing large thermal gradients. These flows would have the effect of carrying the vapors released in the upper plenum as a result of revolatilization into the cooler regions of the primary system where the vapors could recondense. The location of the break in the lower vessel head together with the gradual leakage induced containment depressurization would lead to bulk flow in the opposite direction to natural convective flows and would tend to limit upward relocation of fission products. The net effect of accounting for natural circulation flows in the long term analysis would be to somewhat extend the time during which the revolatilized fission products would be released to the containment atmosphere and reduce the rate at which these releases take place.

Since the heat generated by radioactive decay accounts for only about 10% of the heat absorbed by the structures during the meltdown phase of the accident, retention of fission products in the primary system prior to reactor vessel failure does not depend significantly on the inclusion of fission product heating in the calculation. However, the effect of fission product heating becomes very important after vessel failure when extensive revolatilization takes place solely as a result of fission product heating of structures. This can have a marked effect on the source term if this revolatilization takes place in conjunction with a containment undergoing depressurization or if containment depressurization occurs shortly after the revolatilization in the primary system. Moreover, the calculations show that the inclusion of the natural convection phenomena plays a significant role in the retention capability of the primary system. The net effect of the natural convection phenomenon is to increase the primary system gas temperatures and, thus, structure temperatures which causes a reduced rate of fission product removal from the gas stream. This is primarily due to the inability of the volatiles to condense onto the aerosol surfaces, that are at the gas temperature. Since the aerosol area to volume ratio is much larger than the structural area to volume ratio, the removal rate of volatiles is markedly reduced since the only mechanism of volatile removal other than chemisorption is through condensation on structural walls. In addition, at the time of core collapse, a large gas flow is induced through the primary system which sweeps the vapors out into the containment. This occurs at such a rate that the residence times of the vapors, as they pass through the cooler volumes on their way out to the containment, are insufficient to result in any significant removal of these vapors from the gas stream. The net effect is a considerably reduced retention of volatile fission products in the primary system.

Table 8 summarizes the primary system releases compared to those calculated for a TMLB' sequence in the Zion plant as reported in the BMI-2104 study[6]. It was stated previously and should be reiterated here that the selection of the BMI-2104 Zion plant calculations for purposes of comparison with the present results was somewhat arbitrary. In terms of primary system releases, the Surry or Sequoyah BMI-2104 results could equally well have been used, since both are PWR plants. The primary system releases calculated in the BMI-2104 study were significantly higher for Surry and Sequoyah than for Zion and the differences are not entirely clear. Because of the differences in RCS releases between these three plants, the comparisons made between the present results for Bellefonte and the results for the BMI-2104 Zion plant should not be viewed as being particularly significant. The important conclusions emerging from this study are related to the relative effects on the RCS releases due to the incorporation of new phenomenological models in the primary system fission product transport code package.

For the meltdown phase without natural convection the MCT code predicted CsI and CsOH releases are only slightly higher than the BMI-2104 releases (factor of 1.5). Tellurium releases are higher by a factor of 6. The MARCH code modeling for the melt-progression phase and in particular, the clad oxidation parameters, strongly affect the release of tellurium from the fuel. Consequently the high primary system Te releases are partly due to melt phase fuel releases that are more than twice as large as those in the BMI-2104 Zion analysis.

The net effect on the releases of volatiles up to the time of vessel failure due to the modeling of fission product heatup is seen to be relatively insignificant. There is not sufficient time before vessel failure for the fission products to heat up the primary system heat structures to the extent that would allow reevolution of volatiles in that time frame. Fission product heating as it affects the reevolution of volatiles subsequent to vessel failure is, however, seen to be quite significant. Ultimate releases of CsI and CsOH in the reevolution phase are nearly an order of magnitude high than what was released in the core meltdown phase. Total releases, including pre and post vessel failure releases are a factor of 10 higher than BMI-2104 estimates for Zion.

The present analysis which represents an initial attempt at estimating the effects of natural convection on the melt-phase releases indicates that these may be higher by a factor of 10 for CsI and CsOH. Assuming that the reevolution phase with natural convection produces reevolved releases similar to those shown in Table 8 for reevolution without natural convection, the total releases of CsI and CsOH could well be in excess of 50% of the initial inventory of these species for this accident sequences.

It should be reiterated here that the natural circulation model is quite simplistic and represents an early attempt at treating natural convective processes. The TRAP/MELT code employs lumped parameter modeling throughout the code and would have required massive alterations in order to incorporate the 2 or 3 dimensions which would be necessary to treat natural convection in a completely rigorous manner. The present approach, which does have some precedence in the literature [19,20], employs the Bernoulli equation (ideal flow assumption) together with a buoyancy term to calculate the natural convection flows between adjoining control volumes and appears to somewhat overpredict natural convective processes.

The particle size distribution of the aerosols emerging from the primary system varied only slightly through the accident. The initial aerosol releases came out of the system at about 1.5 microns increasing quickly to about 3.5 microns within the first 300 seconds and then gradually to about 5.5 microns after the release levels became significant. The preponderant fraction of the aerosols, however, were released in the 5.5 micron range (see Table 9) with a standard deviation of about 3 microns.

4.4 CONTAINMENT AEROSOL TRANSPORT AND RELEASES

The thermohydraulic sources from the various codes used, the radiological sources from the primary system releases, direct heating releases, and core/concrete interaction releases were all input to the CONTAIN code. The CONTAIN code was used to calculate the transport and retention of aerosols and fission products in the containment system and to estimate the radiological releases to the environment.

Except for one multiple-volume case, the CONTAIN code analysis of the TMLB' high pressure sequences was performed using a single containment volume connected to a very large "receiver" volume representing the environment. The "receiver" volume was necessary for accumulating the various fission products that were released from the containment either by leakage or by gross containment failure.

The CONTAIN code models aerosol particle size distributions through a user specified number of discrete particle size groups or "bins". The input requires the mass median particle size together with the geometric standard deviation of the particle size distribution for each aerosol species. From this information the code sets up the group particle size ranges and the total masses of aerosols in each size group. For the single volume cases the aerosol size distribution was characterized using 20 particle size groups. The particle size distributions are given in section 4.2 and 4.3.

4.4.1 SINGLE VOLUME CALCULATIONS

A matrix consisting of 15 cases was analyzed for the high pressure ejection scenario. The case matrix is described in section 4.0 (See Table 1). The matrix of cases utilized to assess containment releases for this accident sequence employs combinations of assumptions, parameters, and modeling capabilities applied across the entire set of codes and calculations used in this analysis for the various thermohydraulic and radiological source terms. Direct heating parameters, containment failure mode assumptions and primary system release modeling parameters are combined in such a way as to cover a reasonable range of possible source terms.

Table 5 shows the constituents of each of the fission product groups and their initial total core inventories. Table 10 is a summary table that gives the integrated fission product releases to the environment at 20 hours for each of the fission product groups for the cases in the high pressure ejection matrix. Case-000 represents the most optimistic set of assumptions for the high pressure ejection scenario. This case combines BMI-2104 primary system releases with no ejection of core debris into the containment atmosphere (no direct heating component) and a very small (1 in^2) induced containment leakage. The maximum airborne masses of CsI and CsOH for this case were about

1.4 lbs and 9 lbs and the releases from containment were about 4 x 10^{-2} lbs and 4.4 x 10^{-3} lbs at 20 hours, respectively. These are extremely small releases. The releases from the tellurium, strontium and lanthanum groups result primarily from core/concrete interactions that commence at about 8 hours into the accident sequence when the cavity water was boiled away.

The effect of leakage area on containment releases for this scenario can be seen by comparing Cases-000 and 100 in Table 10. These cases are identical except for the leakage area which is 2.4 times larger in Case-100. As expected, the releases are approximately a factor of 2 larger for Case-100.

The most pessimistic case in the matrix is Case-011B. This case includes a 90% injection of core debris into the containment atmosphere which results in gross containment failure (7 ft^2 hole). The primary system release calculations for this case included a model for natural convection that contributed to quite high releases of volatiles into containment. These are the type "B" releases (see Section 4.3.2). Comparison of the airborne CsI mass (Figure 33) to the mass of CsI leaked to the environment (Figure 34) reveals that a large fraction (about 2/3) of the aerosols released into the containment during the meltdown and vessel failure phases are released into the environment. Table 10 shows that the total releases of the volatiles CsI, CsOH, and Te at 20 hours to be 16%, 12% and 21% respectively. Containment failure coincident with direct heating which was assumed to generate high concentrations of Te, Ru, and Mo aerosols leads to very high releases in these groups. The Ru group, for example, which contains both Ru and Mo has a 41% release fraction for this case.

There are several comparisons that can be made across the set of 90% high pressure injection cases (Cases-001 through 011B in Table 10). Comparing cases that used BMI-2104 Zion RCS releases with those calculated from the MCT code without natural circulation (type "A" release) reveals essentially no differences in the CsI and CsOH releases. The tellurium releases are about twice as large in the MCT prediction due primarily to a difference in the quantity of Te released from the fuel. The ruthenium group releases are about the same because both are dominated by the assumed direct heating releases rather than the RCS releases. The MCT code apparently predicts somewhat lower releases from the strontium group and about the same releases in the lanthanum group. The major differences for the 90% high pressure injection cases results from the use of the MCT Type "B" RCS releases. These are the RCS releases obtained from using the natural convection models in MCT. A comparison between Case-001A and 011B reveals that the CsI and CsOH releases from containment using type "B" RCS release are a factor of 10 larger than those using the BMI-2104 Zion RCS releases. Again, the Te and Ru groups are similar, because, these are dominated by the direct heating releases rather than the RCS releases.

The 50% debris injection direct heating scenario is probably best represented by Case-012A or Case-112A. The difference between the two cases was the size of the induced containment leak area. These cases involve a 50% injection of core debris into the containment atmosphere, which induces a containment leakage (5 in^2 and 12 in^2) rather than a catastrophic failure of containment. The primary system releases for these cases consists of type "A" releases during the core melt down phase (without natural circulation) and type "C" releases for late reevolution of volatile fission products (see Section 4.3).

Because the leak area for Case-012A was relatively small (5 in^2) compared to containment failure scenarios, the containment depressurized rather gradually with adequate time in the containment system for aerosol removal mechanism to have an effect. The total releases of the volatiles CsI, CsOH and Te as well as the ruthenium group at 20 hours were about 1% of the initial inventories for this case. The ultimate releases would have been somewhat higher since, as the graph of leaked CsI (Figure 35) indicates, the release rates had not yet leveled out at 20 hours.

Comparisons made between the various 50% injection cases show very strong enhancement in containment releases due to the reevolution of fission products in the RCS. A comparison of Cases-002A and 012A, for example, shows CsI and CsOH releases to be a factor of 13 or 14 higher with reevolved RCS releases than with the BMI-2104 Zion RCS releases.

A rather surprising result is seen in comparing Cases-112 and 112A. The only differences between these two cases is that Case 112A assumes that the water in the reactor cavity at the time of vessel failure was swept out with the core debris and completely vaporized in the direct heating event, while in Case 112 it is assumed not to participate. A comparison of the CsI and CsOH containment releases for these two cases shows that the case with the additional steam component due to the inclusion of the cavity water (Case-112A) has releases of these volatiles that is higher by a factor of about 1.7. There are two competing effects that explain the results. The additional water in the atmosphere would tend to condense on the aerosols and more readily "wash" them out of the atmosphere. However, the condensation of the additional steam on structures in the containment reduces the containment pressure more rapidly in Case-112A than in Case-112. Also, the containment pressure was higher in Case-112 because the water was not swept out of the cavity and remained as a steam source as it was heated by the debris remaining in the cavity. The more rapid depressurization for Case-112A results in about twice the quantity of revolatilized fission products being released from the RCS. Apparently, the large additional release of revolatilized fission products dominates over aerosol removal by condensation resulting in higher releases for Case-112A.

The particle size distribution of the aerosols which were leaked to the environment for Cases-011B and 012A are compared in Figure 36. The abscissa on this plot represents the fraction of the total mass of aerosols that are in that particle size interval bounded halfway between adjoining points. The effects of aging of the aerosols is clearly illustrated in this figure. The aerosols that were released from containment at the time of containment failure (Case-011B) show the distinct bimodal distribution characteristic of direct heating releases. The aerosols in Case-012A have been released gradually over a 20 hour period and display a size distribution that indicates aerosol aging. The quantity of aerosols in the lower size bins are now a somewhat higher fraction of the total as they are removed by settling less rapidly than larger particles. The larger size particles in the distribution have been depleted for the same reason, and agglomeration has shifted the peak in the size distribution to the right. The bimodal distribution is barely noticeable in the aged aerosols for this case.

The disposition of aerosols between the atmosphere, the various surfaces within the containment and the quantity leaked to the environment is illustrated in Figure 37 and 38. The large fraction of aerosols ejected out of the containment due to the direct heating induced failure is evident in Figure 37 which shows results for Case-011B. The fraction of material ejected from the containment amounts to about 63% immediately after direct heating with the remainder being settled out on the floor (27%) or plated out on the walls (10%). The leakage scenario represented by Case-012A demonstrated a much different disposition of aerosols. In this case (Figure 38), only a very small fraction of the aerosols were leaked from the containment, about 2%, with the largest fraction ending up on the containment floor (72%) and the remainder (26%) was deposited on the vertical walls.

4.4.2 MULTI-VOLUME CALCULATIONS

The calculations that have been presented to this point were performed using a single-cell representation of the Bellefonte containment system. In order to achieve an estimate of the attenuation of fission product releases due to a more realistic representation of the the actual containment configuration, a multi-cell calculation was performed for Case-012A. In this calculation the containment was sectioned into 7 physical volumes with associated flow paths (see Figure 39) The main physical boundaries were chosen according to floor levels within the containment. The volumes for the calculations as numbered in Figure 39 were:

1. Reactor Cavity
2. Steam Generator/Pressurizer Compartment
3. Steam Generator Compartment
4. Lower Level Rooms
5. Mid-Level Rooms
6. Upper Level Rooms
7. Containment Dome.

The Case-012A accident scenario has a complex sequence of hydraulic and aerosol sources which can be broken down into early and late sources. The volumes into which the sources were released were as follows:

Hydraulic Sources---

Reactor Cavity (vessel failure {early}, concrete interaction {late})

Lower Level Rooms (pressure relief valve {early})

Dome (concrete floor degassing due to injected core debris {early and late})

Aerosol Sources---

Reactor Cavity (vessel failure {early})

Lower Level Rooms (pressure relief valves{early})

Containment Dome (direct heating aerosols {early}).

Results from the calculations which compare single and multi-cell leaked masses are given in Table 11. The two multi-cell calculations show a comparison of results with and without natural circulation included in the inter-cell gas flows. The numbers shown in Table 11 are the ratio of the multi-cell releases to the corresponding single-cell releases. These results indicate that the differences between the single and multi-cell releases are minor for this scenario. The main differences that have been observed in previous studies(4) which compared multi-cell to single-cell calculations were the result of different aerosol agglomeration rates that can occur when aerosol concentrations within volumes are significantly disparate. A less pronounced effect is the additional wall and floor deposition which occurs in the multi-cell calculations as fission products are transported through the various cells on their way to the dome region. In the present case the latter effect is dominant. The main source of additional aerosol concentration is sourced directly into the dome in order to approximate a direct heating event. This assumption is consistent with the argument which supports transport of ejected debris by particle inertia rather than gas entrainment.

It should be noted that the magnitude of the effective attenuation factor obtained in the calculations by nodalizing the containment volume is highly sequence dependent. The direct heating event in this particular sequence forced most of the aerosol mass into the upper containment volume, so that no significant differences were seen in any of the aerosol releases. In fact, the multi-cell treatment produced somewhat enhanced releases from the fission product groups most heavily concentrated in the direct heating releases (Ru, La). The fission product groups that were released primarily in lower containment volumes (CsI, CsOH, Te) did , as expected, see some attenuation in their releases (about 10%). In general, therefore, the attenuation factors shown in Table 11 may be applied to the 50% direct heating cases, but should probably not be applied to either the non direct heating or the 90% direct heating scenarios.

5.0 TMLB' PUMP SEAL LOCA

Although this accident sequence was intended to treat the situation in which the seals in the main coolant pumps were induced to fail due to the loss of coolant flow, the only available thermohydraulic analysis for this sequence was performed with the pump seals failed at the outset of the accident. At present there is no information available from which to estimate the mode of pump seal failure or the time required to induce failure under accident conditions. In the absence of the necessary information, and of a RELAP5 calculation that incorporated a lag time for seal failure, the present calculation assumes that the seals fail immediately. In the strictest sense, then, the sequence analyzed here is not actually an induced pump seal LOCA.

The break size, assuming the failure of all four pump seals, is less than 2 in^2 so that this sequence is similar to an S_2D with loss of all primary system makeup and cooling as well as a failure of containment sprays and coolers.

The pump seal LOCA sequence was analyzed assuming that a direct heating event did not occur. The primary system pressure at the time of vessel failure was about 750 psi lower than in the high pressure ejection cases, but there is no reason to believe that an ejection of core debris could not occur with the RCS at 1700 psia. Core debris ejection at the lower pressure would be less severe and probably involve smaller fractions of the core. This being the case, and since direct heating has already been examined in some detail for the high pressure scenario, the pump seal LOCA sequence was analyzed assuming direct heating did not occur.

The assumption has been made in this analysis that as long as there is water in the reactor cavity the debris is coolable and does not attack the concrete basemat. In terms of thermohydraulic loading on containment this is probably a conservative assumption. In terms of radiological sources the assumption delayed the onset of core concrete reactions and the radiological sources arising from that reaction. However, the effect may not be significant, since releases into the containment from core/concrete interactions are inhibited by the scrubbing effect of the overlying water layer.

The sequence of events for the TMLB' Pump Seal LOCA scenario is shown in Table 12 and involves steam generator dryout at 4.5 minutes followed by core uncovery at 26.7 minutes. Incipient core melting commences at about 43.6 minutes with core slump taking place at 60.5 minutes and vessel head failure at 68.6 minutes. Containment leakage was assumed to be induced at the time of vessel breach. The reactor cavity dried out at 455 minutes at which time a core/concrete interaction ensued. Table 13 shows the matrix of cases analyzed for the pump seal LOCA. The main parameters that were varied in this sequence were the size of the containment leak area and the presence or absence of the natural convection heat transfer mode in the RCS fission product transport code calculations. There were no comparable BMI-2104 analysis with which to compare results, and therefore, no calculations were done using BMI-2104 RCS releases.

In the absence of an estimate for leakage in the Bellefonte plant, the leakage curve developed by the Containment Performance Working Group(15) for the Zion plant was used. This curve yielded a leak area of about 1 in^2 at 65 psia which is the containment pressure at vessel failure. The parametric leakage area that was used was arbitrary. Areas of 1 in^2 and 2.4 in^2 were assumed to open at the time of vessel failure and to remain constant thereafter.

5.1 CONTAINMENT LOADING

In the absence of direct heating in this sequence the peak loading was less severe than was calculated in the high pressure ejection cases. The containment pressure and temperature responses for a typical case in the matrix (Case-030) is shown in Figure 40 and 41. Figure 40 shows that the peak pressure occurred at about 5 hours when the water in the reactor cavity had boiled off. The smaller leak area cases (Case-030 and 031), as expected, showed slightly higher pressures (3%). The peak pressures varied between about 65 and 72 psia for the four cases. The cases which incorporated natural convection in the RCS (Cases-031 and 131) showed pressures that were elevated by about 8%. The higher pressures were due to the additional fission product heating of the atmosphere. This is reflected in the containment atmospheric temperatures (Figure 41) which were also slightly elevated for the cases with enhanced RCS releases.

Although the pool of water in the reactor cavity was boiled off by about 5 hours, overflow from the containment sump kept refluxed coolant entering the reactor cavity until about 450 minutes. This water did not accumulate but was revaporized upon contact with the debris. Core/concrete interaction commenced at about 450 minutes and hydrogen began to accumulate in the containment atmosphere. A hydrogen burn did not occur within the 20 hours to which the cases were run, but the hydrogen concentration at 20 hours was about 7.9% mole fraction and a burn would likely have occurred before 24 hours. The magnitude of the burn would have been similar to the one that occurred in Case-000 and would have yielded a pressure spike on the order of 100 psia, assuming it was initiated at 8% hydrogen concentration.

5.2 PRIMARY SYSTEM RADIOLOGICAL RELEASES

Two configurations were analyzed for the TMLB' induced pump seal LOCA sequence using the MCT code package. The analysis was performed both with and without implementation of the natural convection models in MCT. Since this sequence has higher flowrates through the primary system than the TMLB' high pressure case, natural convection has somewhat less of a role in heating the primary system. Nevertheless, the combination of higher primary system temperatures associated with natural convection together with the quantity of flow through the system due to the break, yields a striking increase in primary system releases.

Figure 42 describes the primary system flow path for this sequence. The Bellefonte primary coolant system is a B&W design that has a set of 8 vent valves which allow flow from the outlet plenum back into the inlet plenum. These valves were designed to prevent "steam binding" and assure that ECCS flow can be injected into the vessel during small break LOCAs. The RELAP5 calculations that were performed for this sequence indicated that the loop seals did not clear so that the primary flow path was from the core into the upper plenum, to the outlet plenum, through the vent valves, to the inlet plenum, the cold leg piping, the main coolant pumps, and out the failed pump seals.

Figure 43 shows the core exit gas flow history for the Pump Seal LOCA case. This gas flow rate history was used for both variations of the Pump Seal LOCA sequence described below. The first analysis, discussed below, was performed without modeling natural convection in the RCS (Type A). The second pump seal LOCA analysis was performed for the case which includes the effects of natural convection (Type B). The core exit gas flow during the pump seal LOCA indicates that throughout the core melting process there will be substantial gas flows out of the core until core collapse at approximately 3600 seconds. At that time a large gas flow swept the primary system vapors out into the containment.

5.2.1 PUMP SEAL LOCA ANALYSIS WITHOUT NATURAL CONVECTION (TYPE "A")

Figure 44 shows the temperature response of the primary system for the Pump Seal LOCA when natural convection was not modeled. The hottest structure is in the upper plenum as shown in Figure 44, and reaches a peak temperature of just over $1600^{o}F$ at approximately 3600 seconds. At that time the large gas flow out of the core, which results from core collapse and consists primarily of saturated steam, cools the upper plenum region. The steam flow resulting from core slump accounts for the rapid turnaround in the upper plenum temperature. The structures downstream from the upper plenum remain relatively cool throughout the sequence and thus substantial retention of volatile species throughout the primary system would be expected. Figure 45 shows the fission product heat in each volume of the primary system. The sweeping effect of the large gas flow at core slump occurs at approximately 3600 seconds when a substantial drop in the fission product heat in the upper plenum is observed.

Figure 46 shows the cesium iodide retention factor. The behavior of CsOH was similar. As expected, the fission product retention in the primary system is very high. This is due to the relatively cool temperatures prevailing throughout the accident sequence. Because of the almost continuous flow of gases from the top of the core into the remainder of the primary system, cesium iodide and cesium hydroxide are spread out throughout the primary system with most of the retention occurring in the upper plenum.

Figure 47 shows the behavior of tellurium in the primary system. The turnaround in the upper plenum retention is due to the heating up of the upper plenum structures. The revolatilized tellurium is carried by the gas flow into the downstream volumes where it is readily chemisorbed. Because this revolatilization takes place late in the accident, tellurium is released to the containment in appreciable amounts commencing at approximately 3600 seconds, the core collapse time, as shown in Figure 48. Prior to that, the tellurium release rate was very small as it was readily removed from the gas stream by chemisoption and condensation on structures. The releases to containment of CsI is shown in Figure 49. Like tellurium, CsI was released to the containment throughout the accident sequence at a slow rate until core collapse at 3600 seconds. At that time, the releases to containment increase rapidly as the residence times in the primary system volumes are insufficient to remove the fission products from the gas flow stream. Note that CsI releases to containment are primarily in particulate form (i.e., vapors condensed onto aerosol surfaces which have not yet been deposited). At 3600 seconds, these aerosols, primarily from the upper plenum region, are entrained in the rapid gas flow and swept out into the containment.

The results of the Pump Seal LOCA analysis without natural convection indicate that a large fraction, in excess of 90%, of the fission products released from the fuel during the meltdown process will remain in the primary system after the calculated vessel failure. These remaining fission products, as in the case of the TMLB' sequence, will continue to heat the primary system surfaces on which they are deposited, and eventually the temperature of these surfaces will increase sufficiently to cause revolatilization. Once in vapor form these fission products may be moved from the primary system into the containment through the large opening in the bottom of the reactor vessel.

5.2.2 PUMP SEAL LOCA ANALYSIS WITH NATURAL CONVECTION (TYPE "B")

This section discusses the results of the analysis performed for the pump seal LOCA case in which natural convection is modeled. The results of the thermal analysis are shown on Figures 50 and 51. As in the case of the TMLB' sequence, the effect of modeling natural circulation is to increase the gas temperatures throughout the primary system which in turn increases the heat structure temperatures and affects the retention of fission products. In addition, the increased gas temperatures throughout the primary system result in an increase in the aerosol temperatures which in turn rapidly decrease the condensation of volatiles onto aerosols. The end effect as discussed in conjunction with the TMLB' sequence is that the volatile species, cesium iodide and cesium hydroxide, exist in vapor form rather than condensed on the surfaces of aerosols. This, combined with the continuous gas flow throughout the primary system into the containment, results in a small retention of volatile species in the primary system.

Figure 52 shows the retention factor for cesium iodide. During the early stages of the accident, up to about 3200 seconds, the volatiles are removed from the gas flow stream primarily by means of condensation on structural surfaces. This is because the aerosol temperatures are too high to allow significant condensation to occur onto their surfaces. At about 3200 seconds, the structure temperatures reach a level at which revolatilization of the condensed materials in the upper plenum takes place and the revolatilized vapors are quickly moved into the downstream volumes where they condense. Eventually, at approximately 3500 seconds, the temperature in the cold legs and the main coolant pumps increase sufficiently to revolatilize the material condensed in those volumes and combined with the large gas flow occurring at 3600 seconds, the reevolved vapors are swept into the containment. From Figure 52, it is seen that essentially all of the retention of cesium iodide at the time of reactor vessel failure, is in the cold leg inlet plenum and it amounts to less than 10%. Cesium hydroxide behavior is similar except that chemisorption plays an additional role in retaining some of the revolatilized cesium hydroxide and, therefore, the final retention of cesium hydroxide is somewhat higher, approximately 25%. The behavior of tellurium, shown in Figures 53 and 54, is due almost entirely to chemisorption. Because of the substantial gas flow through the primary system and the high temperatures in the upper plenum and outlet plenum, essentially no tellurium was retained there. The cold-leg inlet plenum and the cold-leg piping retained most of the tellurium with a small fraction retained in the main coolant pumps. From approximately 3600 seconds until vessel failure there is a large flow of gases throughout the primary system which carries the remainder of the released tellurium from the fuel matrix through the primary system at such rate that the residence time of tellurium in any given volume is insufficient for significant removal.

The difference between the pump seal LOCA case without natural convection and this case is due to the increased gas temperatures in the primary system combined with the relatively large gas flow rates through the primary system into the containment. The increased gas temperature has the effect of keeping the volatile species in vapor form whereas the significant gas flow rates have the effect of carrying these vapors through the primary system at a rate which results in a short residence time in the primary system and, thus, results in low removal rates by condensation or chemisorption. In addition, the high gas temperatures increase the heat structure temperatures to a level at which the condensed volatiles reevolve back into vapor form and are carried out of the primary system into the containment. The main difference between the first and the second case (type "A" verses type "B" releases) is a drastic decrease in the retention of both cesium iodide and cesium hydroxide by the primary system. This difference was not as noticeable in the TMLB' cases because for most of the sequence duration, the gas flow rates through the primary system and into the containment were quite low. In both, the second TMLB' case and the second pump seal LOCA case the primary form of the volatiles was the vapor form. Because in the TMLB' case the gas flow rates were so much lower than in the pump seal LOCA case, the residence times in the TMLB' case were considerably longer and therefore condensation and chemisorption of volatiles was more significant in removing these species from the gas stream. In the pump seal LOCA case, as stated before, the gas flow rates were large and, therefore, resulted in insufficient residence times in the primary system volumes to allow significant removal of the volatiles fission products from the gas stream by condensation and chemisorption.

A summary of the primary system releases of the volatile fission products for the pump seal LOCA sequences is presented in Table 14. The Type A releases (without natural circulation) are on the order of 7 to 8% of initial inventories for CsI and CsOH with CsOH releases slightly less than that for CsI due to the small contribution of chemisorption for the former. Tellurium Type "A" releases were about 9% of inventory. The Type "B" releases as discussed already were markedly high for CsI and CsOH, 93% and 77% respectively, primarily due to the much higher RCS temperatures and relatively constant gas flows that tended to sweep these materials into the containment. Due to a high removal rate by chemisorption the primary system releases of tellurium were only about 50% greater (13%) than for the Type "A" releases.

5.3 CONTAINMENT AEROSOL TRANSPORT AND RELEASES

The same procedure that was used for analyzing the fission product transport, deposition, and release from containment for the TMLB' high pressure sequences was also employed for the pump seal LOCA sequences (see Section 4.4). The case matrix, Table 13, consists of four cases with the parameters being the primary system releases (Type "A" or "B", Table 14) and the magnitude of the assumed containment leak areas, 1 in^2 and 2.4 in^2.

Case-030 as indicated in Table 13 utilizes the MCT calculated Type 'A' primary system releases together with a 1 in^2 leak area in the containment boundary. The mean particle size for the MCT calculated RCS releases was about 5 microns and these relatively large aerosol particles do not remain in the atmosphere for long periods. This is clearly seen in Figure 55. The peak mass of CsI in the containment was about 4.5 lbs, but was quickly removed primarily by settling within an hour, and the accumulated releases to the environment at 20 hours amounted to only about .004 lb. (Figure 56). The release of tellurium from the primary system was quite small for this case reaching only about 5 lbs in containment. Releases from the core/concrete interaction which commenced at about 8 hours produced significantly larger Te aerosol concentrations in containment and a total release to the environment of about 0.24 lbs.

The Type "B" RCS releases for CsI and CsOH were an order of magnitude greater than the Type "A" releases and this fact is clearly distinguished in the graphs of airborne concentration for these species, Figures 57 and 58 (Case-031). The containment releases also reflect the high releases from RCS, being about .06 lbs at 20 hours for CsI. Type 'B' Te releases from the primary system were not significantly different from Type "A" releases, and in any case the core/concrete interaction releases of Te tended to swamp the RCS releases with the result that the containment releases for Te were not significantly changed from Case-030.

The effects of a larger leak area, as expected, showed an increase in the quantity of fission products released to the environment. Figure 59 shows the CsI concentration for Case-131 which incorporates Type "B" releases along with a larger leak area (2.4 in^2) and, therefore, represents the worst case (considered here) for the pump seal LOCA sequence. The releases of volatiles for this case are a factor of about 2.4 times greater than for the 1 in^2 leak area case. Thus, for these small leak areas the total releases appear to be nearly proportional to the leak area.

A summary of the containment releases for all the cases in the pump seal LOCA matrix is given in Table 15. In general, for the same RCS release type ("A" or "B") the containment leakage for each fission product group was nearly proportional to the leak area. The CsI and CsOH containment releases for the two RCS release types were, of course, in nearly the same ratio (factor of 10) as the RCS releases. The tellurium releases which were dominated by core/concrete releases were essentially the same, while rutherium releases were higher for the Type "B" by about 70%. The Sr and La groups, as expected, remained unchanged between the two RCS release types as their RCS releases are governed by their release from the fuel matrix and not by their transport through the primary system.

An absence of a mechanism for early containment failure or for larger induced leakage areas early in the accident makes the containment releases for the pump seal LOCA quite small compared to those for the direct heating scenario. The releases are, in fact, similar to those of Cases-000 and 100 in the TMLB' high pressure scenario which were assumed not to have direct heating. It should be recalled, however, that the primary system pressure at vessel failure as calculated by MARCH was about 1700 psia for the Pump Seal LOCA. This pressure is probably high enough to induce direct heating with the result that this sequence could have results very much like some of the TMLB' high pressure cases discussed in section 4.0.

6.0 CONCLUSIONS

A number of conclusions can be drawn from the results of this analysis. A principal conclusion is that even for large, dry containments, direct heating probably represents one of the most severe threats to containment integrity, and, since it has the potential for failing the containment early and at a time when fission product concentrations are at or near maximum levels, it probably also represents one of the most severe radiological releases to the environment. The magnitude of the threat presented by direct heating may require the generation of a set of operator action guidelines in an attempt to mitigate the problem. Possible operator action might include a timely depressurization of the primary systems before core slump. There is probably a small window between the time at which it becomes apparent that core meltdown cannot be prevented and the time at which RCS venting must commence in order to prevent direct heating. Since a critical decision which has to be made during a short period of time would require very accurate knowledge of conditions in the RCS and particularly in the core, such a decision capability may require additional in-core instrumentation. It is not within the scope of this report to make recommendations regarding strategies for preventing direct containment heating, but there are some points that can be made without recourse to detailed studies. Clearly, the information regarding water level, core temperatures, and vessel pressure that are available during normal operation are even more critical during accident conditions. An obvious strategy for obtaining critical parameters during severe accidents is to "harden" the existing instrumentation systems by extending their range into the severe accident regime as, for example, employing thermocouple that function and are reliable at higher temperatures. Locating temperature measurements in the core in such a manner as to yield information about the extent of core damage would also be advantageous. Finally, the addition of a manual depressurization system to PWRs in general could be considered.

Calculated estimates of the primary system temperature history using the MCT code package indicate that primary system temperatures are well into the regime in which failure would be expected to occur at the elevated pressures characteristic of the TMLB' sequence (refer to Figure 22). If a failure of the RCS boundary occurred of sufficient magnitude to depressurize the RCS in advance of core slump, direct heating could be eliminated or mitigated. A preliminary evaluation of the natural circulation model has indicated that it is overpredicting the transfer of heat from the core to the downstream volumes in the RCS. It is uncertain whether a more realistic heat transfer rate would significantly change the primary system heatup characteristics. It is likely, however, that the RCS heatup would be somewhat slower, delaying the time at which failure might occur and, thus, limiting the mitigating effect it would have on the direct heating pulse. The effect of natural circulation flows in cooling the core, which has been neglected in this analysis, will tend to delay core slump and supply some additional time for RCS failure to occur before core slump. Taken together, the results of this analysis seem to suggest a high probability for a breach in the RCS before core slump and, thus, a low probability for the direct heating sequence of events. Several recent analyses [21, 22, 23] using multi-dimensional codes also tend to substantiate this conclusion.

In terms of primary system releases, the incorporation of models for natural convection between control volume in the RCS and post-vessel-failure fission product heatup and reevolution of volatiles has suggested that the releases of these materials from the primary system could be significantly higher than has been estimated in previous analyses. There are competing factors operating which affect the calculated transport of fission products through and out of the RCS. The previously mentioned overprediction of natural convection heat and mass transfer in the RCS tends to move fission products through the system more rapidly than they would actually be moved, while the underpredicted heat structure surface temperatures associated with the lumped parameter models tend to move materials through the system more slowly than they actually would be moved. These effects would obviously tend to counteract each other. In any event, there is considerable range for improving the models in the existing analytical tools.

The magnitude of the releases to the environment clearly depends very strongly on the size of the pathway leading to the environment. For direct heating events involving more than about 50% of the core debris there exists a high probability of an induced gross failure of the containment boundary. For direct heating that does not result in gross containment failure but which induces leakage pathways,* it is presently not possible to predict the magnitude of the leakage as a function of the magnitude of the containment loading. The work that has been conducted to date to estimate containment leakage rates have involved the situation in which there is a gradual increase in containment loading conditions and have not addressed the situation in which the loading is of a pulsed nature as is the case in the direct heating or hydrogen burn situation. Additional work may be required in this area in order to characterize induced leakage resulting from pulsed loading.

REFERENCES

1. A. M. Kolaczkowski, et al., Interim Report on Accident Sequence Likelihood Reassessment, SAI Report, Aug 1983.

2. J. E. Brockman, W. W. Tarbell, "Aerosol Source Term in High Pressure Melt Ejection," Nuclear Science and Engineering, V. 88, pp. 342-356, 1984.

3. M. Pilch, W. W. Tarbell, J. E. Brockman, Influence of Reactor Geometry On The Behavior of Dispersed Debris, SAND-1725C, The 13th Water Reactor Safety Meeting, Gaithersburg, MD, Oct 1984.

4. R. J. Lipinski, et al., Uncertainty in Radionuclide Release Under Specific LWR Accident Conditions, SAND84-0410, V. 2, Feb 1985.

5. P. P. Bieniarz, Source Term Analysis of Fitzpatrick Power Plant, Risk Management Associates, Albuquerque, NM, Report Under Review, Jan 1986.

6. J. A. Gieseke, et al., Radionuclide Release Under Specific LWR Accident Conditions-PWR-Large, Dry Containment design (Zion Plant), BMI-2104, V. 6, Battelle Columbus Laboratories, July 1984.

7. C. A. Dobbe, R. Chambers, Analysis of a Station Blackout Transient for the Bellefonte Pressurized Water Reactor, EGG-NTP-6704, Idaho National Engineering Laboratories, Oct 1984.

8. R. J. Dallman, Transmittal of Bellefonte TMLB' Calculations with Pump Seal Leakage, Letter of Transmittal-RJDS-12-85, EG&G, Idaho National Engineering Laboratories, May 20, 1985.

9. C. J. Shaffer, Marcon2.OP: A Version of MARCH With State-of-the-Art Core Concrete Modeling, NUREG/CR4-5779, Sandia National Laboratories, Feb 1986.

10. K. D. Bergeron, D. C. Williams, "CONTAIN Calculations of Containment Loading of Dry PWR's," Sandia National Laboratories, Nuclear Science and Engineering, V. 90, pp. 153-159, 1985.

11. D. K. Gabrielson, et al., ONEDIM-A Computer Code for Solving Non-Linear Heat Transfer Problems, Report No. SCL-DR-69-99, Sandia National Laboratories, Feb 1970.

12. D. A. Powers, J. E. Brockman, A. W. Shiver, Vanesa: A Mechanistic Model of Radionuclide Release and Aerosol Generation During Core Debris Interaction with Concrete, NUREG/CR-4308, SAND85-1370, Sandia National Laboratories, July 1985.

13. K. D. Bergeron, et al., Users Manual for CONTAIN1.0, A Computer Code for Severe Nuclear Reactor Accident Containment Analysis, NUREG/CR-4085 SAND84-1204, Sandia National Laboratories, May 1985.

14. J. Jung, Ultimate Strength Analyses of the Watts Bar, Maine Yankee, and Bellefonte Containments, NUREG/CR-3724, SAND84-0660, Sandia National Laboratories, July 1984.

15. Containment Performance Working Group, Draft Report, NUREG-1037, May 1985.

16. F. Gonzalez, I Huhtiniemi, M. Corradini, Transient Model for Direct Heating in a LWR, UWRSR-35, University of Wisconsin, Feb 1986.

17. Lichung Pong, M. Corradini, G. A. Moses, Surry S_2D Severe Accident Containment Loads Calculations Using HMC, UWRSR-34, Jan 1986.

18. Reactor Safety Study--An Assessment of Accident Risks in U.S. Commercial Nuclear Power Plants, WASH-1400, NUREG-75/014, Oct 1975.

19. W. G. Brown, K. R. Solvason, "Natural Convection TGhrough Rectangular Openings in Partitions-1, Vertical Partitions", International Journal of Heat and Mass Transfer, V. 5, pp. 859-868, 1962.

20. W. G. Brown, A. G. Wilson, K. R. Solvason, "Heat and Moisture Flow Through Openings by Convection," ASHRAE-Transactions, V. 69, p. 351-357, 1963.

21. B. C-J. Chen, et al., "Degraded Core Studies Using the Multidimensional COMMIX Code", Transaction of the American Nuclear Society, Annual Meeting, Boston, MA, V. 49, pp. 453-454, June 1985.

22. R. Henninger, "Preliminary 2-D MELPROG Calculation for the TMLB Accident in Surry," Presented at Direct Containment Heating Meeting, Held at Bethesda, MD, April 23, 1986.

23. V. Shah, "Structural Failure Studies of RCS," Presented at Direct Containment Heating Meeting, Held at Bethesda, MD, April 23, 1986.

TABLE 1

TMLB'-HPE
SEQUENCE OF EVENTS
(MARCH 2.0 CODE)

STEAM GENERATOR DRYOUT	5.83 MIN
CORE UNCOVERY	30.0 MIN
CORE STARTS MELTING	53.4 MIN
CORE SLUMP	75.8 MIN
FRACTION CORE MELTED	65%
FRACTION CLAD REACTED	50%
THERMAL ATTACK ON BOTTOM HEAD	75.9 MIN
BOTTOM HEAD FAILURE	82.1 MIN
DIRECT HEATING EVENT	82.1-82.6 MIN
CONTAINMENT INDUCED LEAKAGE OR FAILURE	82.6 MIN

TABLE 2
CASE MATRIX
TMLB' HIGH PRESSURE EJECTION

CASE	% INJECT	CAVITY WATER	BREAK AREA	RCS REL.	F.P. REL.	NAT. CONV.	REEV.	CORE/CONC RELEASES
000	0	--	1 in^2	*	NO	NO	NO	YES
100	0	--	2.4 in^2	*	NO	NO	NO	YES
001	90	NO	7 ft^2	*	NO	NO	NO	NO
011	90	NO	7 ft^2	MCT	YES	NO	NO	NO
001A	90	YES	7 ft^2	*	NO	NO	NO	NO
011A	90	YES	7 ft^2	MCT	YES	NO	NO	NO
011B	90	YES	7 ft^2	MCT	YES	YES	NO	NO
002	50	NO	5 in^2	*	NO	NO	NO	NO
102	50	NO	12 in^2	*	NO	NO	NO	NO
012	50	NO	5 in^2	MCT	YES	NO	YES	NO
112	50	NO	12 in^2	MCT	YES	NO	YES	NO
002A	50	YES	5 in^2	*	NO	NO	NO	NO
102A	50	YES	12 in^2	*	NO	NO	NO	NO
012A	50	YES	5 in^2	MCT	YES	NO	YES	YES
112A	50	YES	12 in^2	MCT	YES	NO	YES	YES

*BMI-2104 ZION RELEASES

TABLE 3

HIGH PRESSURE EJECTION
DIRECT HEATING EVENT
ASSUMPTIONS

CORE DEBRIS EJECTED (UO_2, Zr, ZrO_2).................. 100%

AVAILABLE STEEL EJECTED..................... 53% (100,000 lbs)

INITIAL DEBRIS TEMPERATURE........... (CORIUM EUTECTIC) 2550^{O}K

ZIRCONIUM REACTED IN-VESSEL................................ 50%

ZIRCONIUM REACTED IN DIRECT HEATING EVENT..100% OF INJECTED Zr

DEBRIS COMES TO THERMAL EQUILIBRIUM WITH ATMOSPHERE

ADIABATIC CALCULATIONS

PARAMETERS VARIED

<u>FRACTION OF DEBRIS INJECTED INTO CONTAINMENT</u>

90%
50%
0%

<u>STEEL REACTED</u>

0%
100% (OF THAT INJECTED)

<u>HYDROGEN REACTED</u>

0%
100% (OF THAT IN CONTAINMENT, 3 VOL. %)

<u>CAVITY WATER INJECTED WITH DEBRIS</u>

0%
100% (75,000 lbs)

TABLE 4

RESULTS OF DIRECT HEATING CALCULATIONS

CASE	% EJECT.	%* WATER	H_2 BURN	Fe BURN	T_F (°F)	P_F (psia)	H (GJ)
001	90	0	NO	NO	2009	159.9	281
001	90	0	YES	NO	2288	178.0	330
001A	90	100	NO	NO	1462	148.8	305
001A	90	100	YES	NO	1719	168.8	356
002	50	0	NO	NO	1314	116.8	172
002	50	0	YES	NO	1681	138.6	226
002	50	0	NO	YES	1913	158.4	265
002	50	0	YES	YES	2223	173.8	318
002A	50	100	NO	NO	789	96.6	181
002A	50	100	YES	NO	1111	121.6	239
002A	50	100	NO	YES	1326	138.2	213
002A	50	100	YES	YES	1609	160.1	334

* % OF WATER IN REACTOR CAVITY THAT IS INJECTED INTO CONTAINMENT WITH THE CORE DEBRIS

TABLE 5
INITIAL FISSION PRODUCT
GROUP INVENTORIES

Group 1	Mass (Kg)
CsI	27.90
RbI	3.97
Total Group 1	31.87
Group 2	
CsOH	180.16
RbOH	21.46
Total Group 2	201.62
Group 3	
Te	33.3
Group 4	
Sr	63.8
Ba	81.4
Total Group 4	145.2
Group 5	
Ru	138.0
Rh	27.9
Pd	70.0
Tc	49.4
Mo	206.0
Total Group 5	491.4

TABLE 5 (Cont.)
INITIAL FISSION PRODUCT
GROUP INVENTORIES

Group 6	Mass (Kg)
La	82.9
Y	30.4
Eu	11.9
Nd	227.0
Np	34.5
Sm	45.2
Pm	9.6
Pu	624.0
Zr	238
Ce	175
Nb	3.7
Pr	67.6
Total Group 6	1549.8

Group 7	
Kr	17.8
Xe	346.0
Total Group 7	363.8

TABLE 6

DIRECT HEATING FISSION PRODUCT RELEASES
TMLB'-HIGH PRESSURE EJECTION*

FISSION PRODUCT GROUP**	50% INJECTION (Kg)		90% INJECTION (Kg)	
	FINE (.7 micron)	COARSE (30 micron)	FINE (.7 micron)	COARSE (30 micron)
Te	6.75	.11	12.1	.20
Sr	--	.59	--	1.06
Ru	61.6	2.34	111	4.20
Mo	83.5	***	150	***
La	--	7.69	--	13.8

* Calculated using fission product inventories remaining in the fuel at vessel failure in the BMI-2104 Zion analysis.
** Molybdenum has been broken out separately here. It is actually a member of the Ruthenium group
*** Included in Ruthenium group total

TABLE 7

DIRECT HEATING FISSION PRODUCT RELEASE
TMLB'-HIGH PRESSURE EJECTION*

FISSION PRODUCT GROUP**	50% EJECTION (Kg) FINE (.7 micron)	50% EJECTION (Kg) COURSE (30 micron)	90% EJECTION (Kg) FINE (.7 micron)	90% EJECTION (Kg) COURSE (30 micron)
Te	3.31	0.52	5.96	.10
Sr	--	.611	--	1.10
Ru	61.8	2.44	111	4.40
Mo	86.4	***	156	***
La	--	7.75	--	13.9

* Calculated using fission product inventories remaining in the fuel at vessel failure in the present study

** Molybdenum has been broken out separately here. It is actually a member of the Ruthenium group

*** Included in Ruthenium group total

TABLE 8

SUMMARY OF PRIMARY SYSTEM RELEASES[+]
FOR TMLB' HIGH PRESSURE EJECTION CASES

FISSION PRODUCT	BMI-2104	MCT WITHOUT NATURAL CONVECTION: MELTDOWN PHASE** TYPE A	MCT WITHOUT NATURAL CONVECTION: REEVOLUTION PHASE*** TYPE C	TOTAL	MCT W/NATURAL CONVECTION** TYPE B
CsI	.02*	.028	.21	.24	.35
CsOH	.02*	.030	.18	.21	.28
Te	.04*	.24	---	.24	.17

[+] FRACTIONS OF INITIAL INVENTORIES

* ZION STUDY

** UP TO AND INCLUDING VESSEL FAILURE

*** RELEASES SUBSEQUENT TO VESSEL FAILURE - CALCULATED USING THE DEPRESSURIZATION HISTORY FOR CONTAINMENT LEAKAGE SCENARIOS

Table 9
PARTICLE SIZE DISTRIBUTION
FOR PRIMARY SYSTEM RELEASES

TYPE	F. P. HEATING	REEVOLUTION	NAT. CONV.	DIAMETER (MICRONS)	STAN. DEV. (MICRONS)
A	Yes	No	No	4.58	1.76
B	Yes	No	Yes	4.52	2.01
C	Yes	Yes	No	5.60	1.98

TABLE 10
CONTAINMENT RELEASES* (TO 20 HRS)
TMLB' HIGH PRESSURE EJECTION

CASE	CsI	CsOH	Te	Ru	Sr	La	Xe	Kr
000	5.7E-5	9.8E-5	.018	2.1E-5	.0054	.0032	.071	.071
100	1.3E-4	2.3E-4	.043	4.9E-5	.013	.0077	.16	.16
001	.014	.014	.29	.38	.024	.0052	.77	.77
011	.015	.016	.13	.39	.0058	.0052	.77	.78
001A	.014	.014	.29	.38	.024	.0053	.78	.78
011A	.015	.016	.30	.40	.0054	.0048	.79	.79
011B	.16	.12	.21	.41	.0073	.0048	.79	.79
002	8.0E-4	8.0E-4	.0097	.012	.0012	4.0E-5	.31	.31
102	.0018	.0018	.022	.028	.0027	9.4E-5	.59	.59
012	.0061	.0056	.010	.012	8.5E-5	3.7E-5	.31	.31
112	.013	.012	.023	.028	2.0E-4	8.8E-5	.60	.60
002A	7.2E-4	7.2E-4	.0088	.011	.0011	3.8E-5	.30	.30
102A	.0017	.0017	.020	.025	.0025	8.9E-5	.57	.57
012A	.0101	.0092	.0092	.011	8.5E-5	3.5E-5	.30	.30
112A	.022	.02	.021	.025	2.3E-4	8.5E-5	.53	.53

*FRACTION OF INITIAL INVENTORIES RELEASED TO ENVIRONMENT

TABLE 11

COMPARISON OF MULTI-CELL RELEASES TO SINGLE-CELL RELEASES*
CASE-012A

FISSION PRODUCT GROUP	ATTENUATION FACTOR NO BUOYANCY	BUOYANCY
CsI	.77	.90
CsOH	.75	.88
Te	.99	.92
Sr	.90	1.07
Ru	1.17	.97
La	1.17	1.30
Xe	.95	1.03
Kr	.95	1.03

* CUMULATIVE RELEASES AT 15.5 HOURS

TABLE 12

TMLB'-PSL
SEQUENCE OF EVENTS
(MARCH 2.0 CODE)

STEAM GENERATOR DRYOUT	4.50 MIN
CORE UNCOVERY	26.7 MIN
CORE STARTS MELTING	43.6 MIN
CORE SLUMP	60.5 MIN
FRACTION CORE MELTED	65%
FRACTION CLAD REACTED	50%
THERMAL ATTACK ON BOTTOM HEAD	60.9 MIN
BOTTOM HEAD FAILURE	68.6 MIN
CONTAINMENT LEAKAGE INDUCED	82.6 MIN
REACTOR CAVITY DRYOUT	454.5 MIN

TABLE 13
CASE MATRIX
TMLB' PUMP SEAL LOCA

CASE	% INJECT	BREAK AREA	RCS REL.	F.P. REL.	NAT. CONV.	REEV.	CORE/CONC REL
030	0	1 in^2	MCT	YES	NO	NO	YES
130	0	2.4 in^2	MCT	YES	NO	NO	YES
031	0	1 in^2	MCT	YES	YES	NO	YES
131	0	2.4 in^2	MCT	YES	YES	NO	YES

TABLE 14

SUMMARY OF PRIMARY SYSTEM RELEASES+
FOR TMLB' PUMP SEAL LOCA CASES

FISSION PRODUCT	BMI-2104*	MCT WITHOUT NATURAL CONVECTION MELTDOWN PHASE**	 REEVOLUTION PHASE***	 TOTAL	MCT W/NATURAL CONVECTION**
		TYPE A	TYPE C		TYPE B
CsI	----	.084	---	.084	.93
CsOH	----	.073	---	.073	.77
Te	----	.089	---	.089	.13

+ FRACTIONS OF INITIAL INVENTORIES

* ZION STUDY

** UP TO AND INCLUDING VESSEL FAILURE

*** RELEASES SUBSEQUENT TO VESSEL FAILURE - CALCULATED USING THE DEPRESSURIZATION HISTORY FOR CONTAINMENT LEAKAGE SCENARIOS

TABLE 15
CONTAINMENT RELEASES* (TO 20 HRS)
TMLB' PUMP SEAL LOCA

CASE	CsI	CsOH	Te	Ru	Sr	La	Xe	Kr
030	6.1E-5	1.2E-4	.0032	1.1E-6	.0049	8.2E-4	.070	.070
130	1.4E-4	2.9E-4	.0078	2.6E-6	.012	.0020	.16	.16
031	8.8E-4	8.1E-4	.0034	1.9E-5	.0050	8.4E-4	.072	.072
131	.0020	.0019	.0082	8.9E-6	.012	.0020	.16	.16

*FRACTION OF INITIAL INVENTORIES RELEASED TO ENVIRONMENT

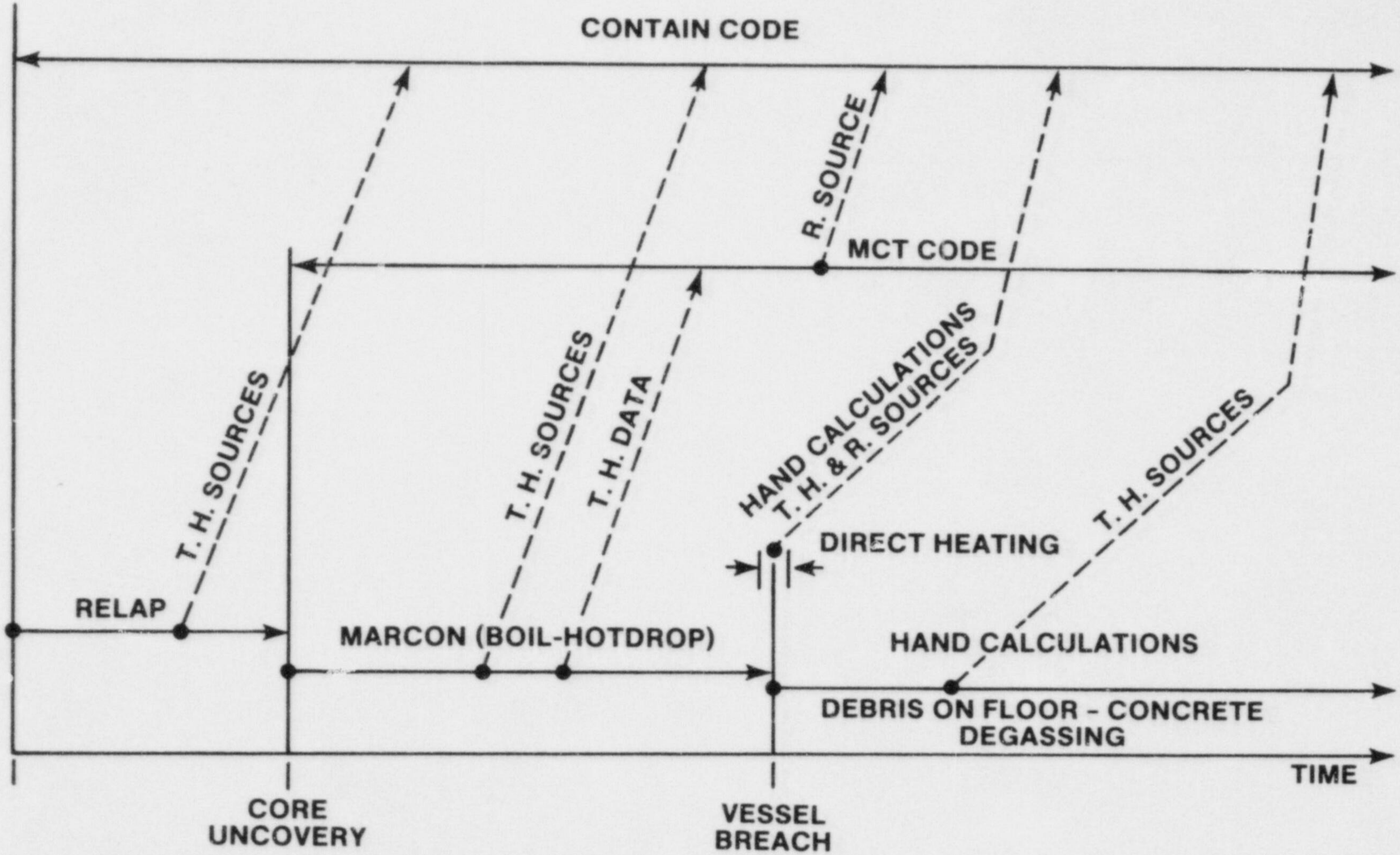

Figure 1. Diagram of Code Linkages

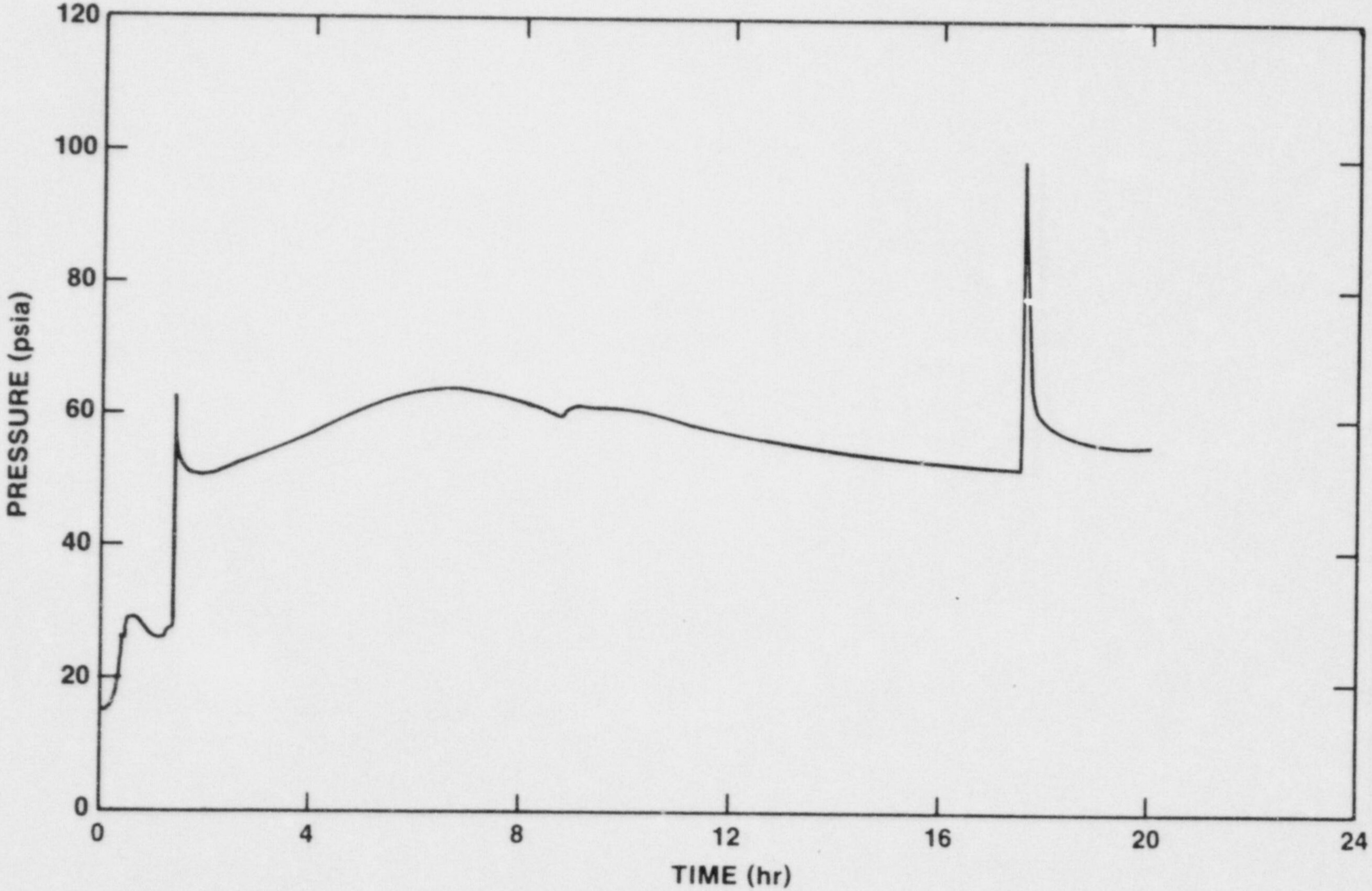

Figure 2. Containment Pressure TMLB' without Direct Heating (Case-000)

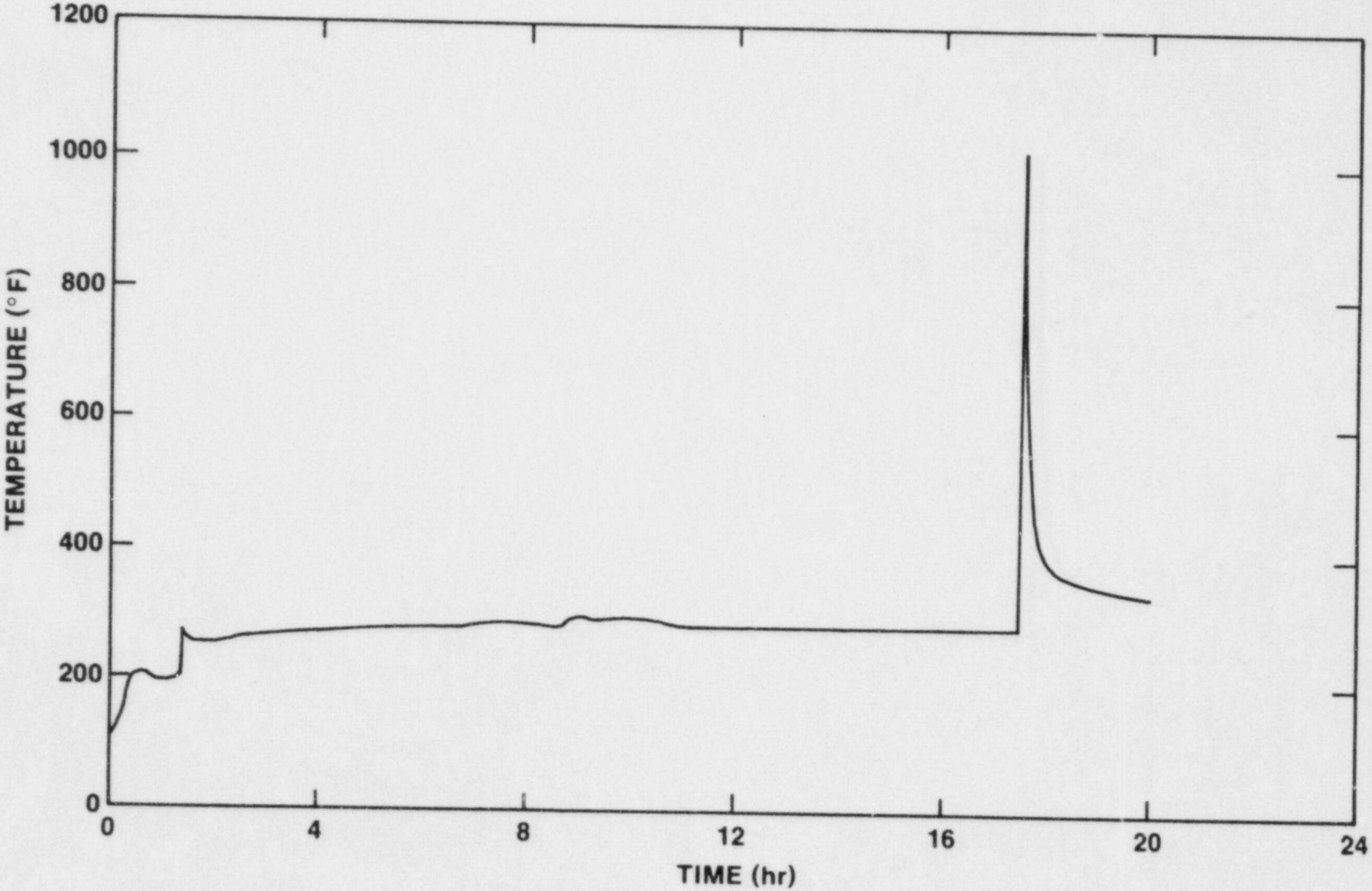

Figure 3. Containment Temperature TMLB' without Direct Heating (Case-000)

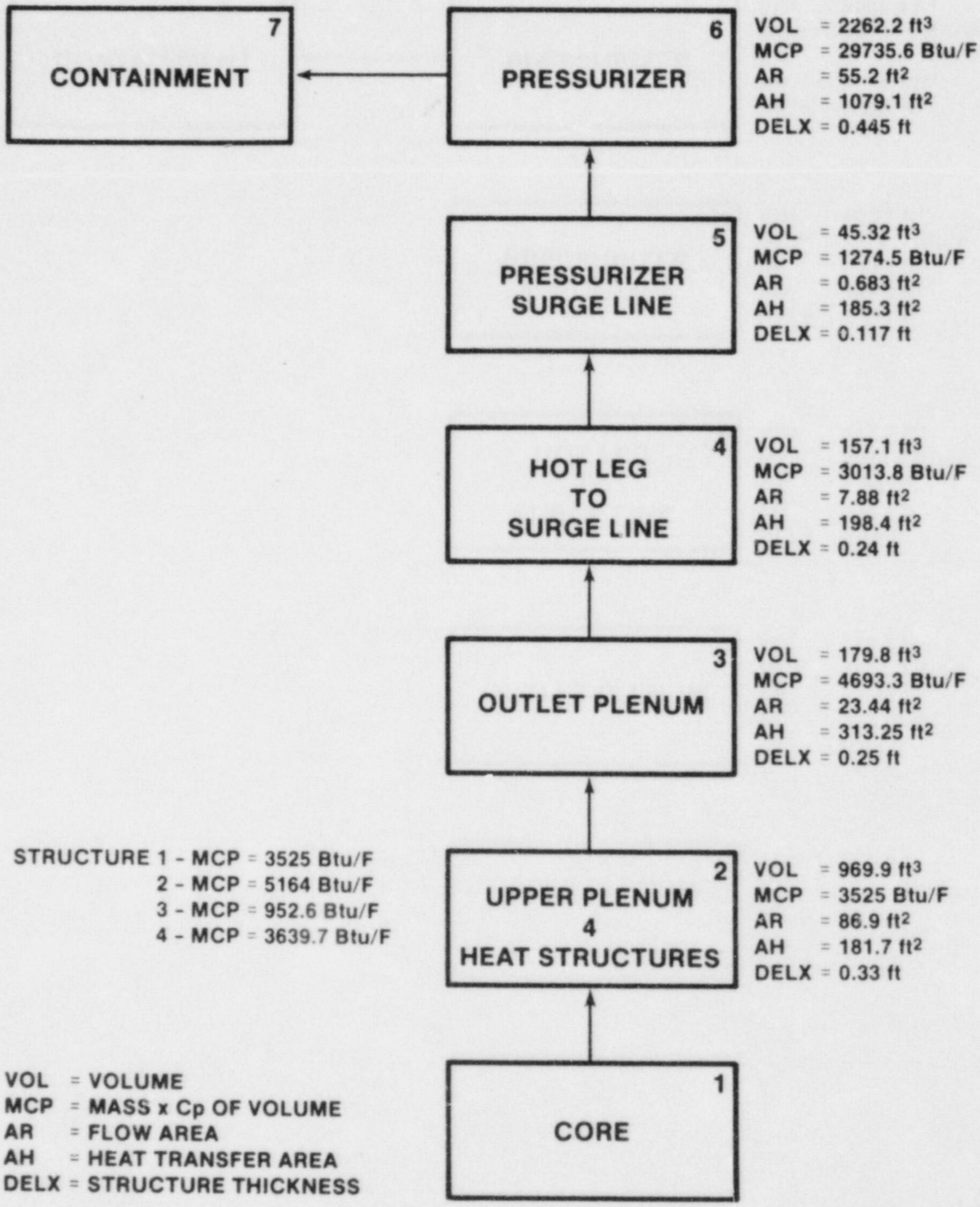

Figure 4. Primary System Flow Path TMLB' High Pressure Ejection

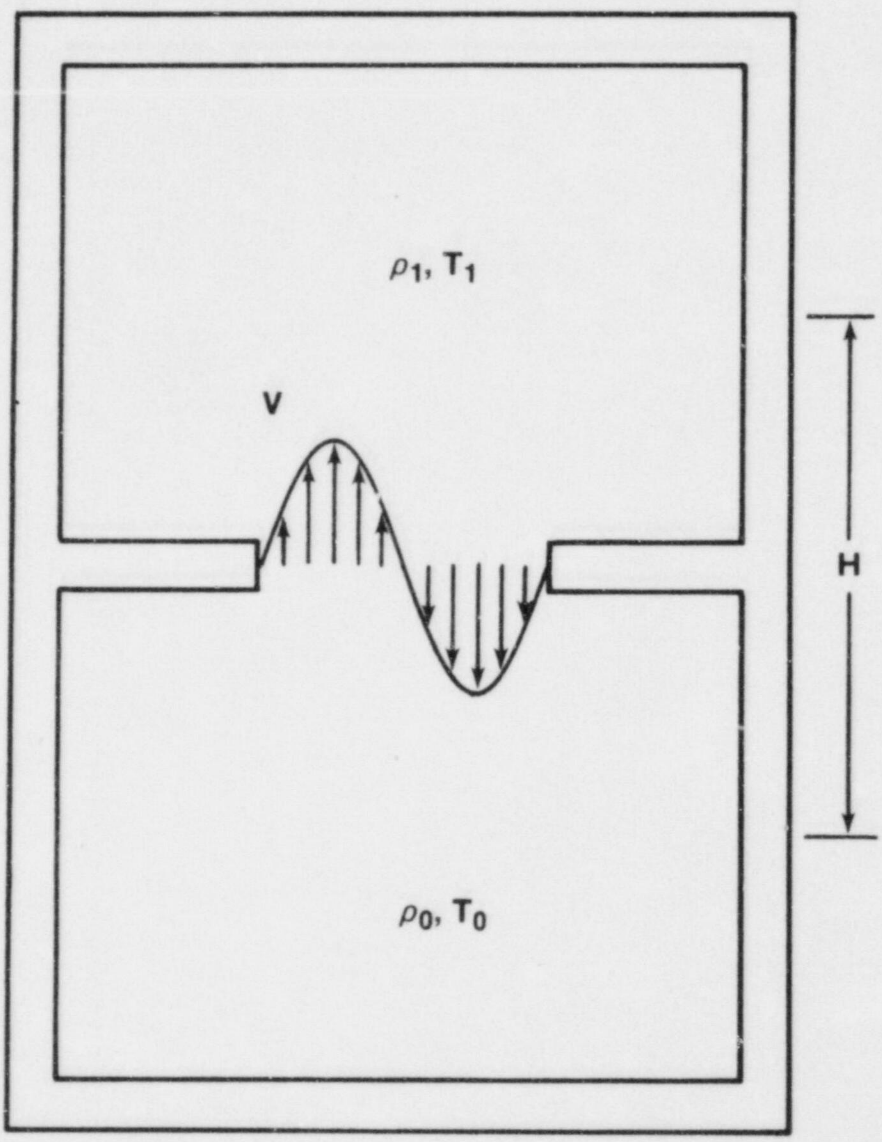

Figure 5. Description of Natural Convection Model

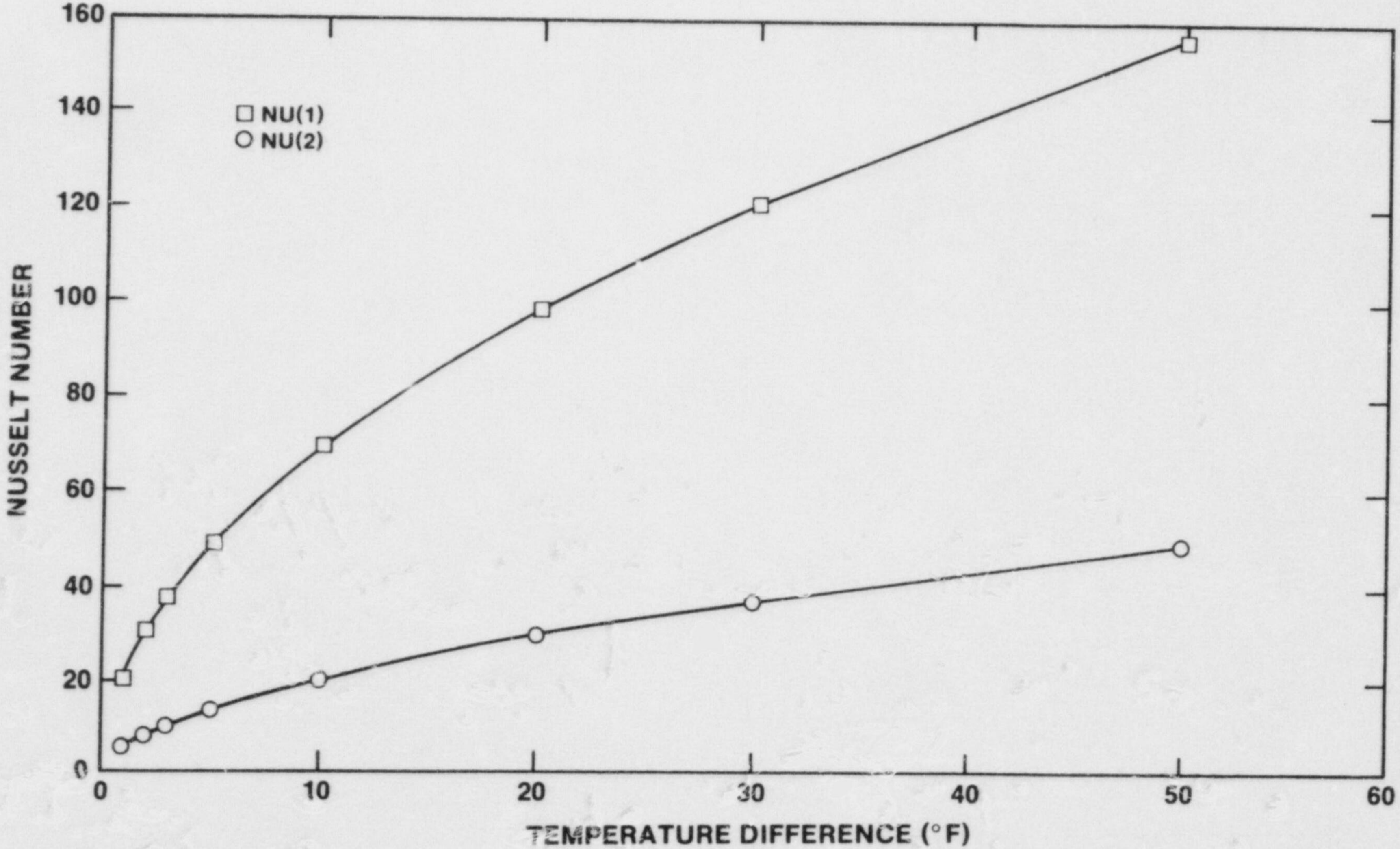

Figure 6. Nusselt Number Correlations for Natural Convection

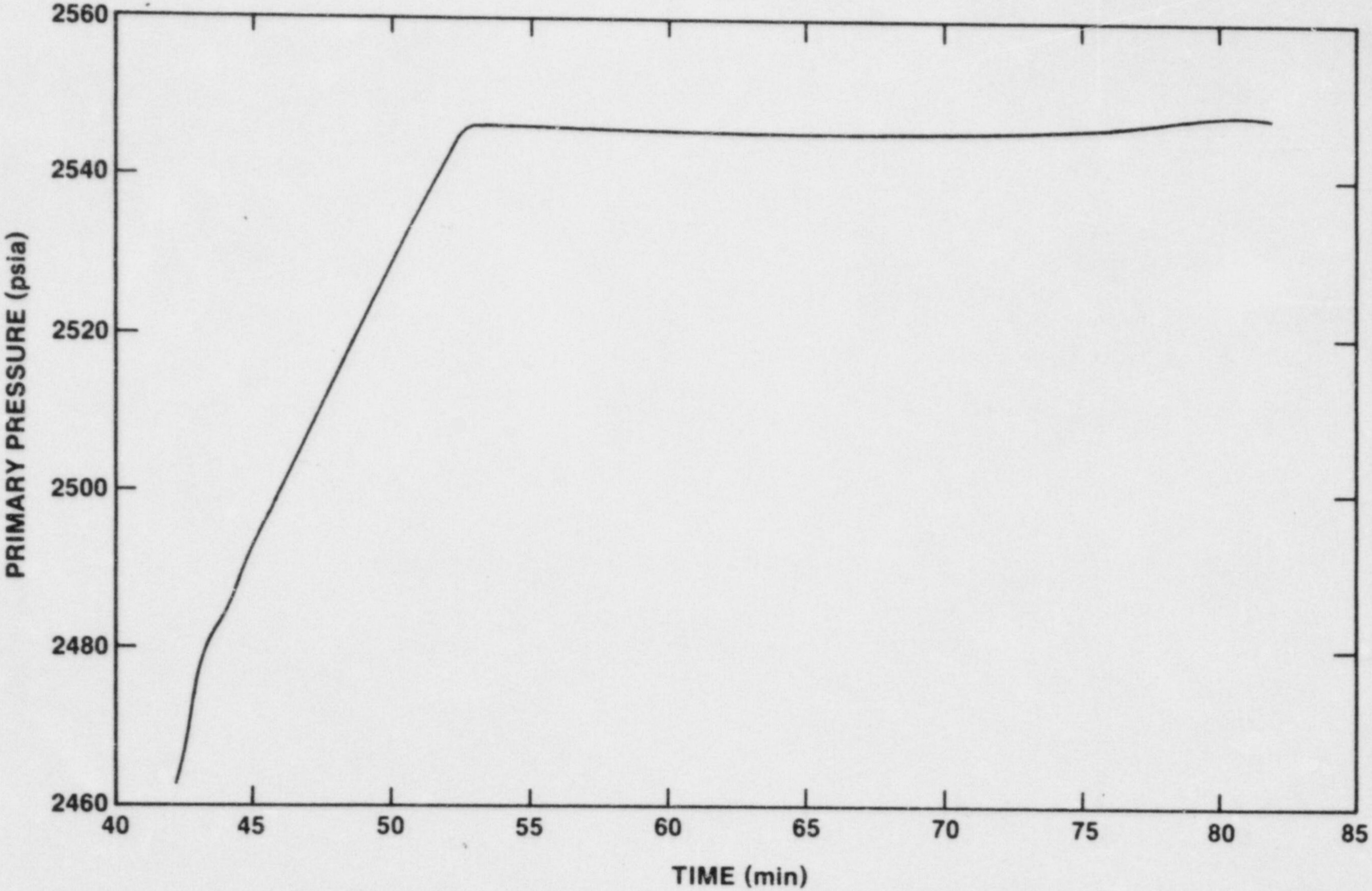

Figure 7. Primary System Pressure TMLB' High Pressure Ejection

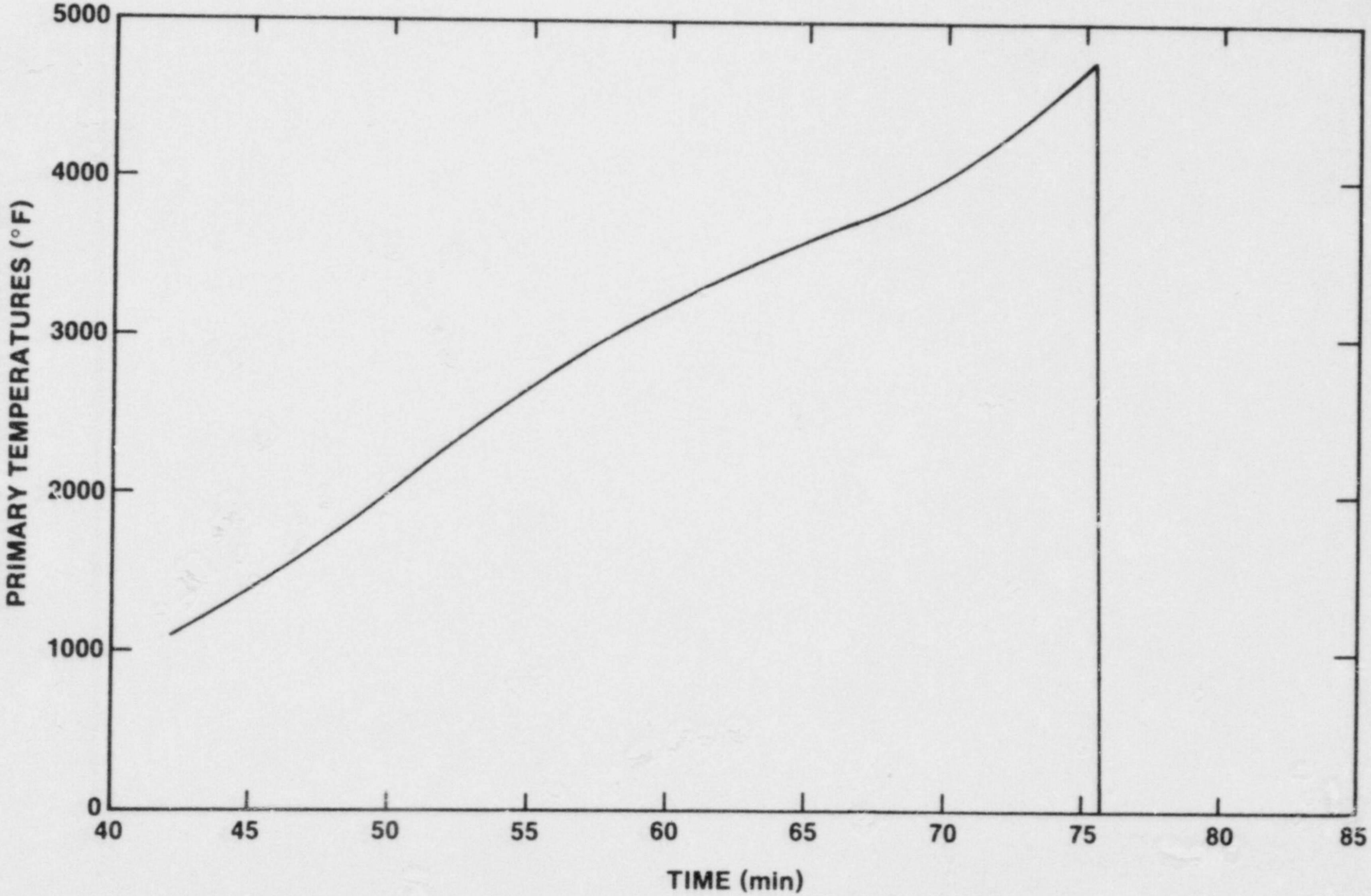

Figure 8. Average Core Temperature TMLB' High Pressure Ejection

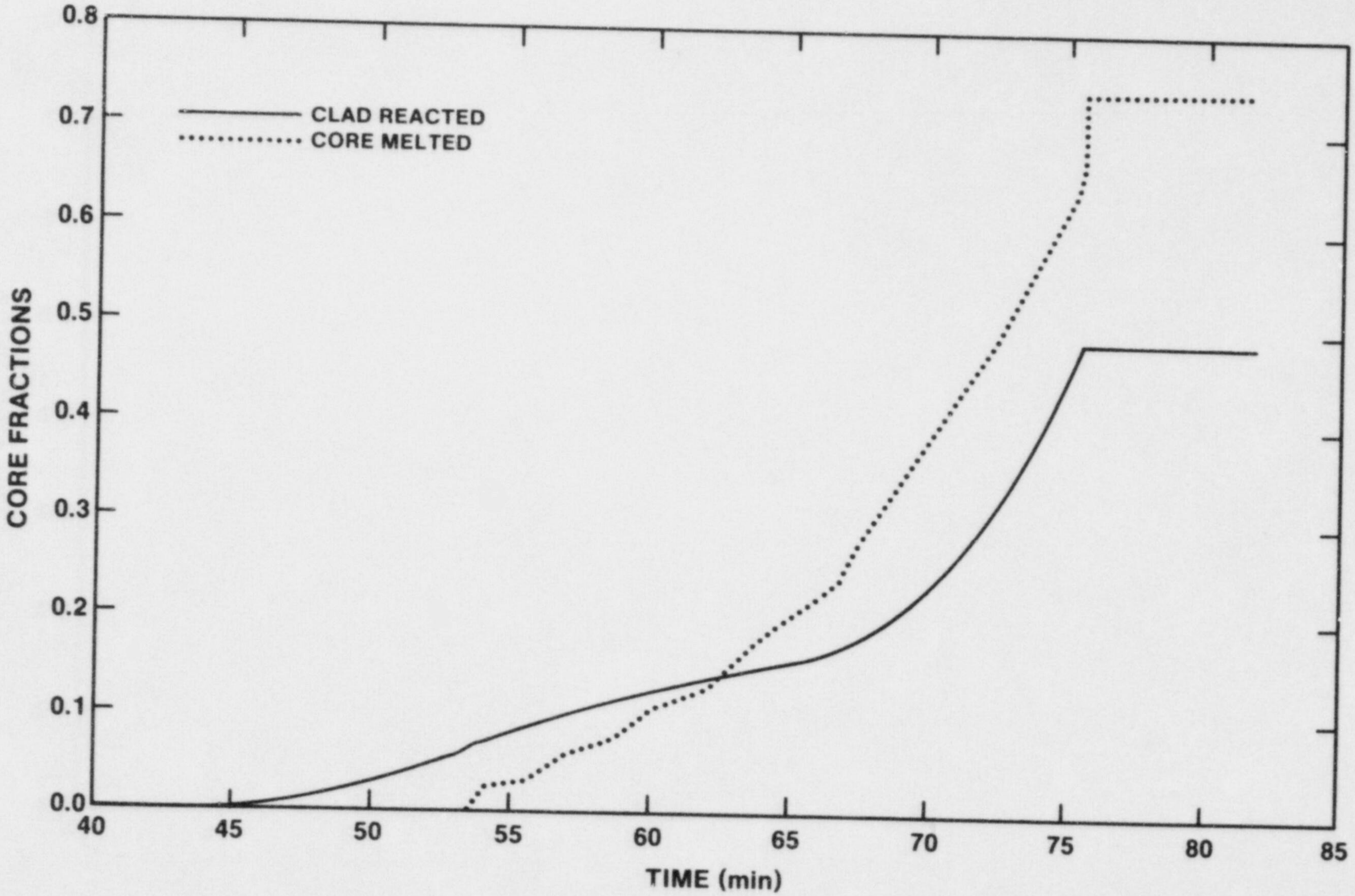

Figure 9. Core Melt and Clad Oxidation Fractions TMLB' High Pressure Ejection

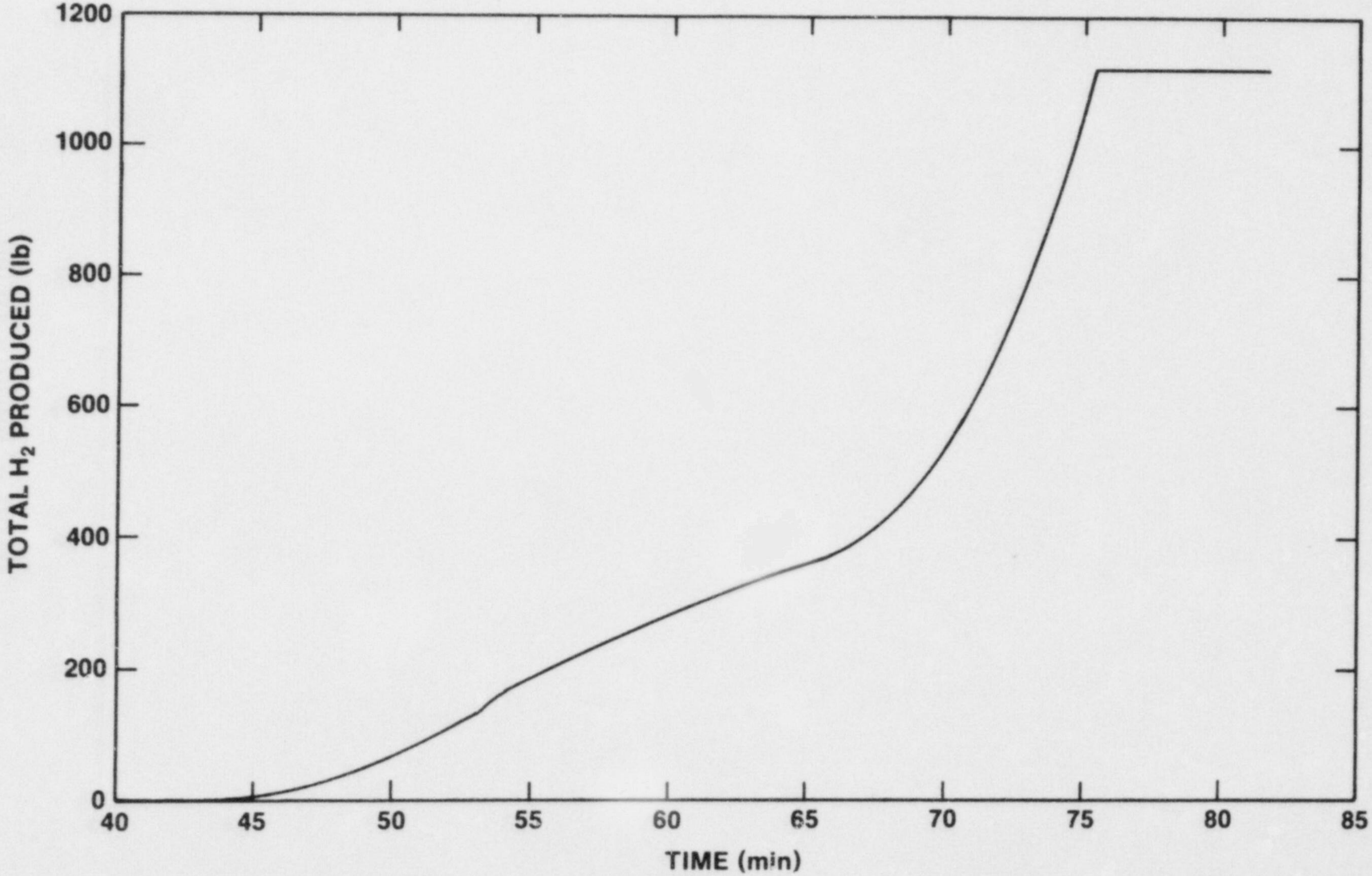

Figure 10. Hydrogen Generation Rate TMLB' High Pressure Ejection

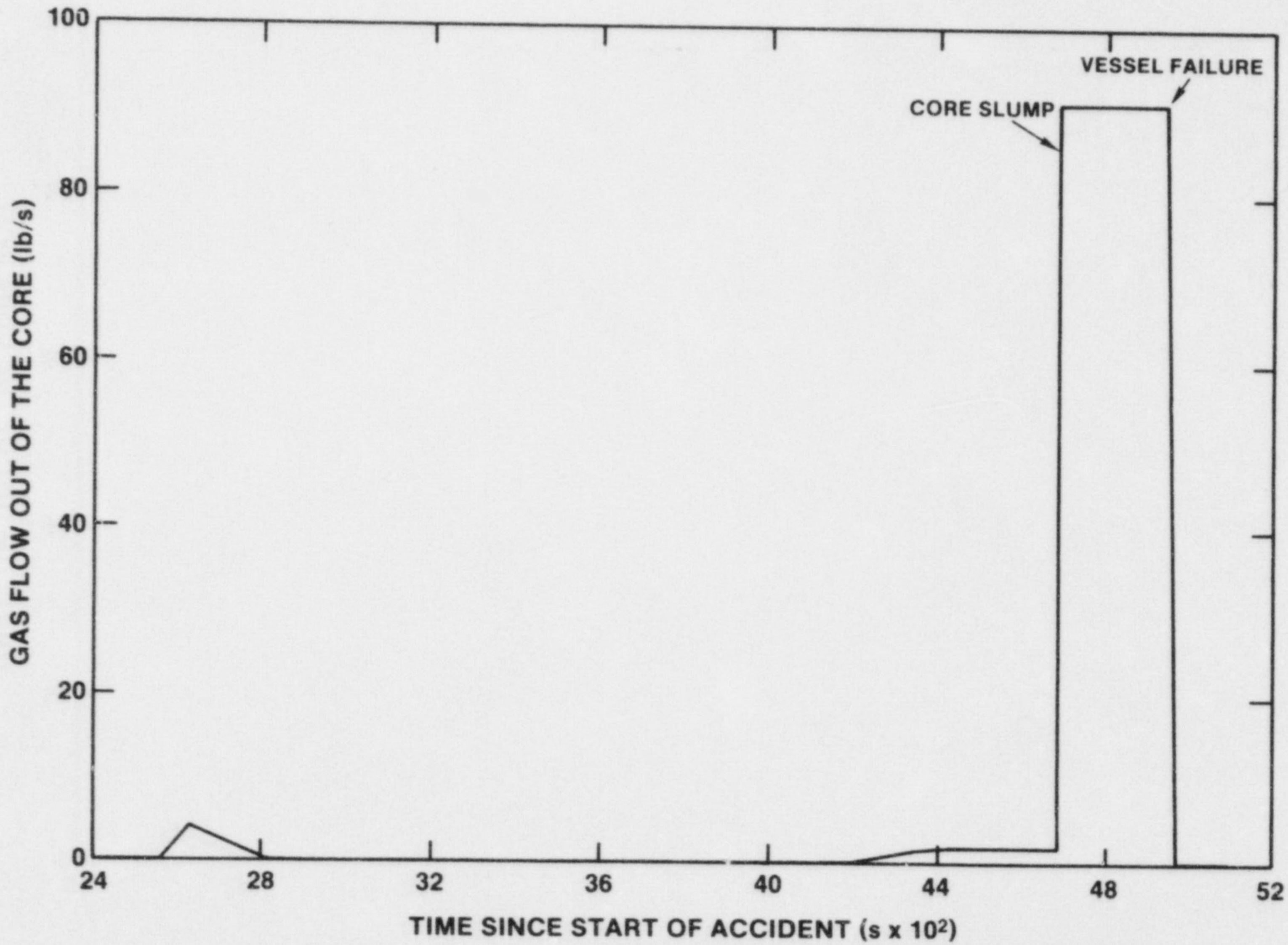

Figure 11. Outlet Gas Flow TMLB' High Pressure Ejection

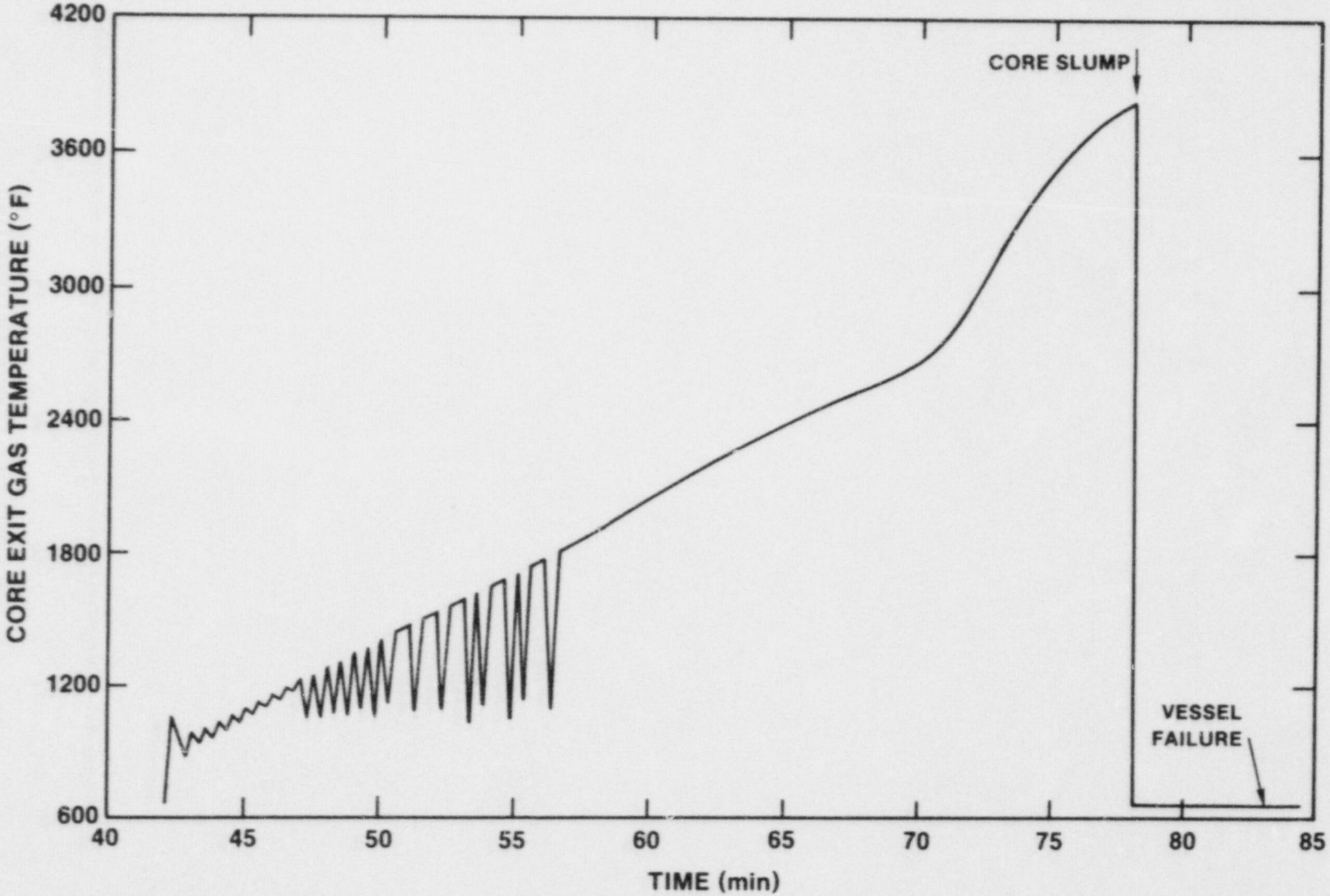

Figure 12. Outlet Gas Temperature TMLB' High Pressure Ejection

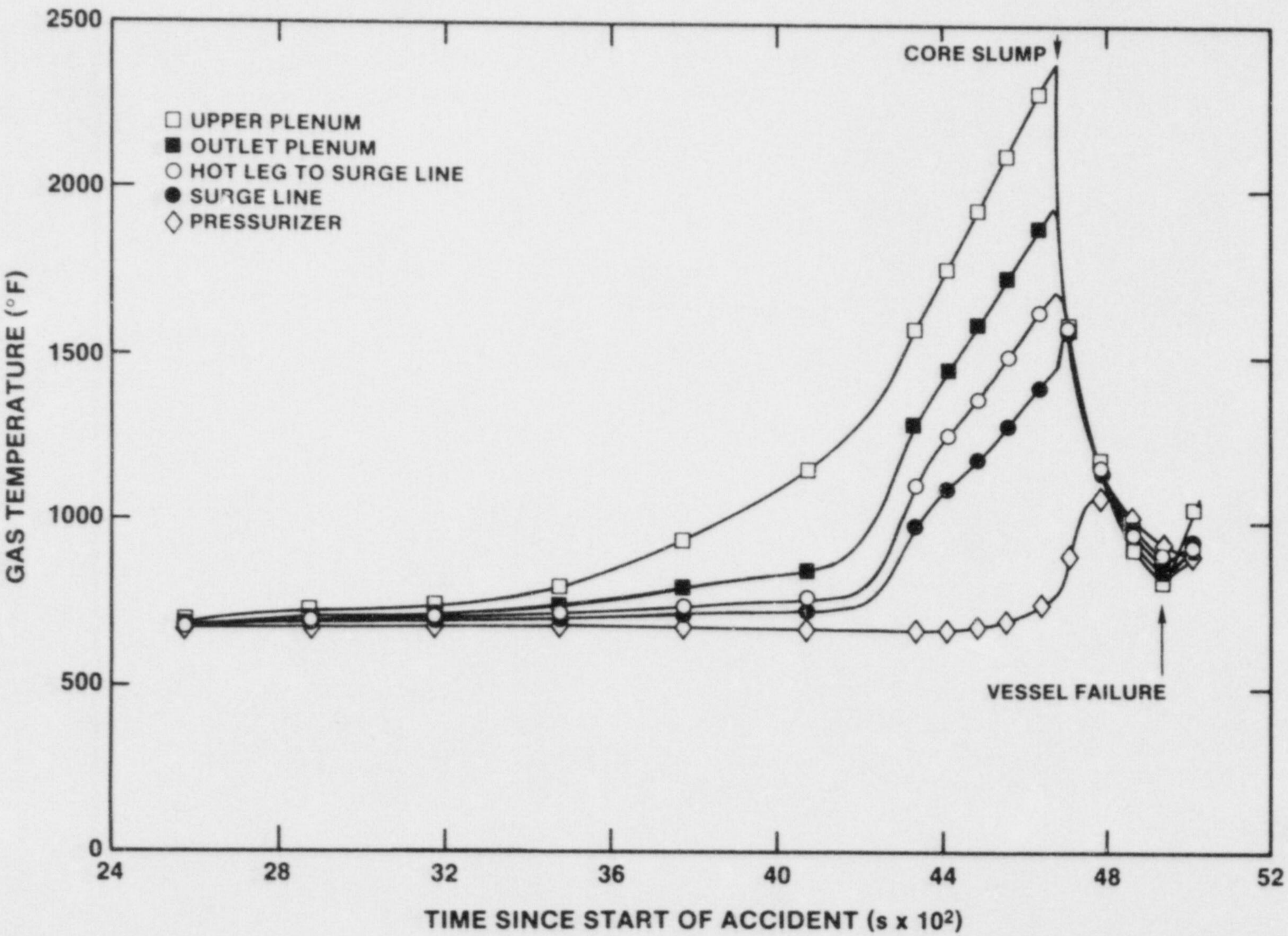

Figure 13. Primary System Gas Temperatures TMLB' High Pressure Ejection (Case A)

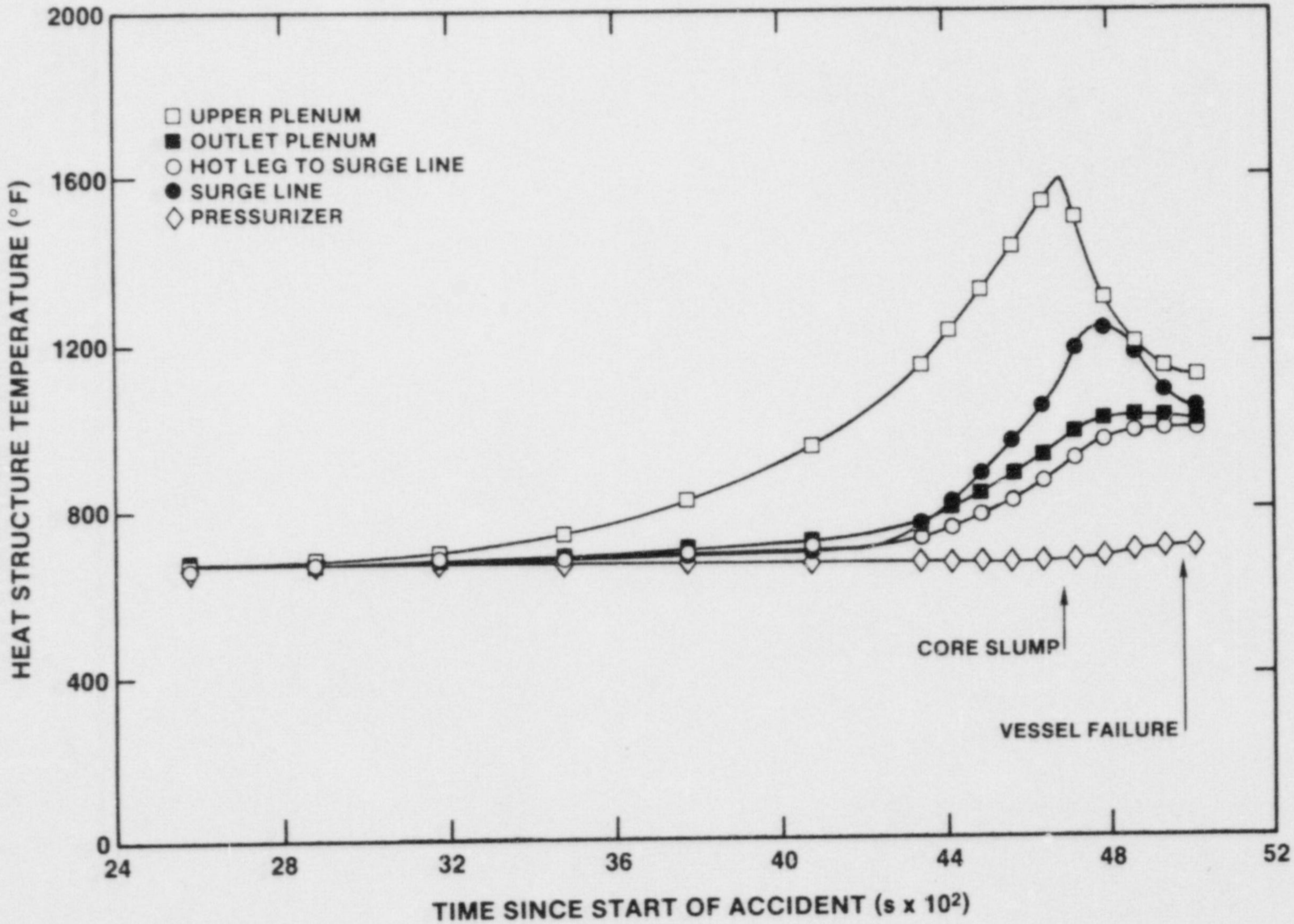

Figure 14. Primary System Structure Temperatures TMLB' High Pressure Ejection (Case A)

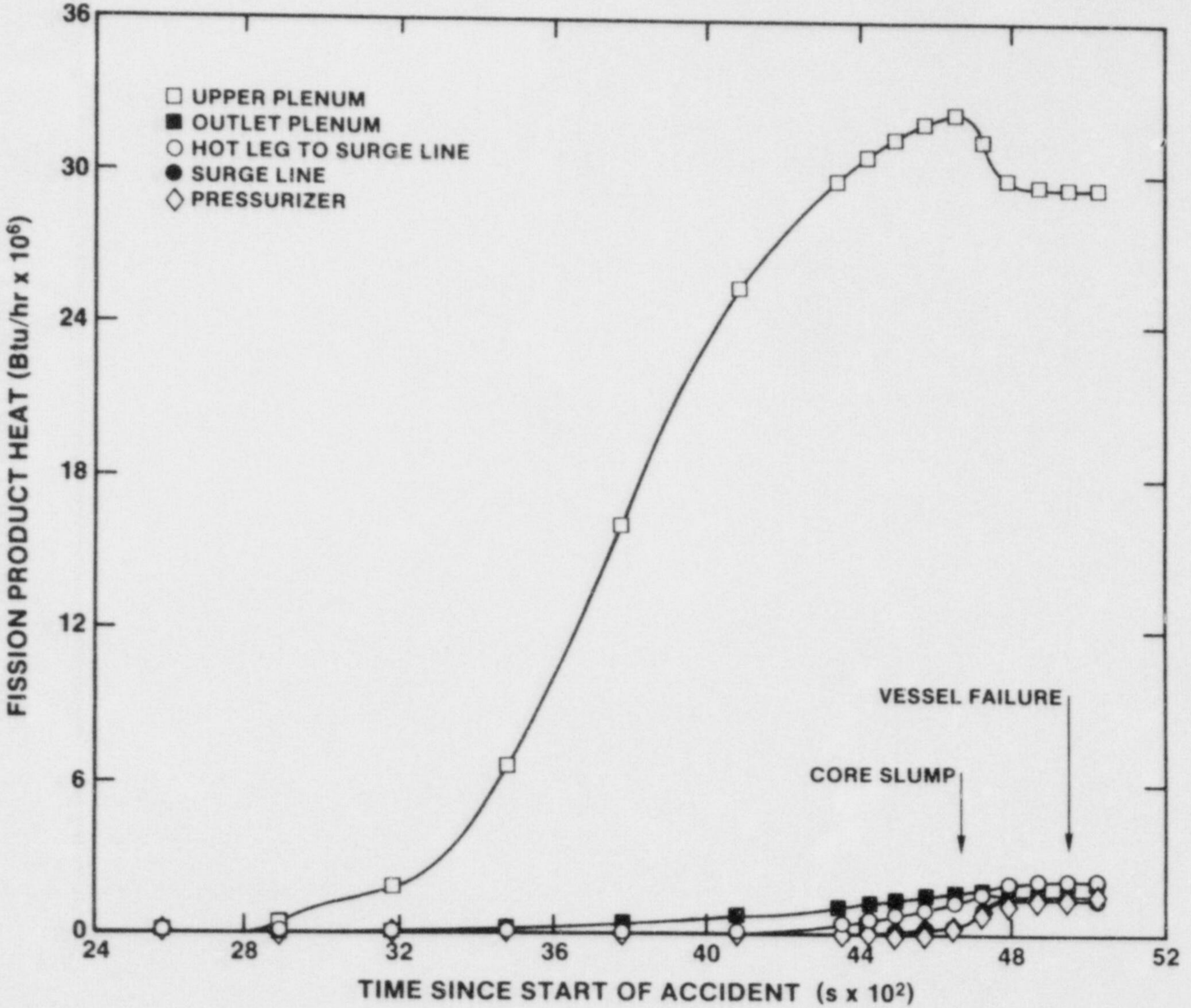

Figure 15. Fission Product Heating TMLB' High Pressure Ejection (Case A)

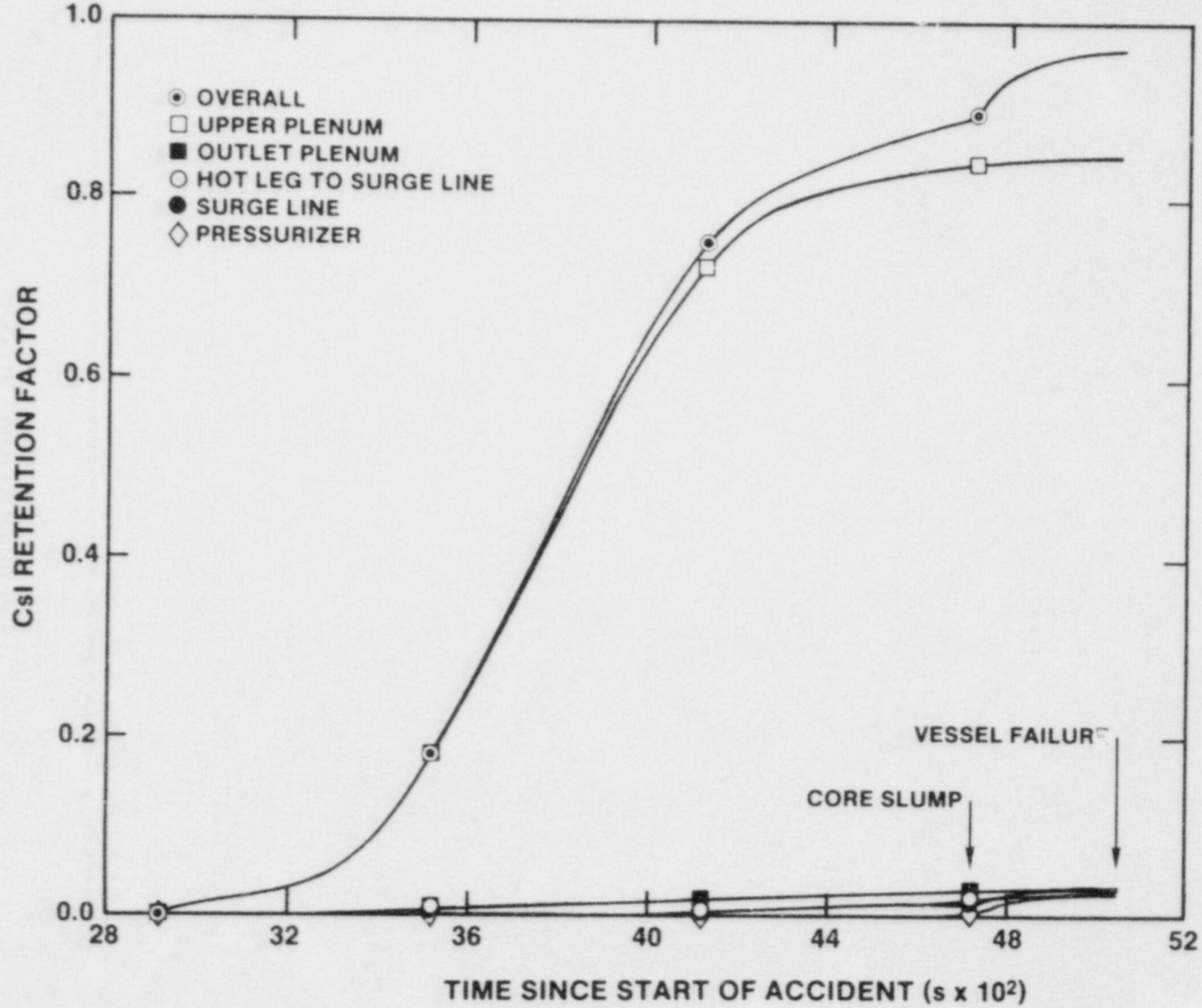

Figure 16. CsI Retention Factor TMLB' High Pressure Ejection (Case A)

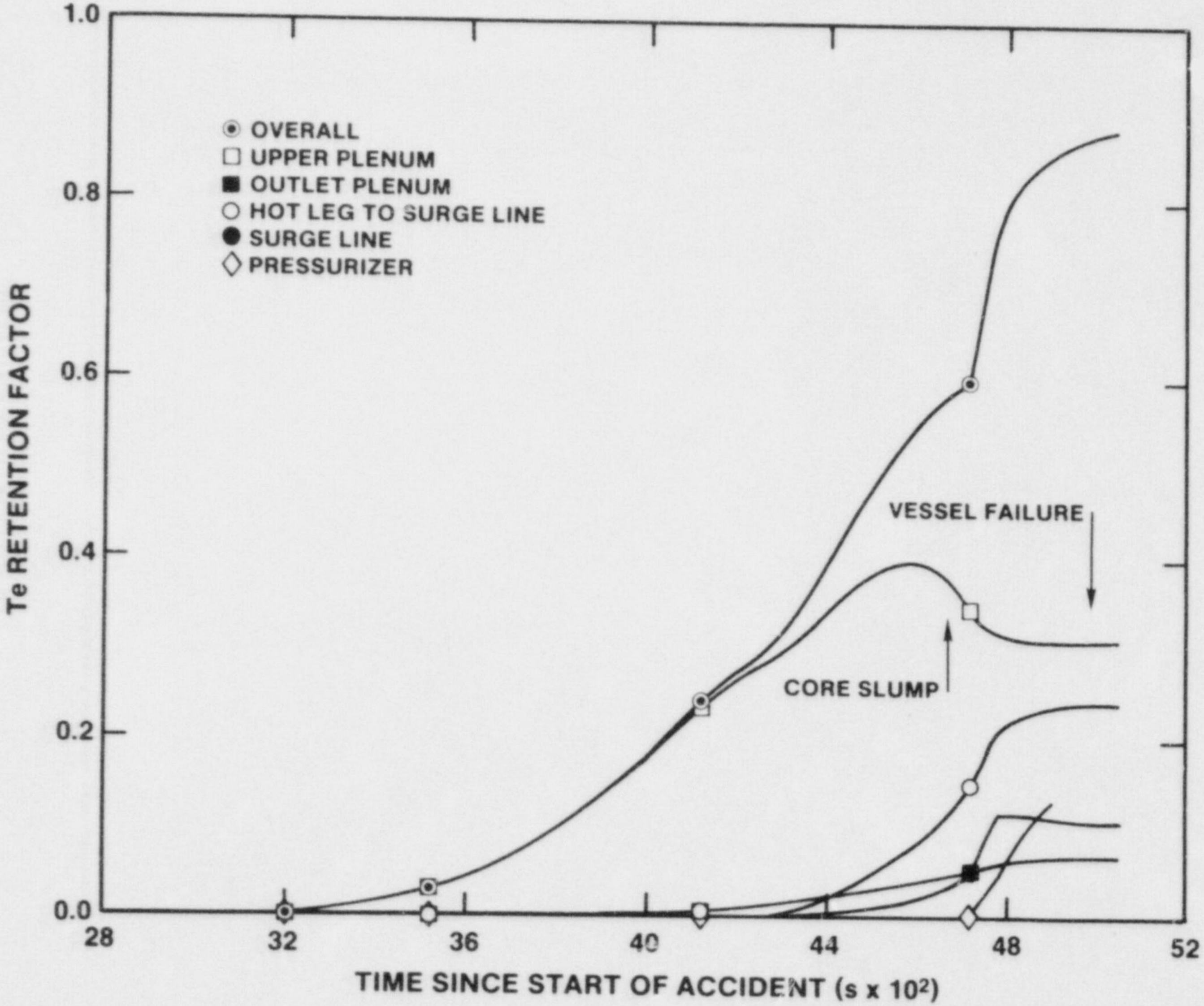

Figure 17. Te Retention Factor TMLB' High Pressure Ejection (Case A)

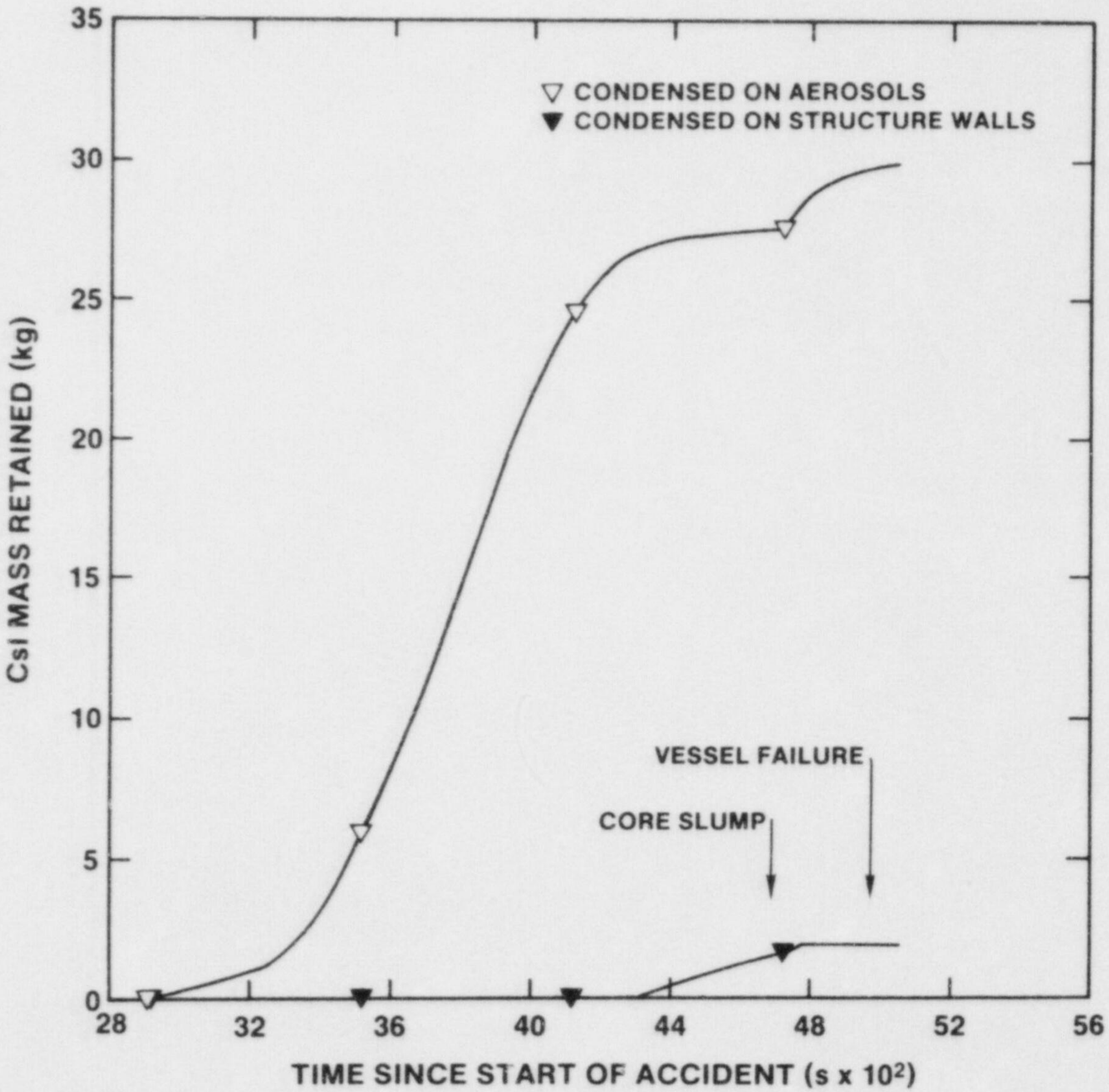

Figure 18. CsI Mass Retained TMLB' High Pressure Ejection (Case A)

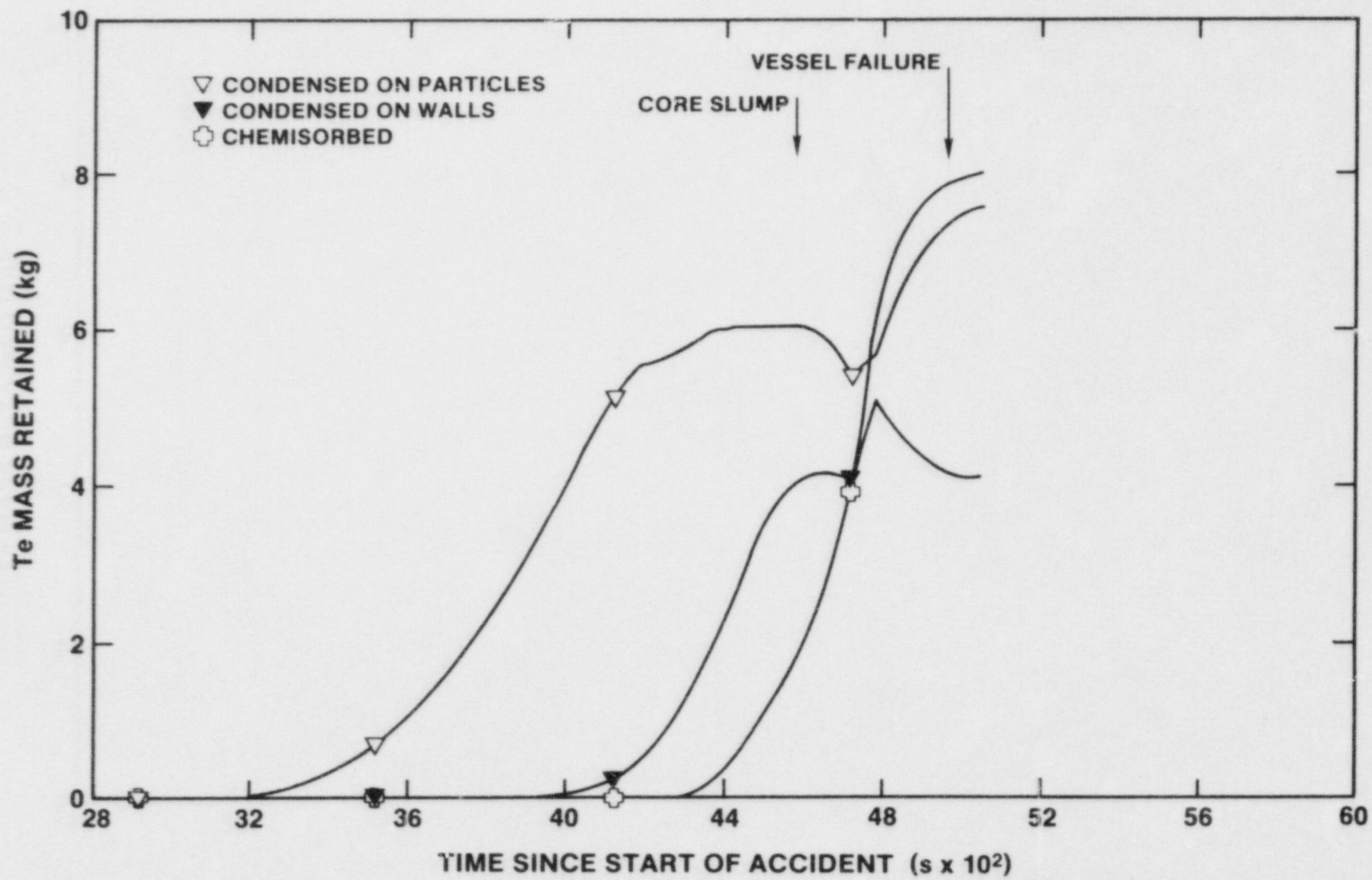

Figure 19. Te Mass Retained TMLB' High Pressure Ejection (Case A)

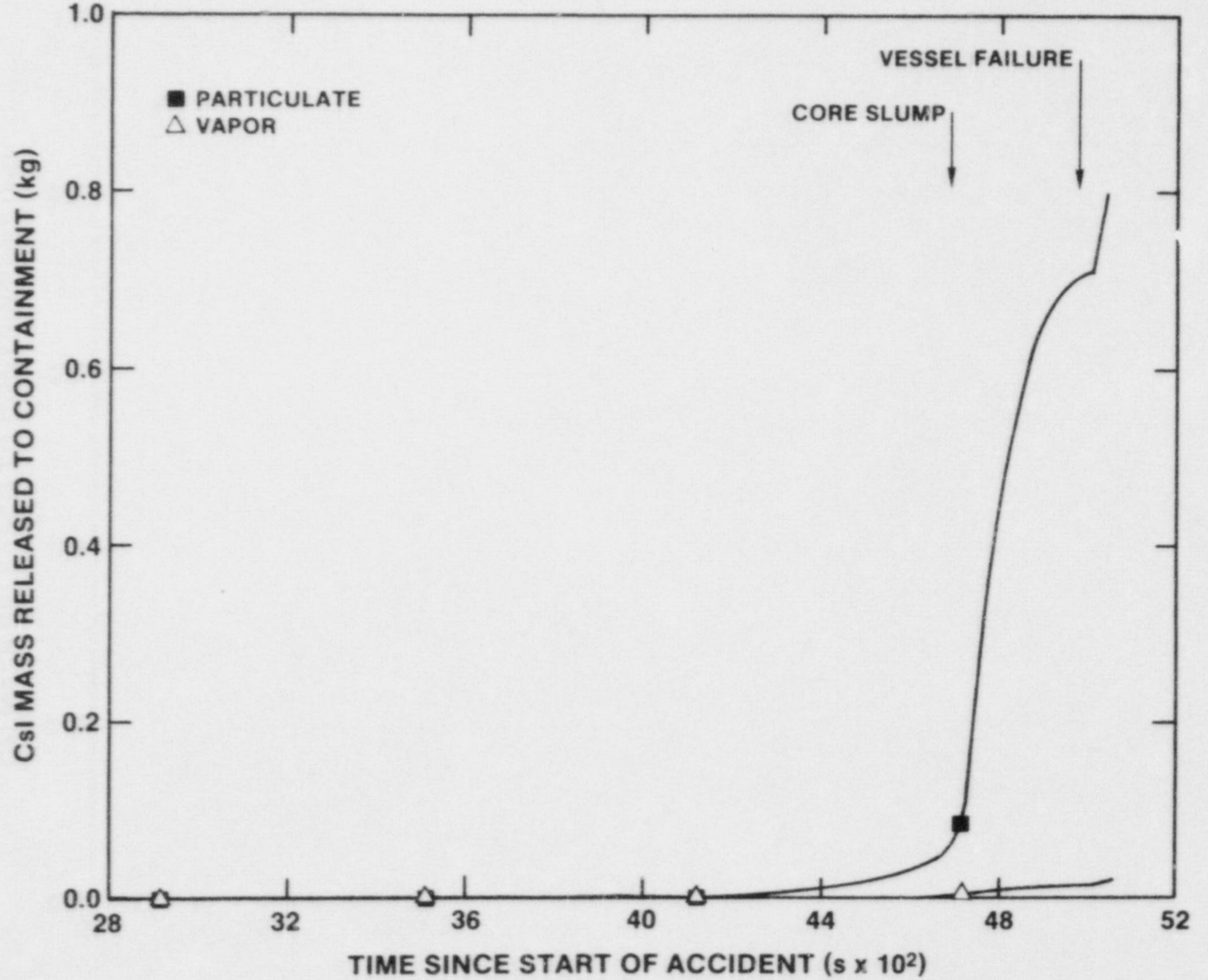

Figure 20. CsI Mass Released TMLB' High Pressure Ejection (Case A)

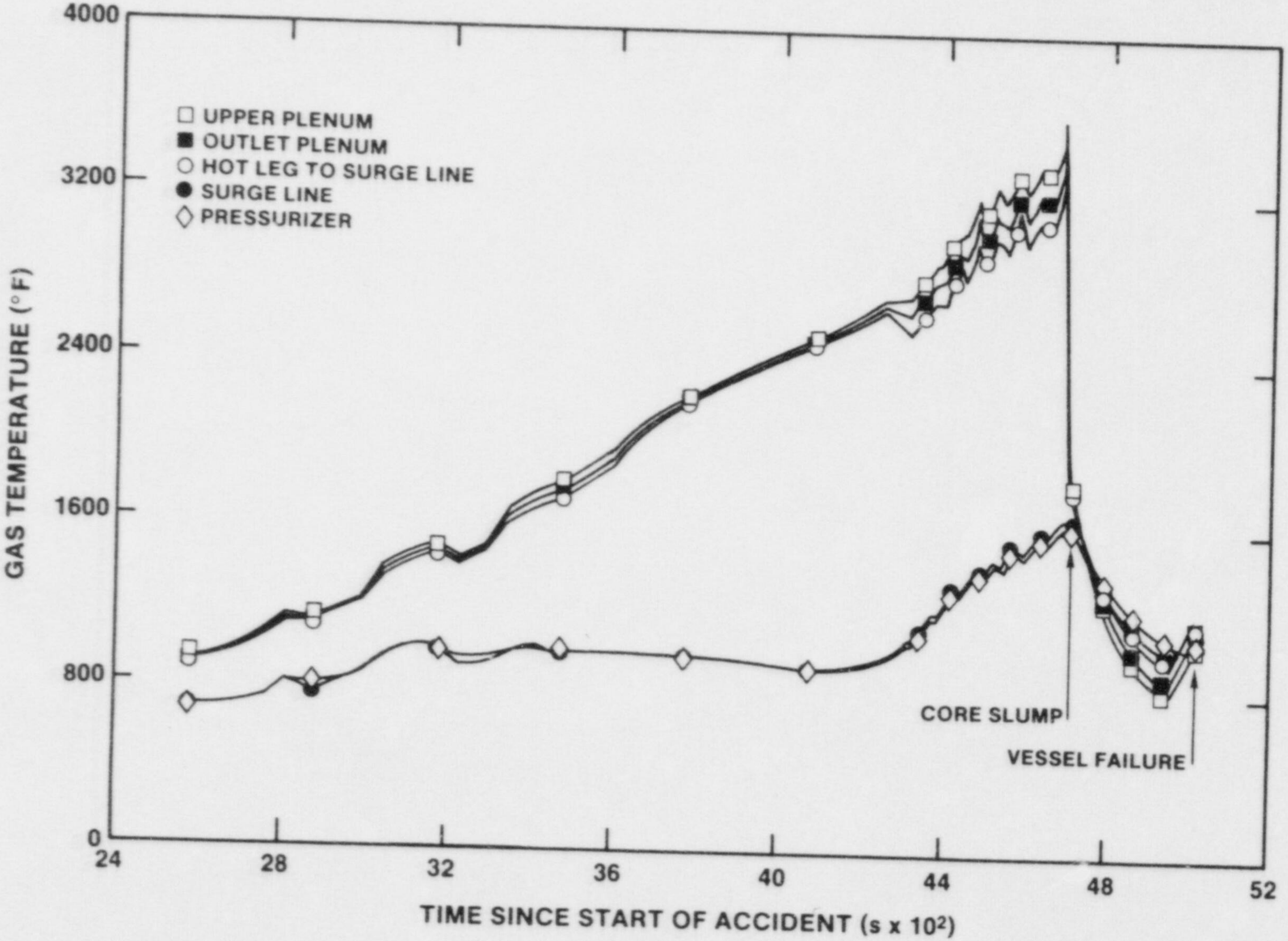

Figure 21. Primary System Gas Temperatures TMLB' High Pressure Ejection (Case B)

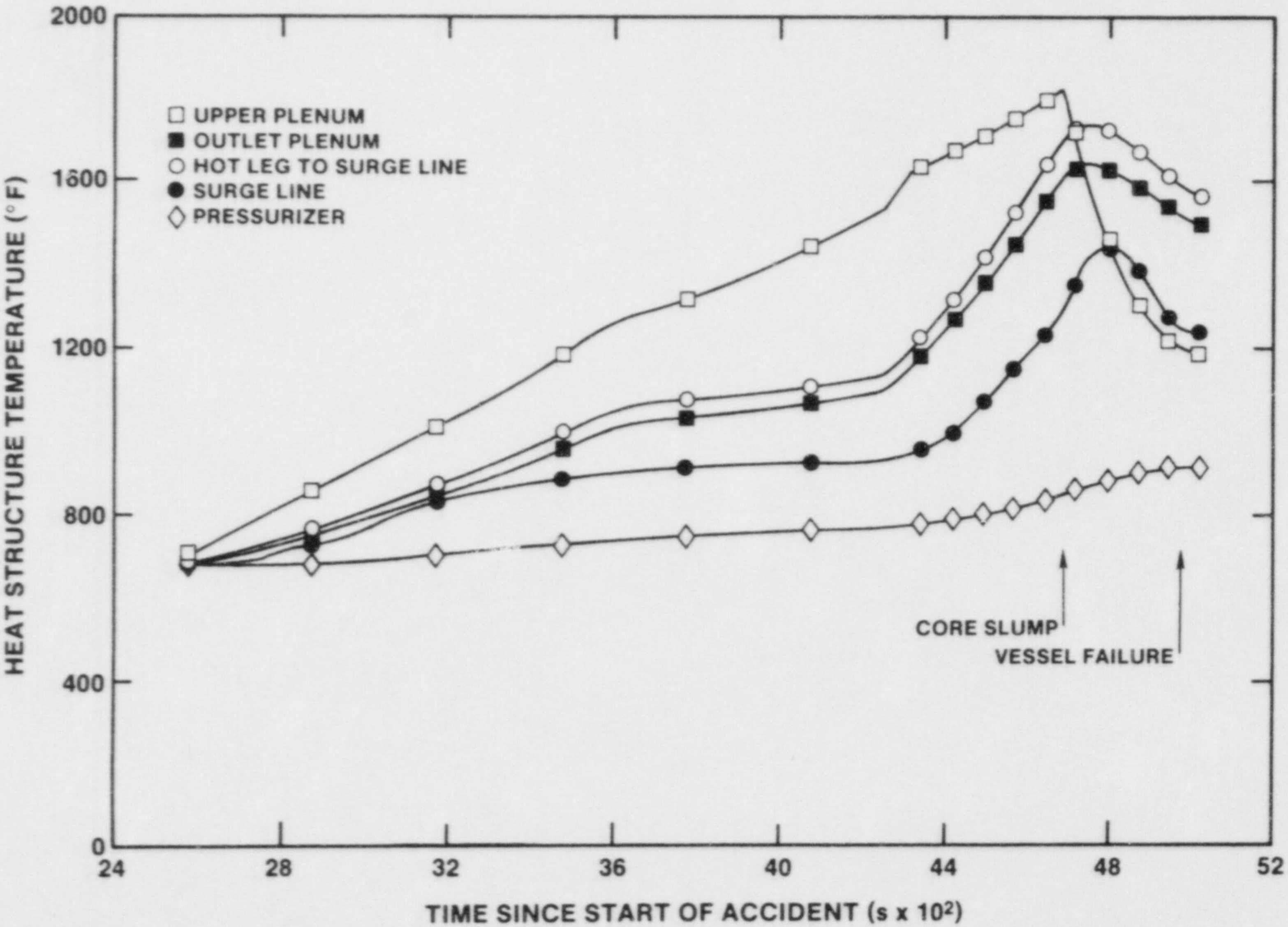

Figure 22. Primary System Structure Temperatures TMLB' High Pressure Ejection (Case Б)

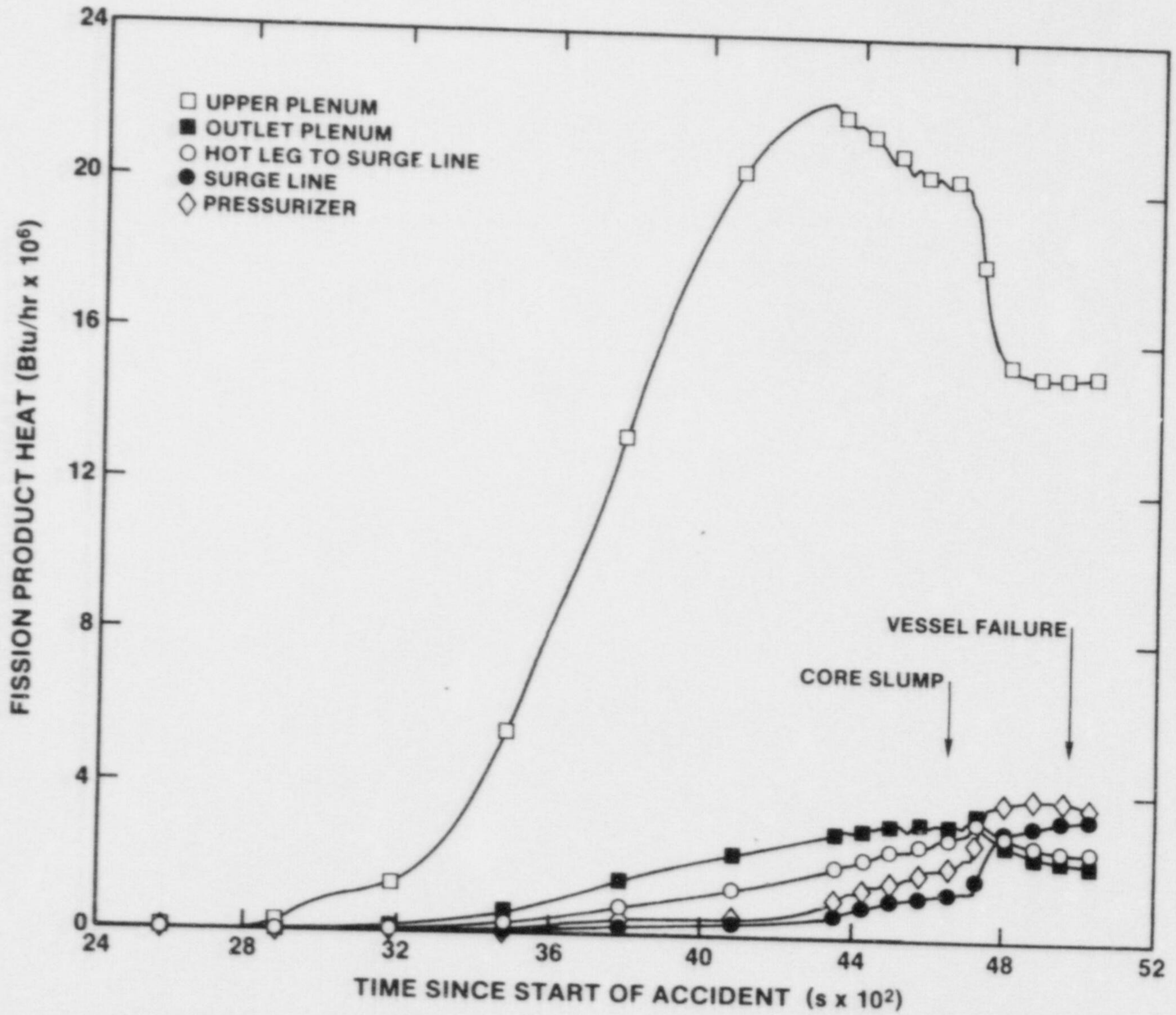

Figure 23. Fission Product Heating TMLB' High Pressure Ejection (Case B)

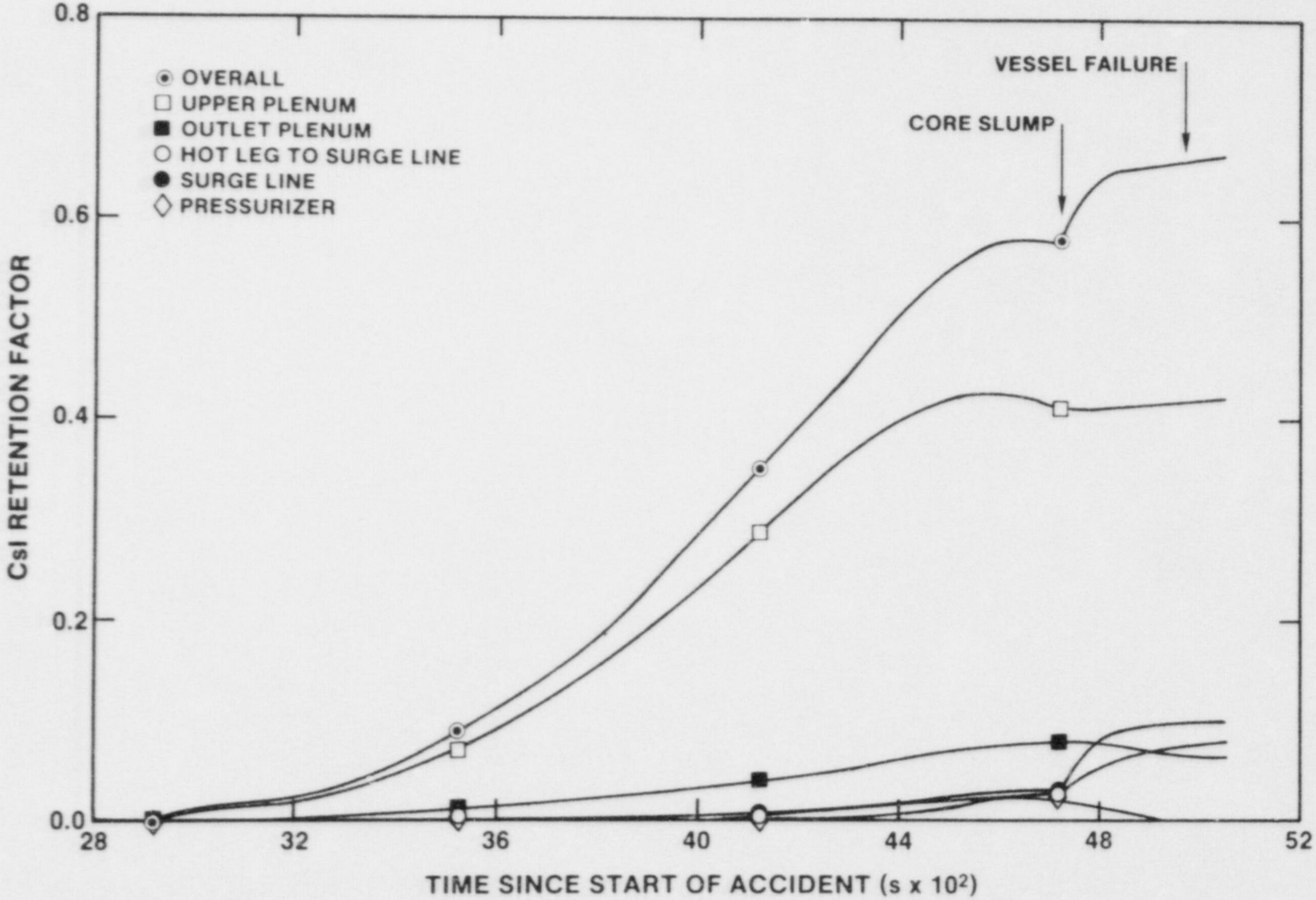

Figure 24. CsI Retention Factor TMLB' High Pressure Ejection (Case B)

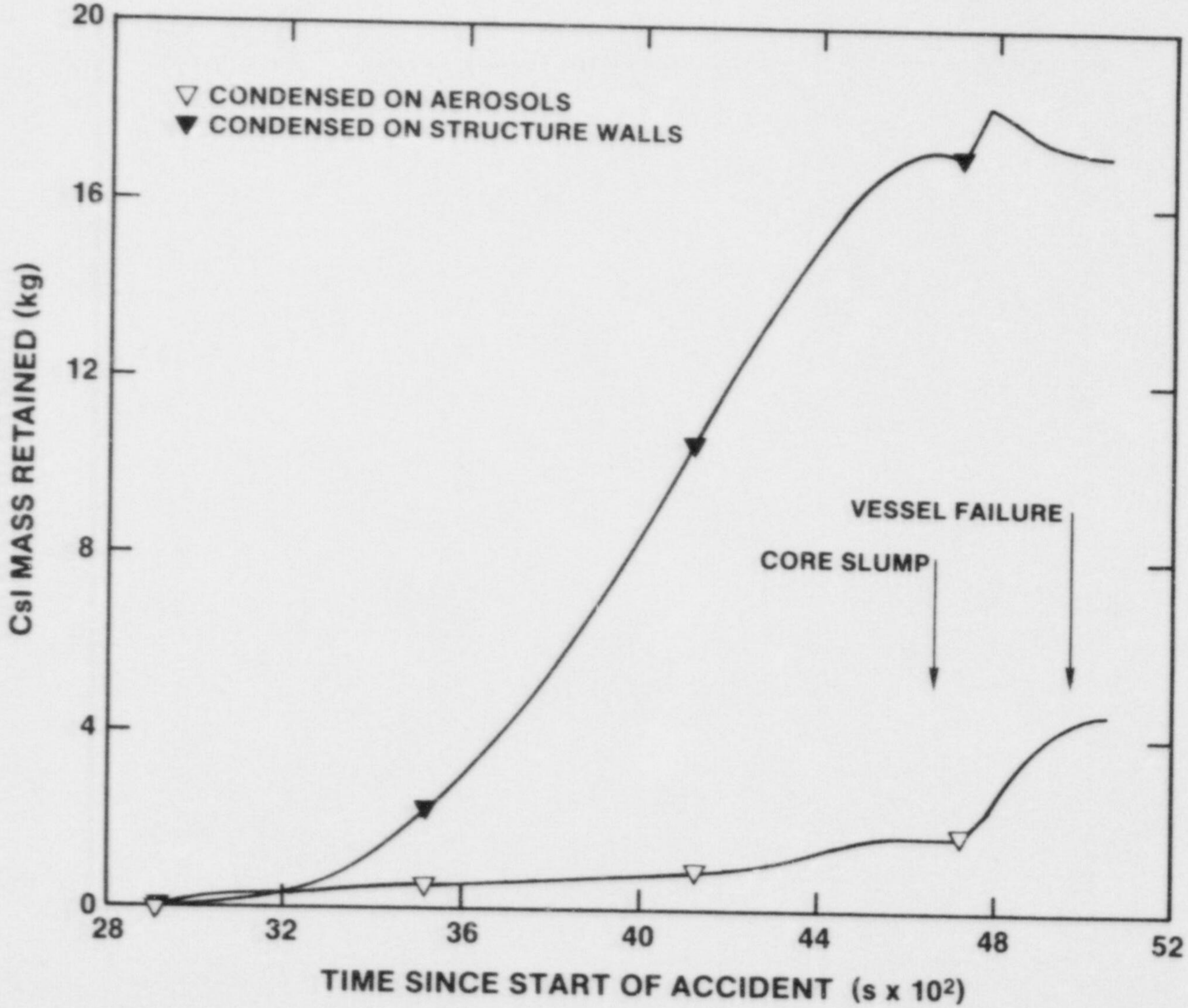

Figure 25. CsI Mass Retained TMLB' High Pressure Ejection (Case B)

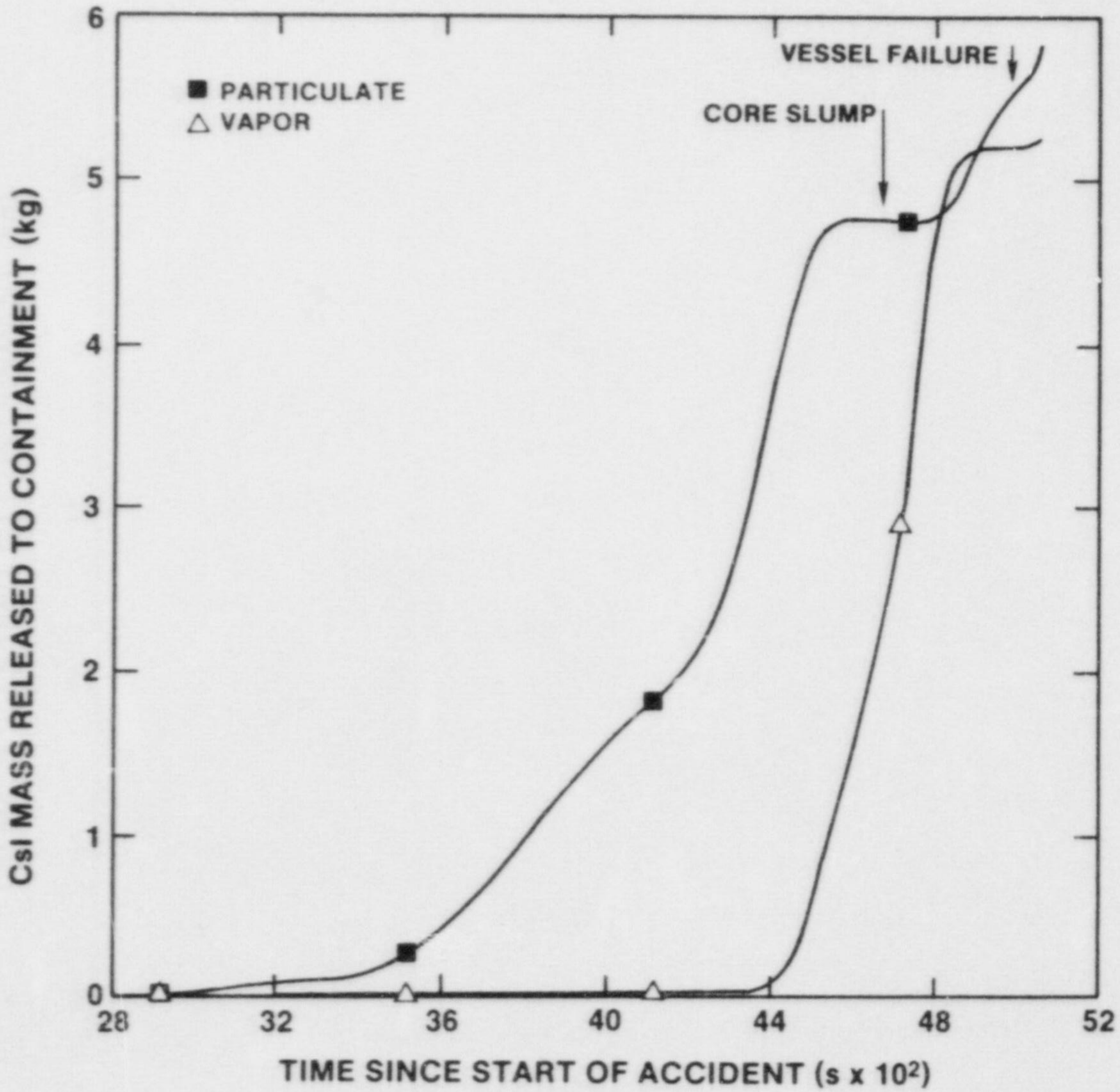

Figure 26. CsI Mass Released TMLB' High Pressure Ejection (Case B)

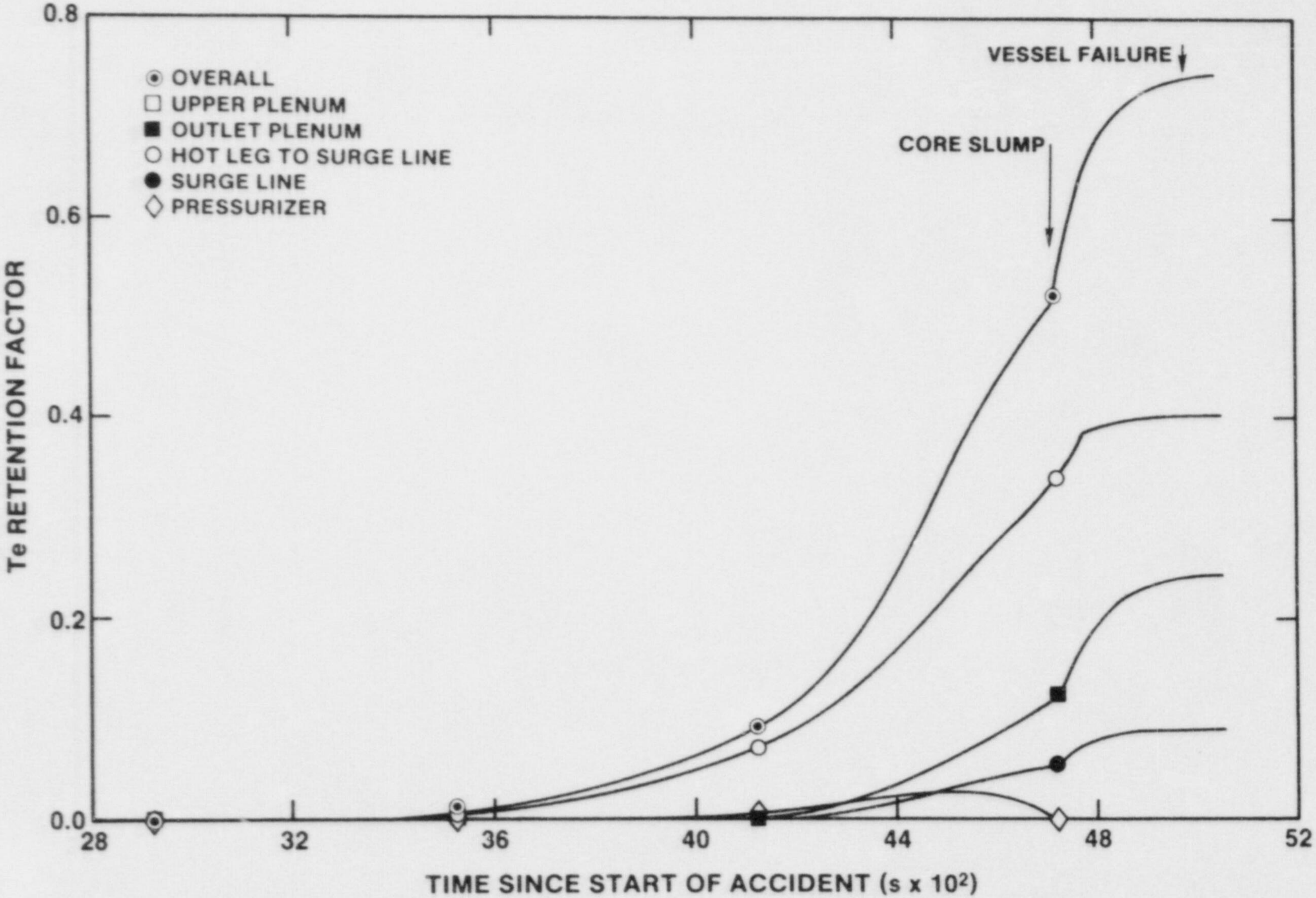

Figure 27. Te Retention Factor TMLB' High Pressure Ejection (Case B)

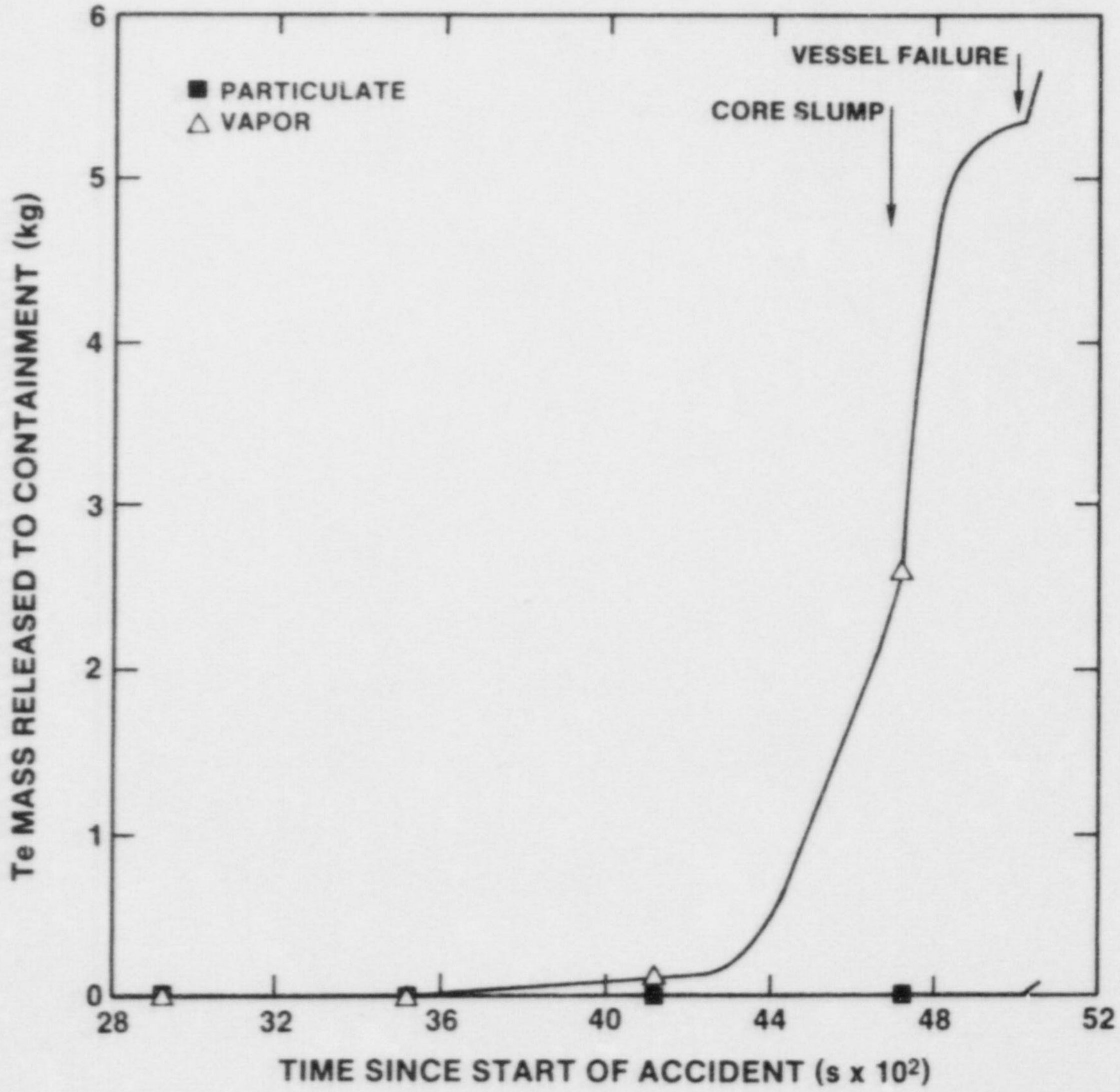

Figure 28. Te Mass Released TMLB' High Pressure Ejection (Case B)

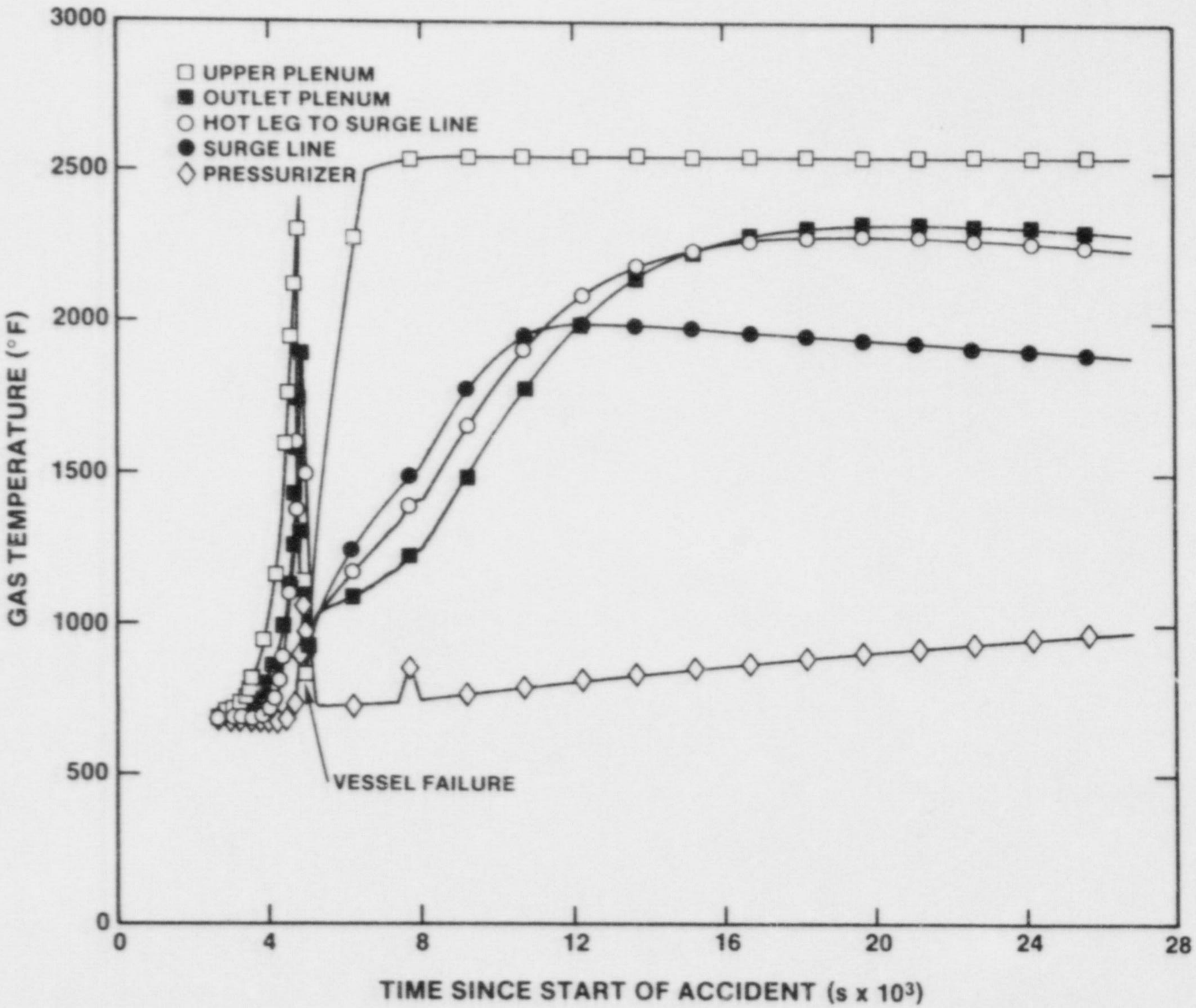

Figure 29. Primary System Gas Temperature TMLB' High Pressure Ejection (Case C)

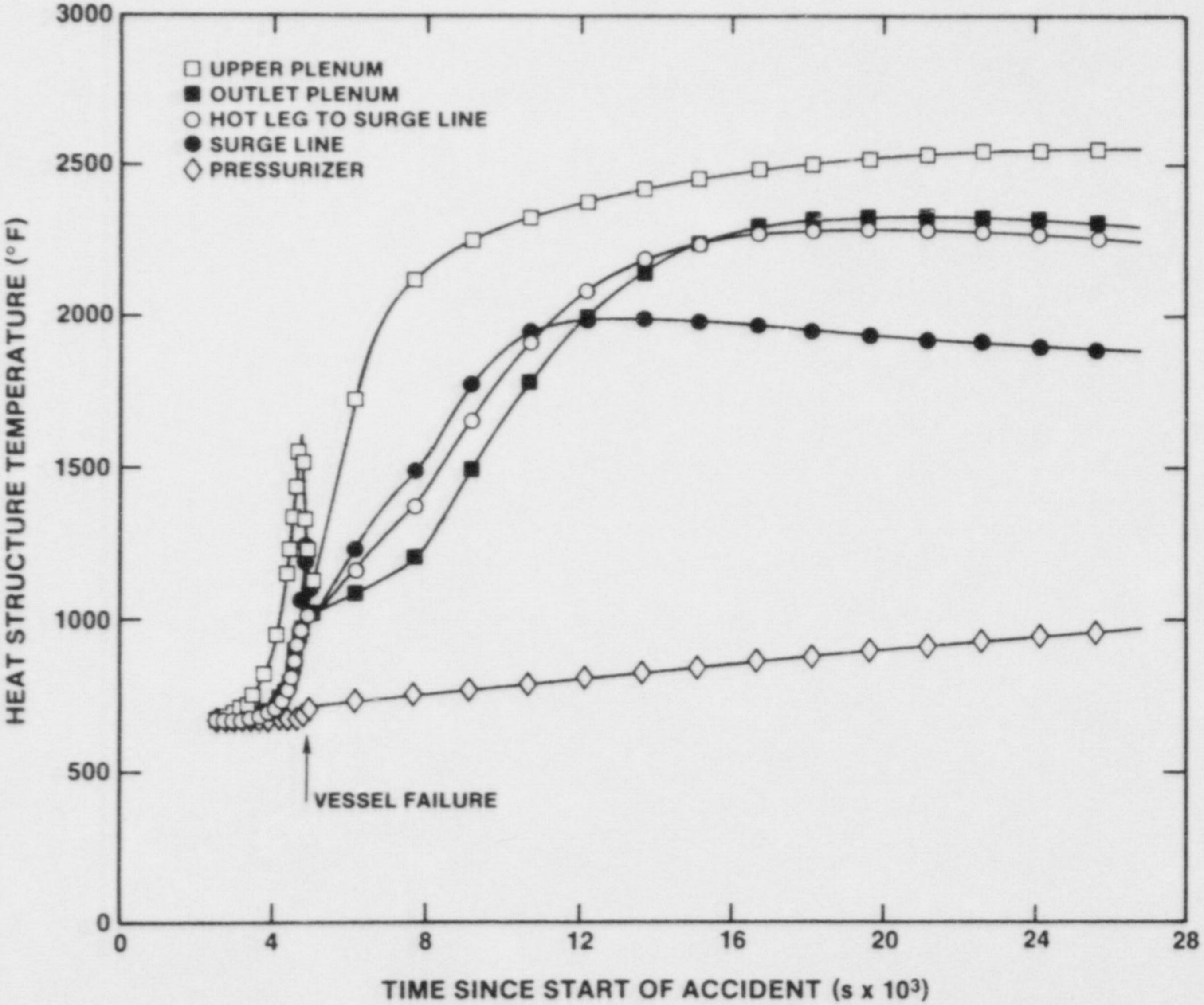

Figure 30. Primary System Structure Temperatures TMLB' High Pressure Ejection (Case C)

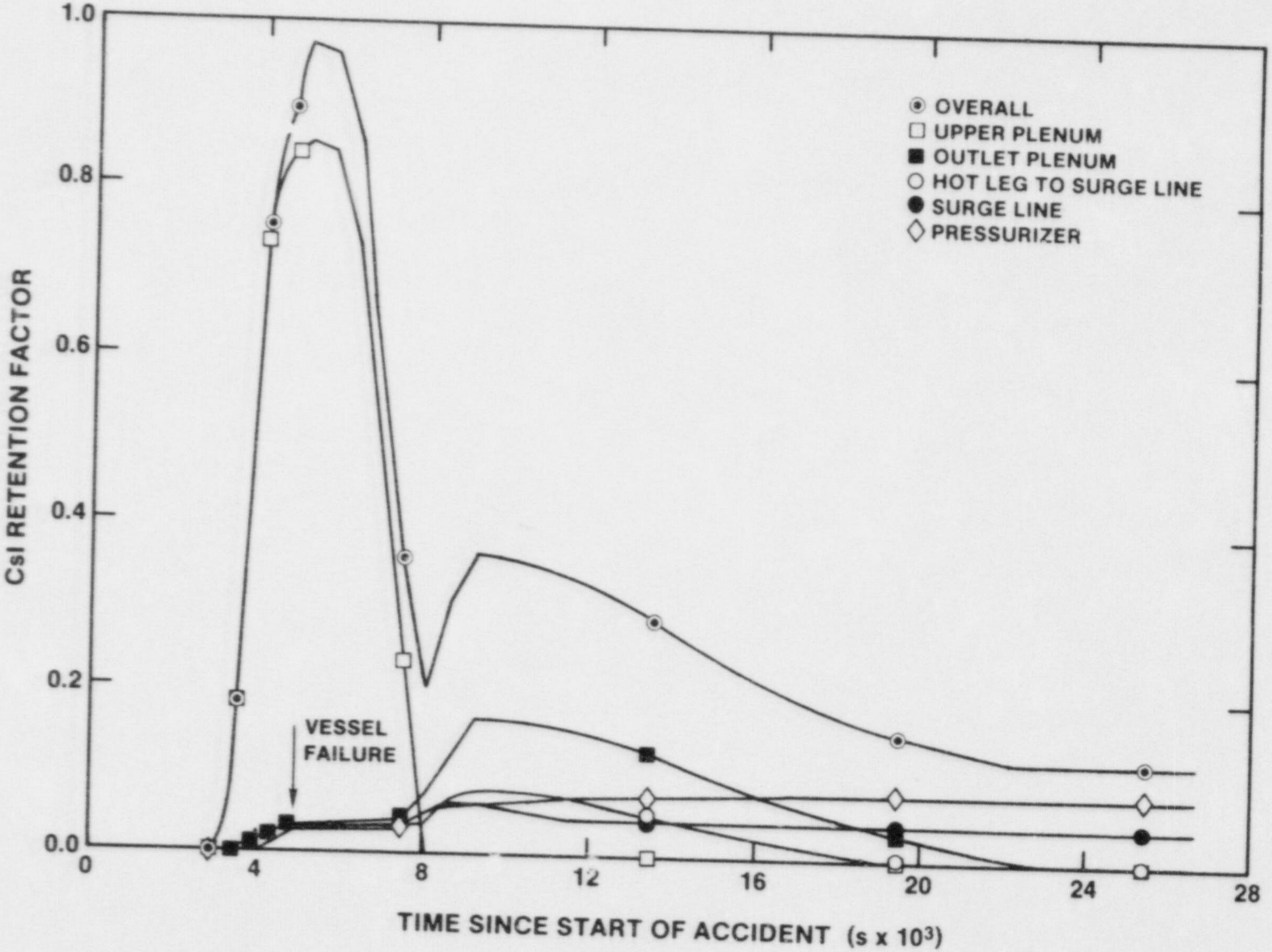

Figure 31. CsI Retention Factor TMLB' High Pressure Ejection (Case C)

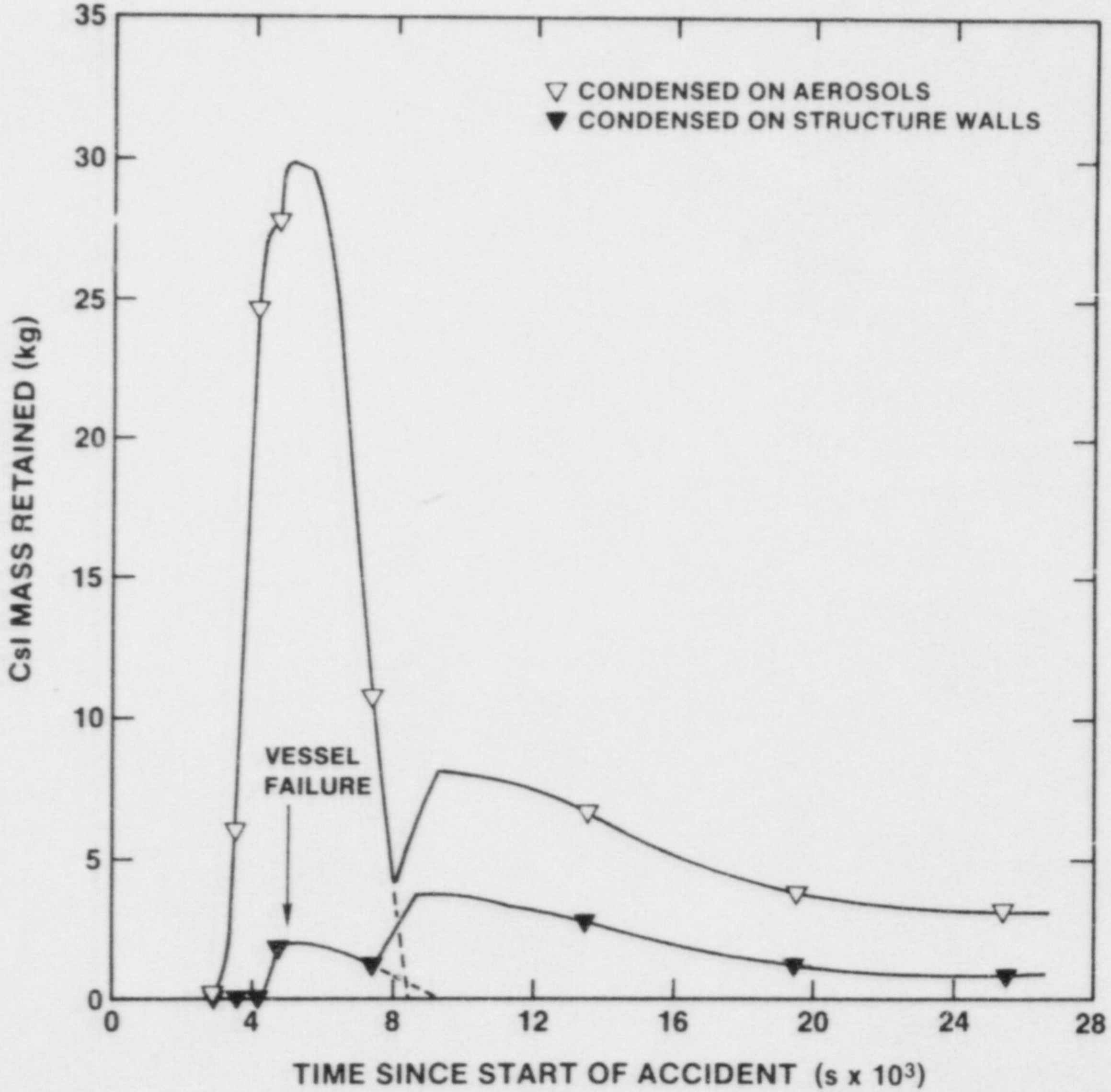

Figure 32. CsI Mass Retained TMLB' High Pressure Ejection (Case C)

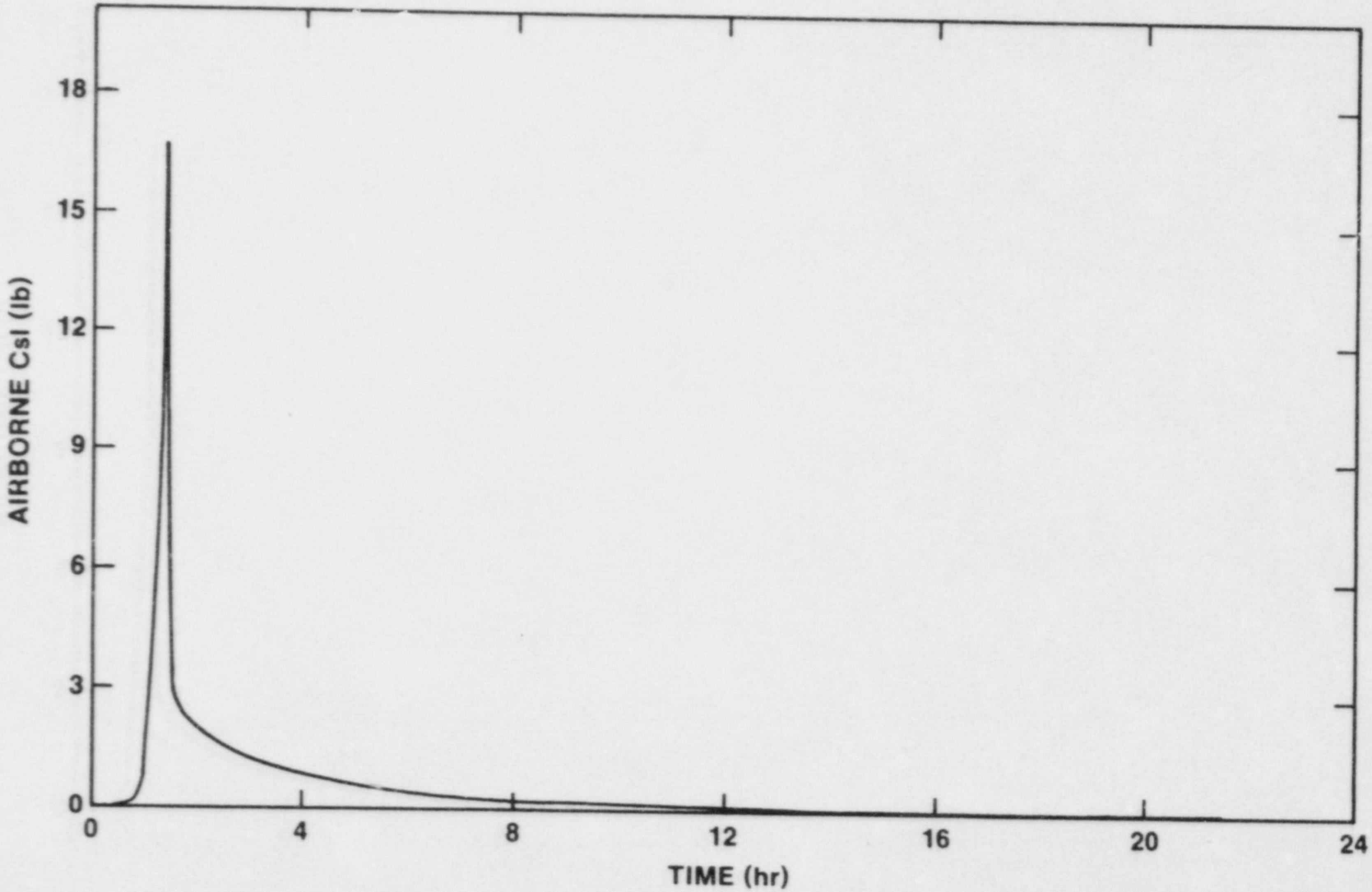

Figure 33. Airborne CsI TMLB' High Pressure Ejection (Case-011B)

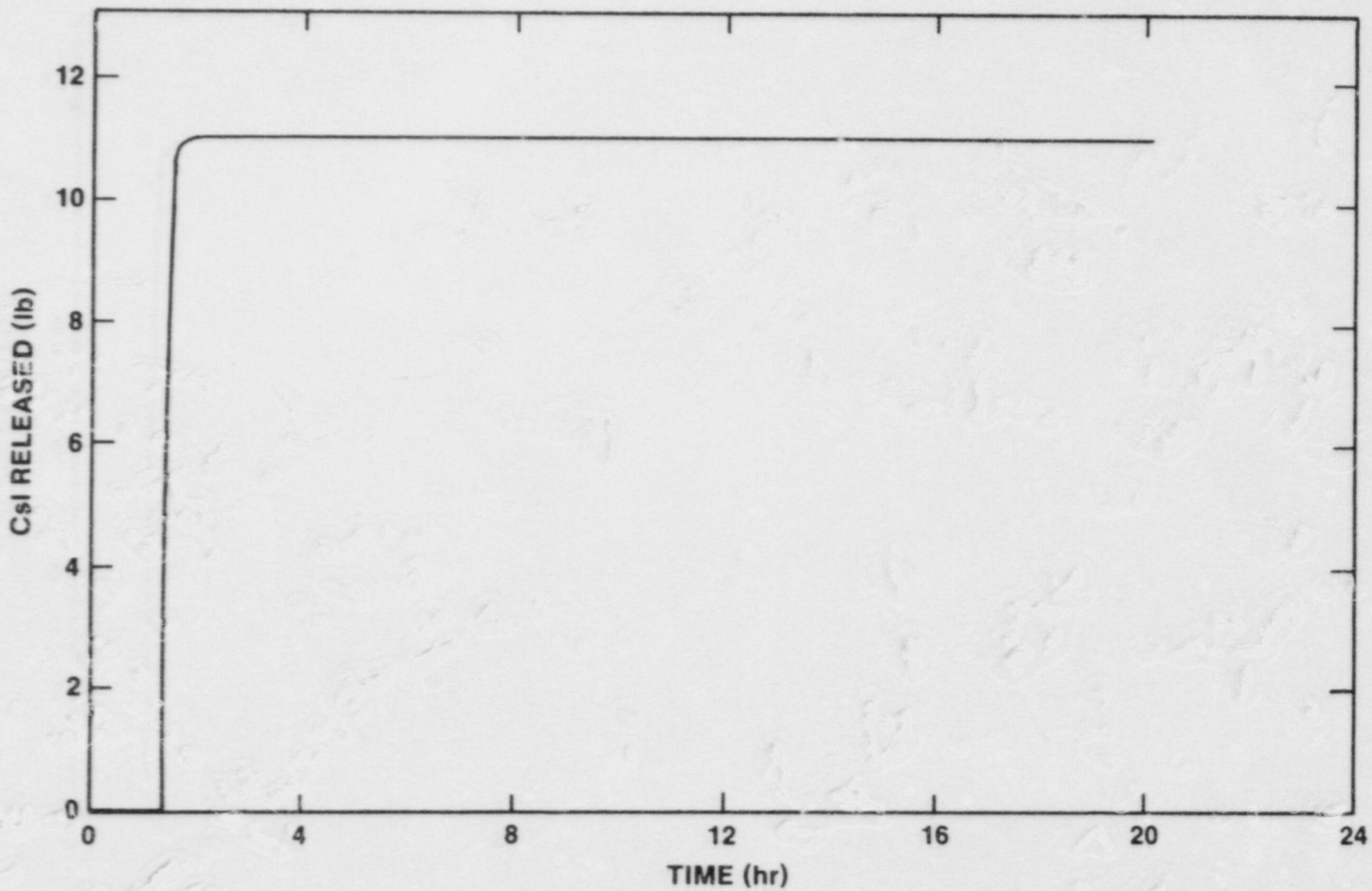

Figure 34. Leaked CsI TMLB' High Pressure Ejection (Case-011B)

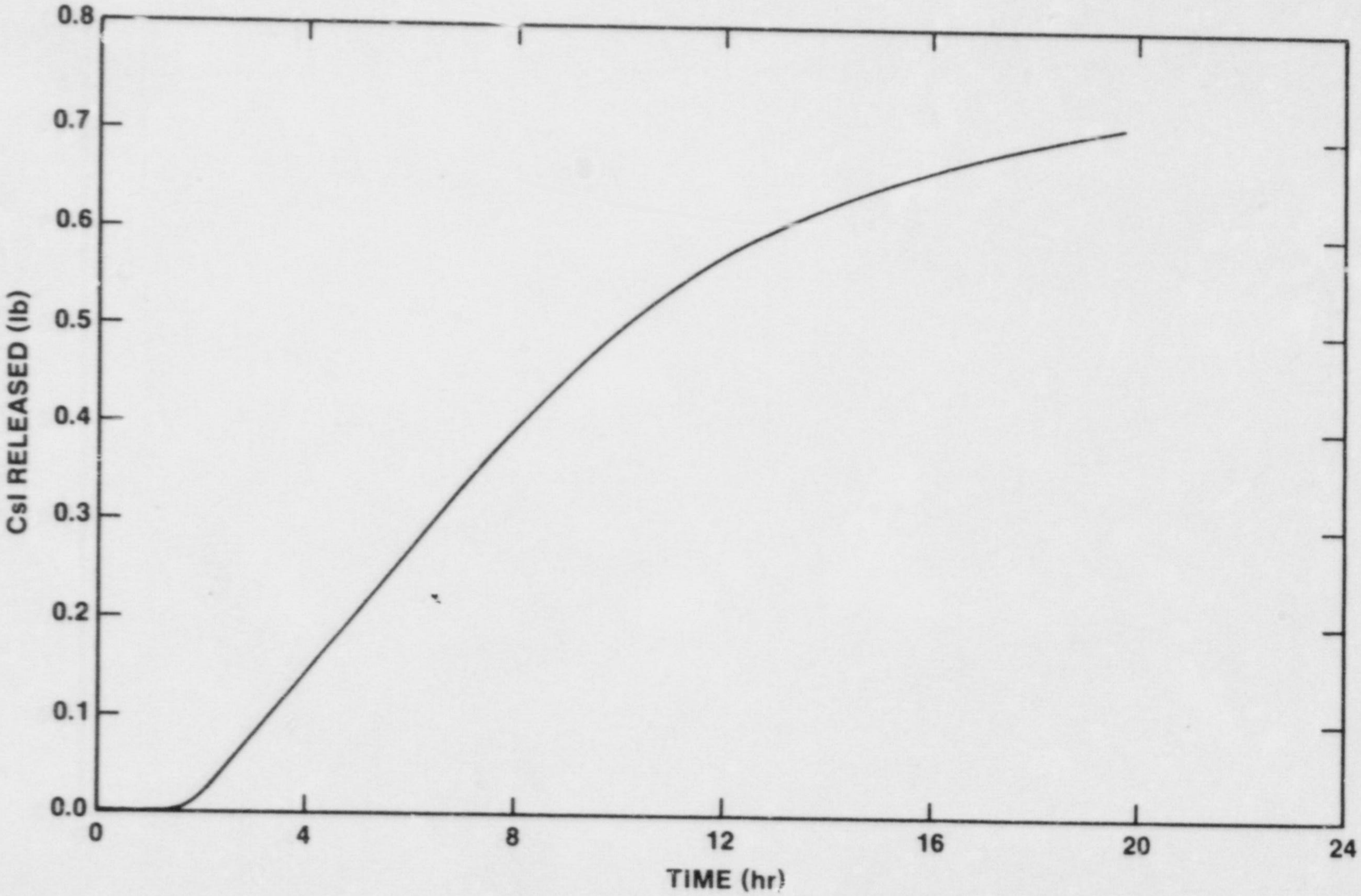

Figure 35. Leaked CsI TMLB' High Pressure Ejection (Case-012A)

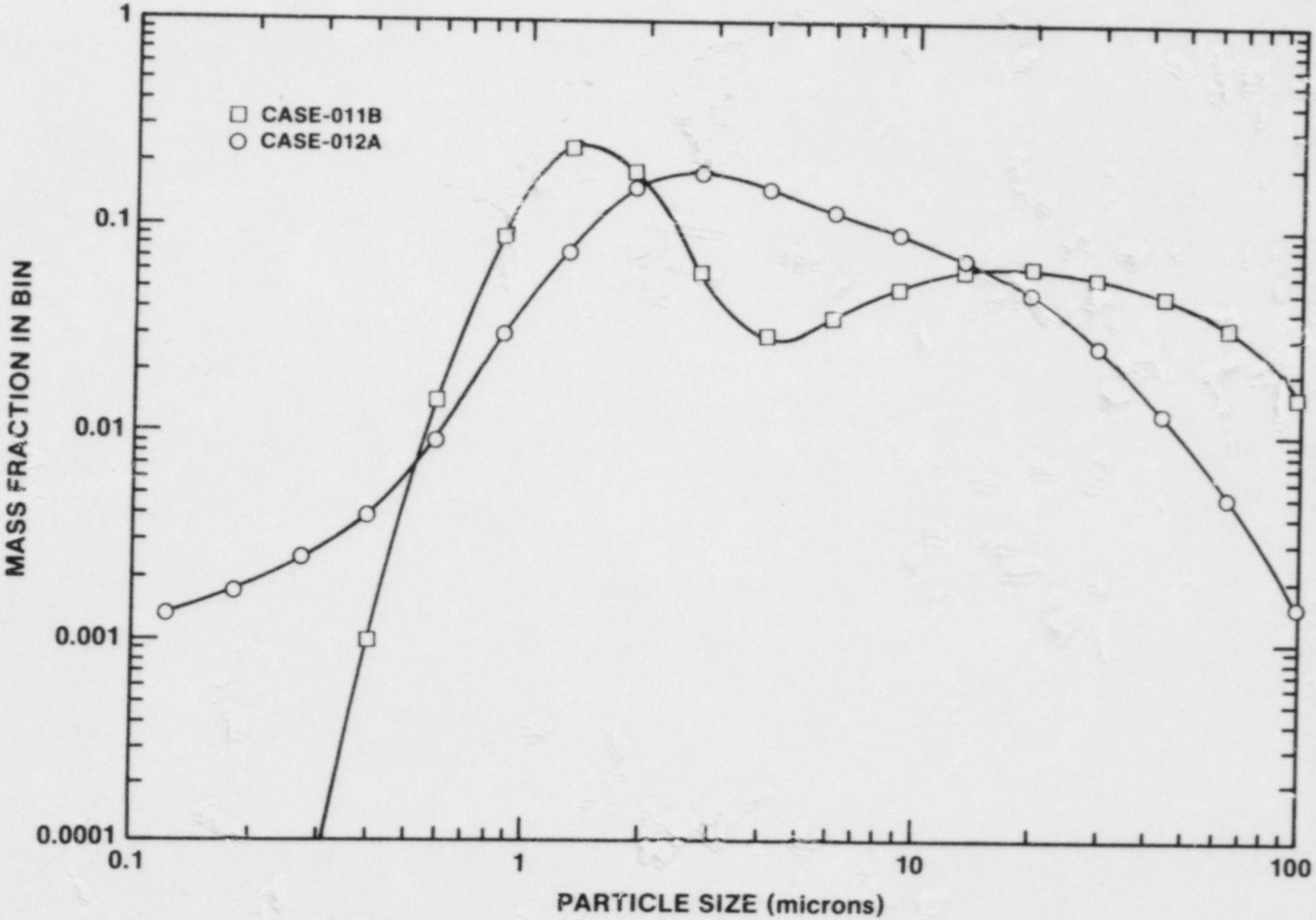

Figure 36. Leaked Aerosol Size Distribution TMLB' High Pressure Ejection

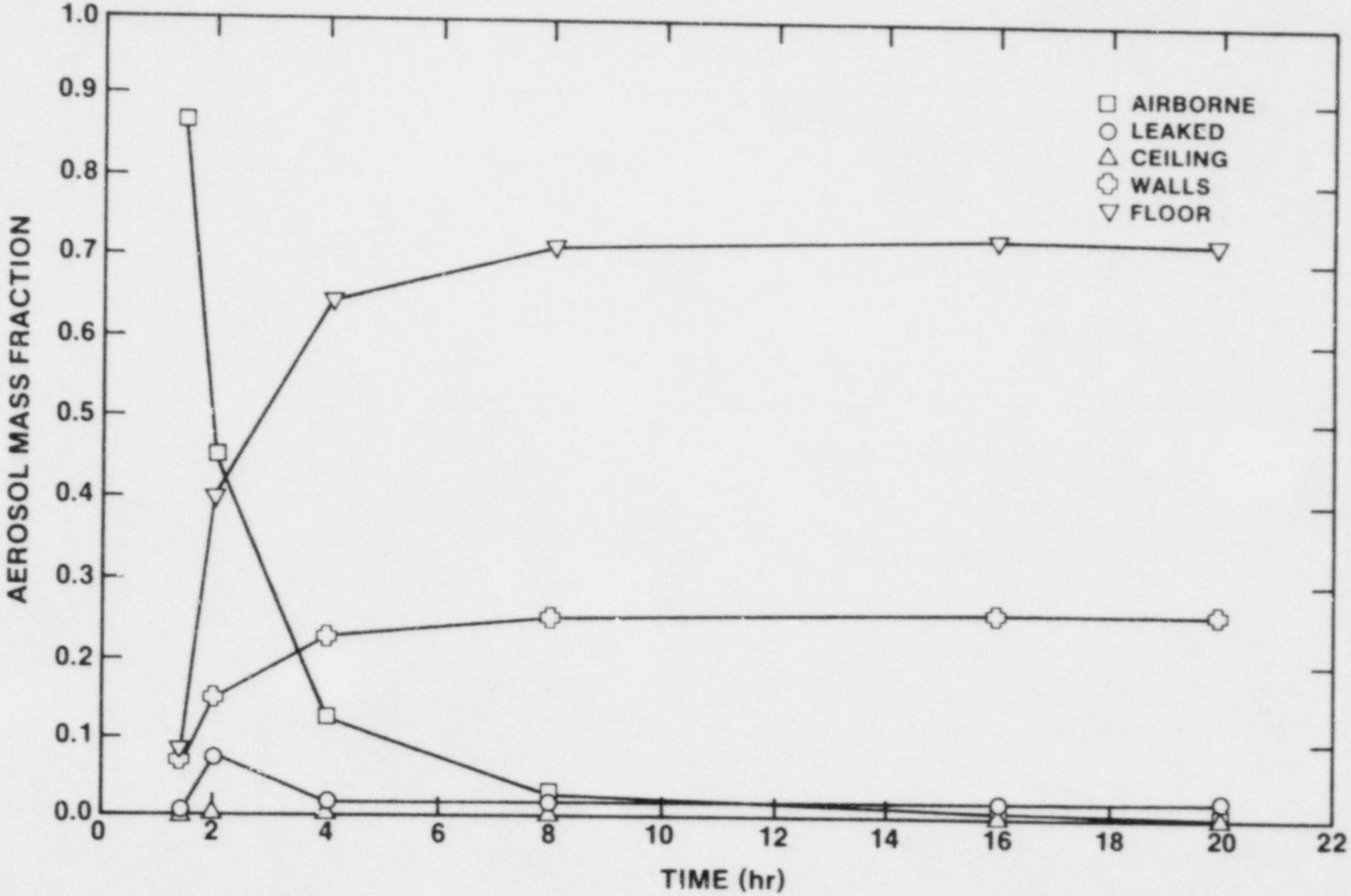

Figure 38. Aerosol Disposition TMLB' High Pressure Ejection (Case-012A)

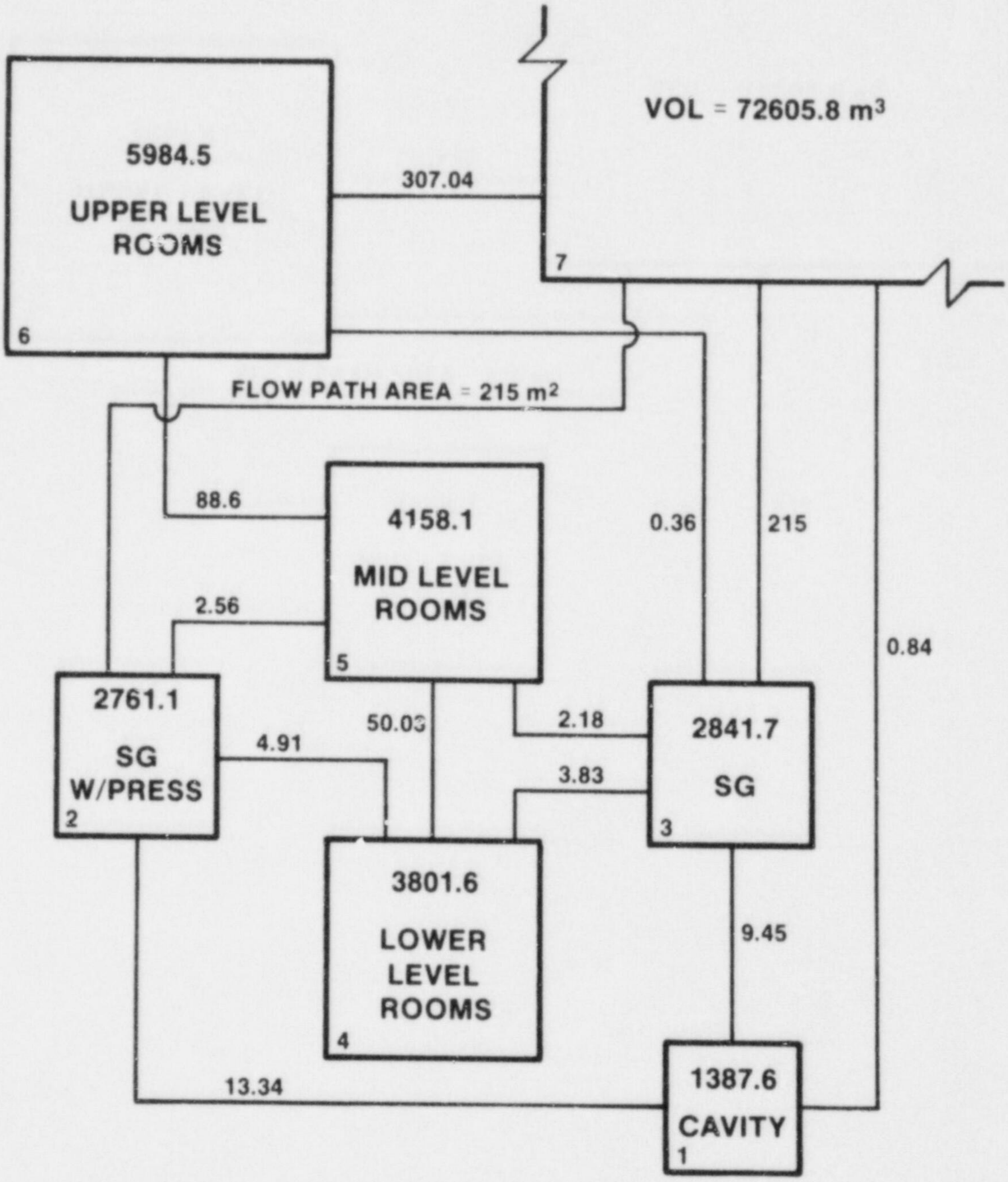

Figure 39. Diagram of Multi-Cell CONTAIN Code Model

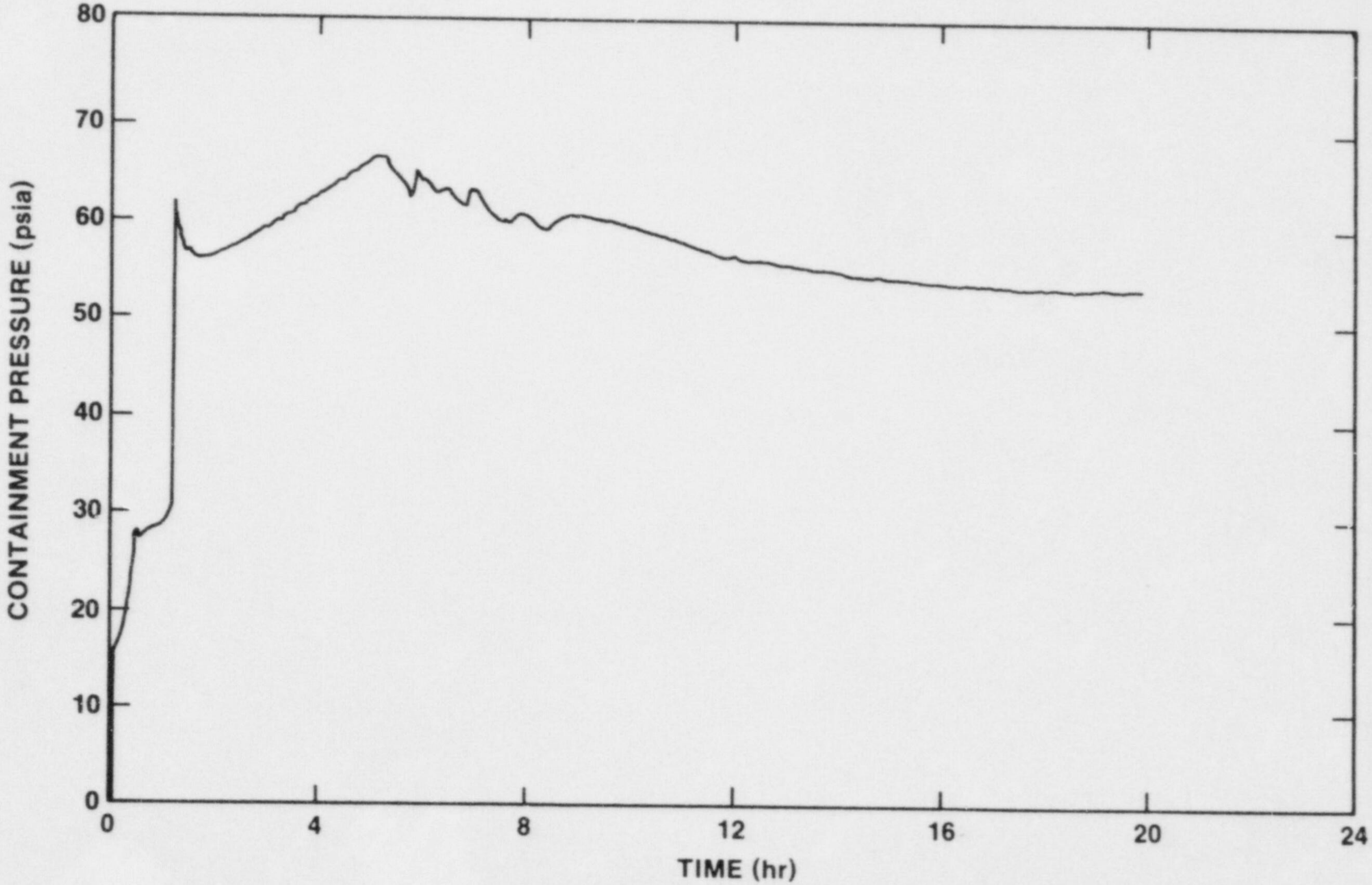

Figure 40. Containment Pressure TMLB' Pump Seal LOCA (Case-030)

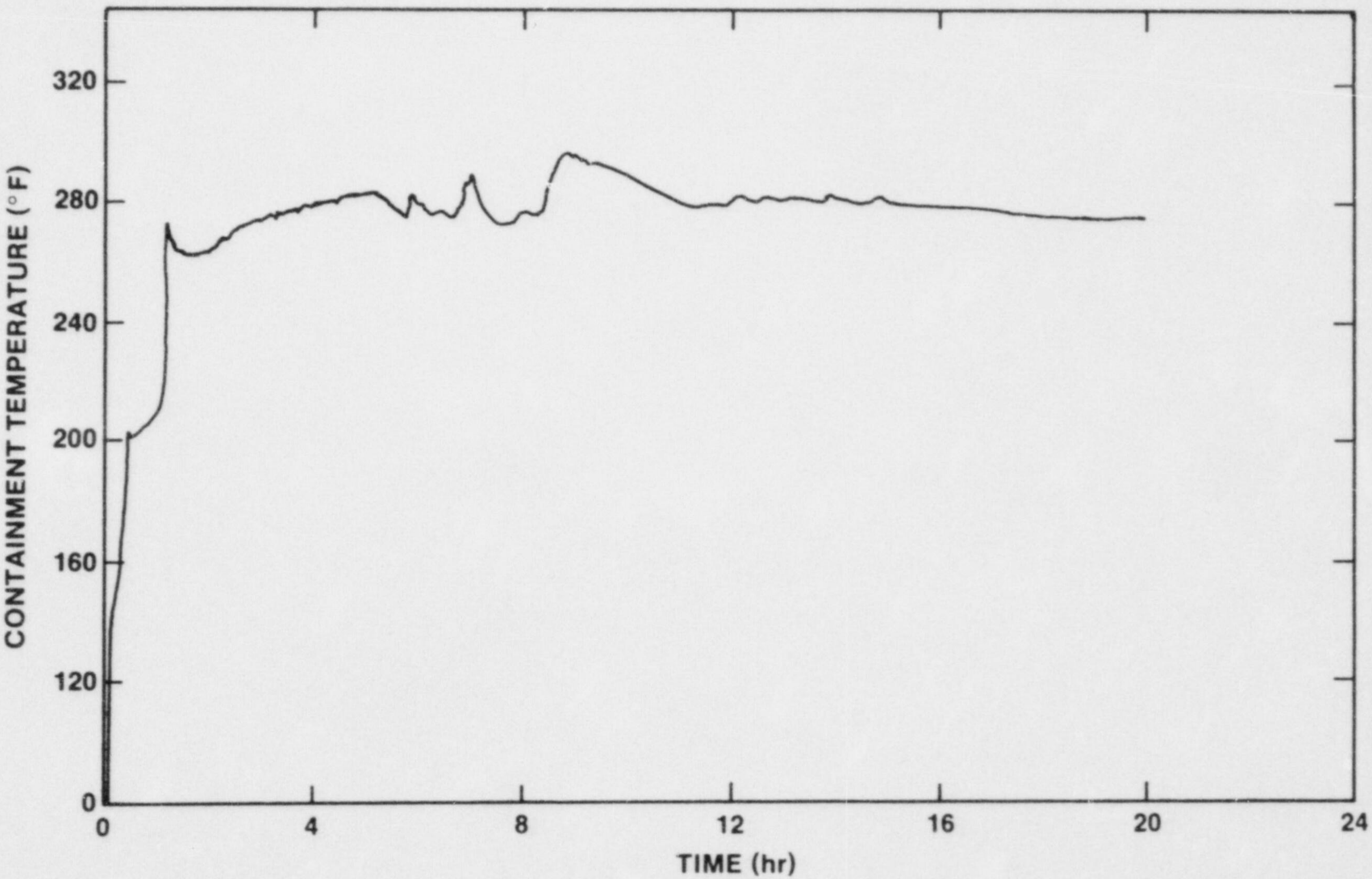

Figure 41. Containment Temperature TMLB' Pump Seal LOCA (Case-030)

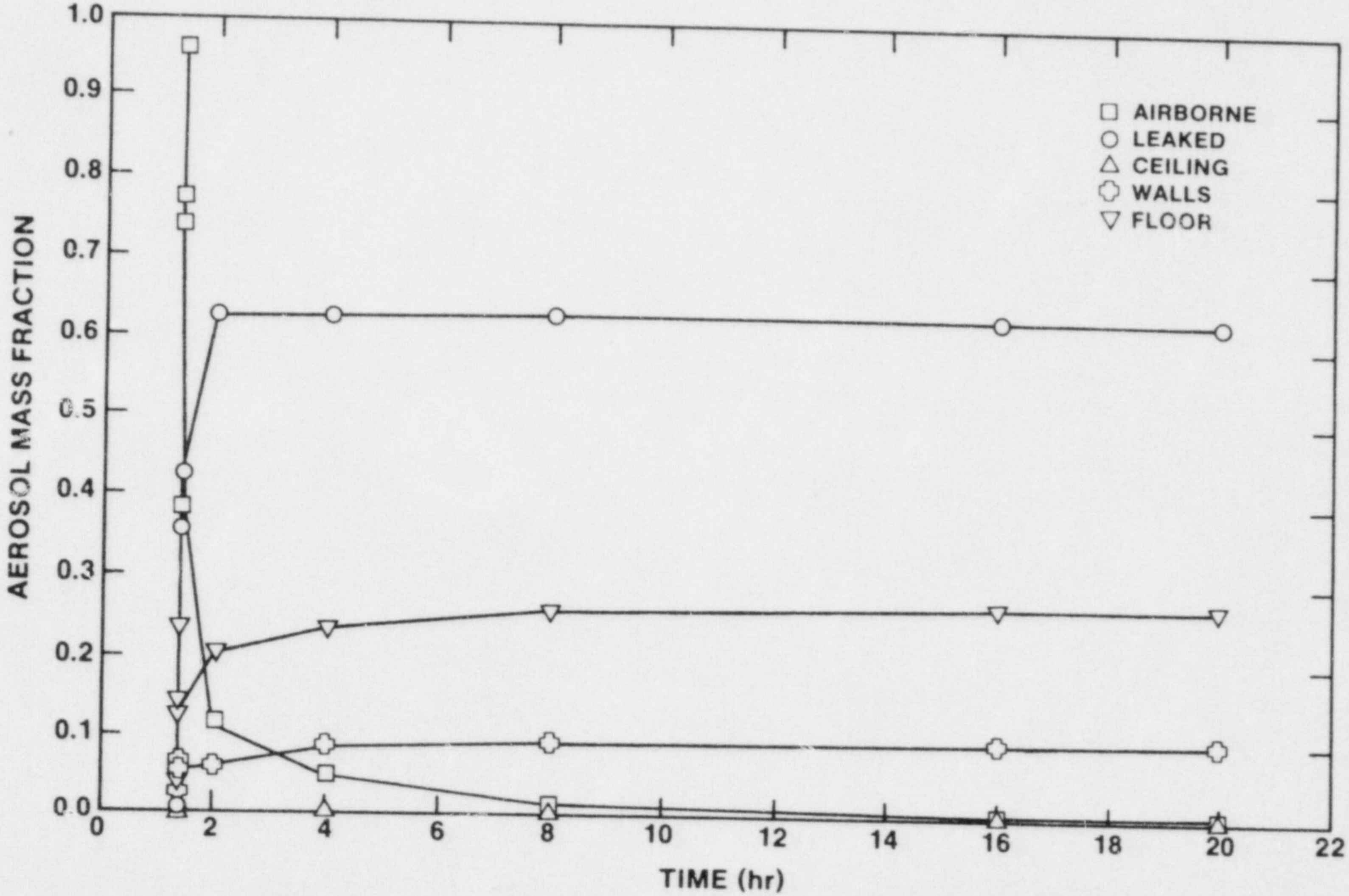

Figure 37. Aerosol Disposition TMLB' High Pressure Ejection (Case-011B)

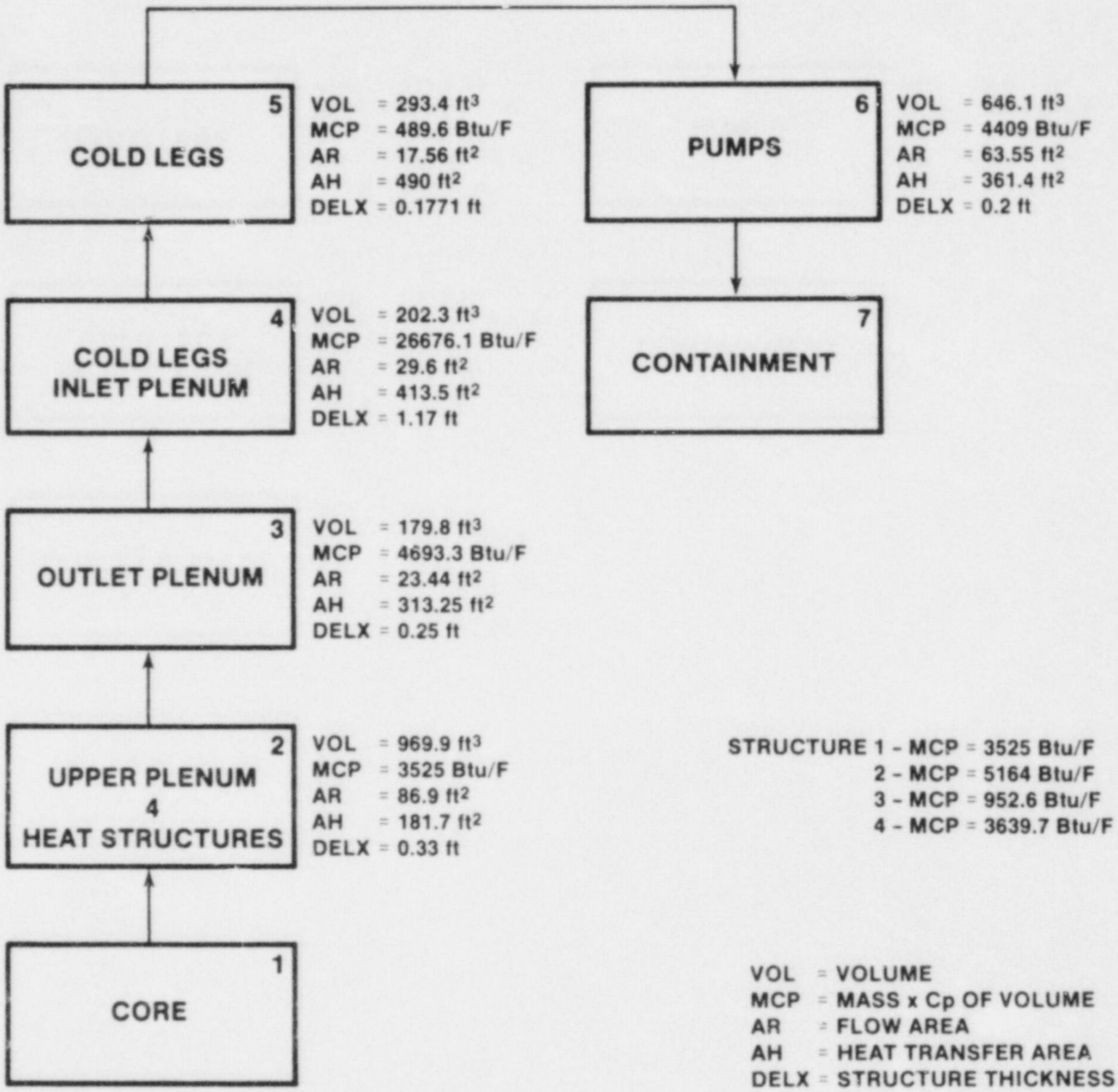

Figure 42. Primary System Flow Path TMLB' Pump Seal LOCA

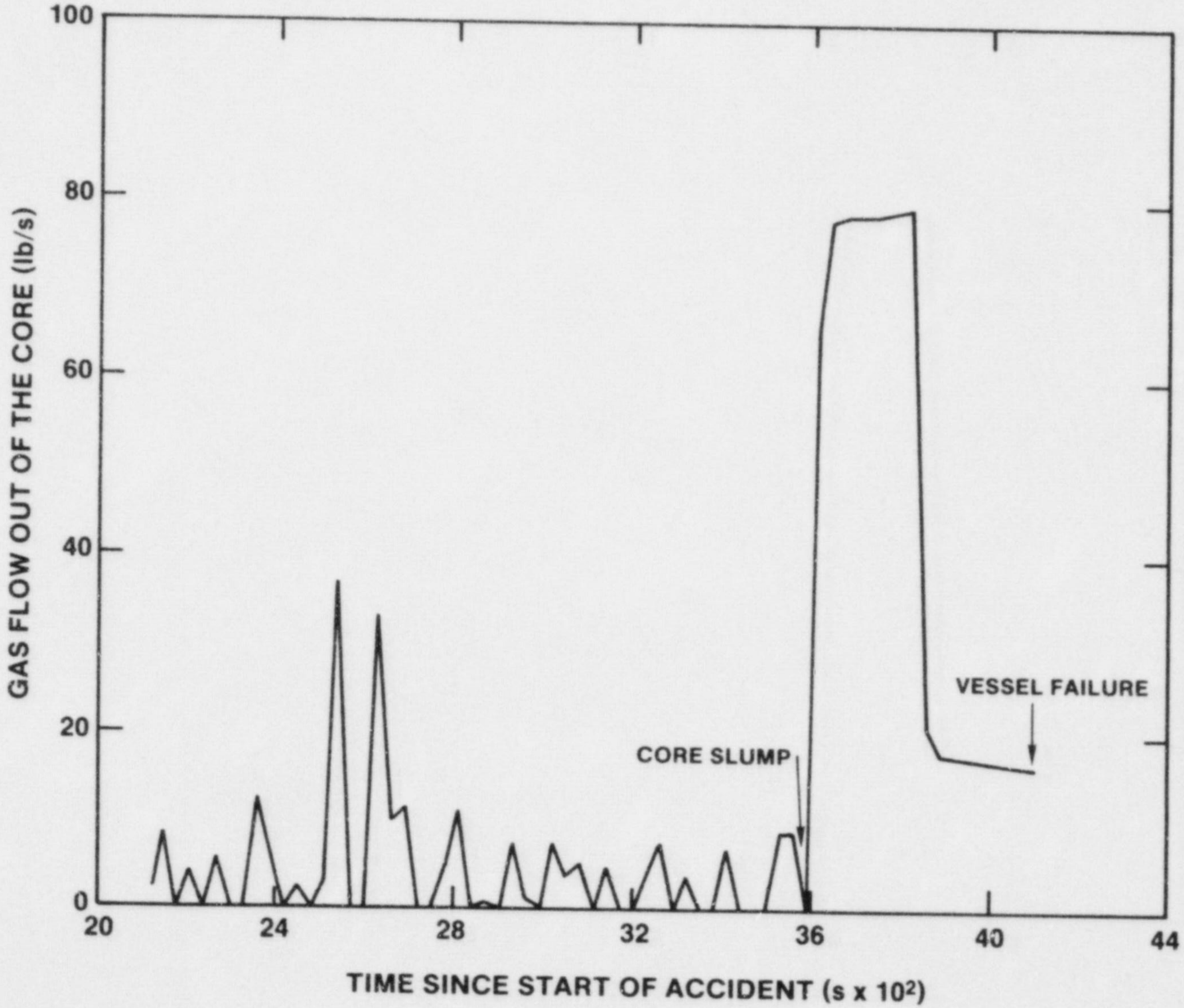

Figure 43. Outlet Gas Flow TMLB' Pump Seal LOCA

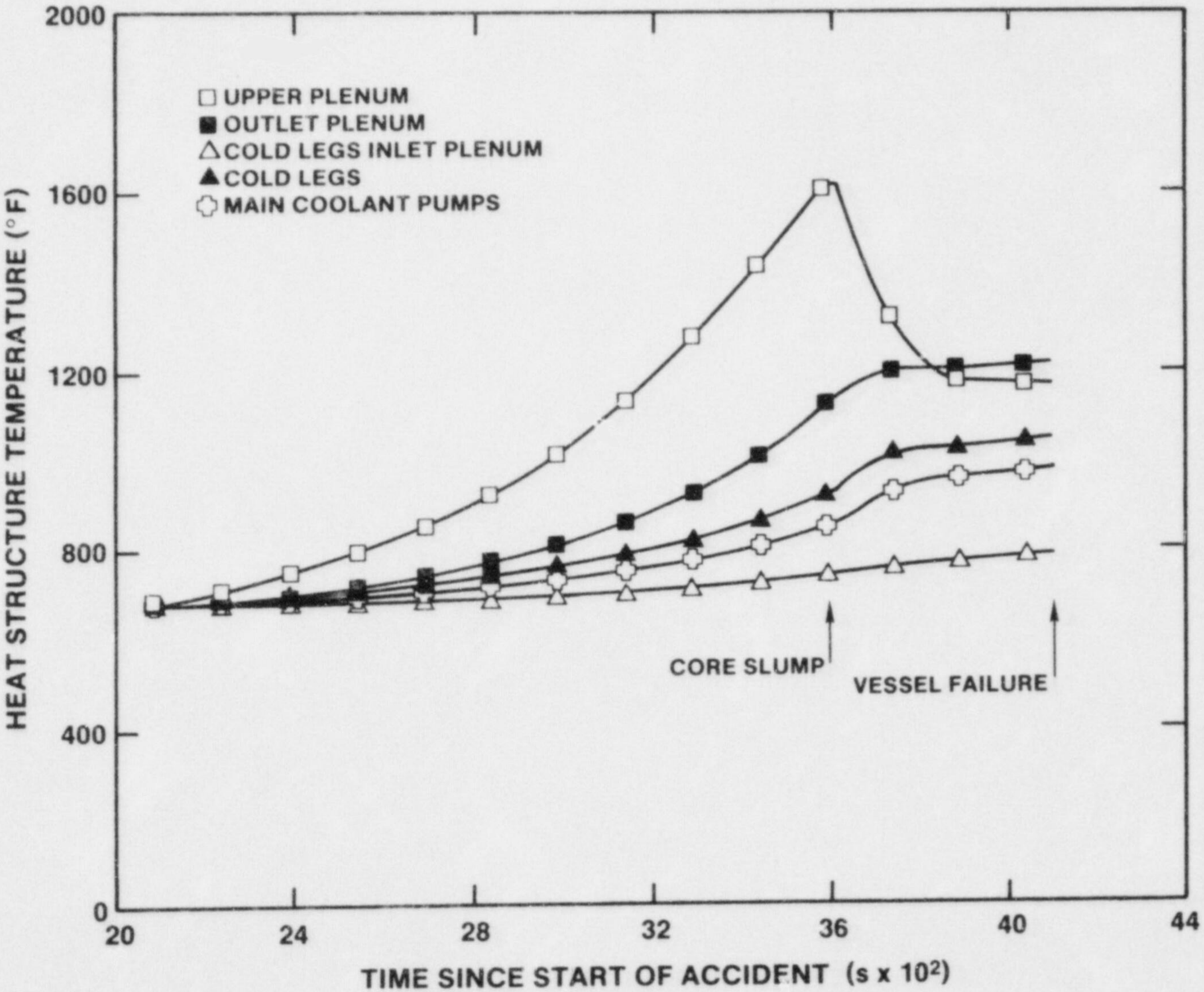

Figure 44. Primary System Structure Temperatures TMLB' Pump Seal LOCA (Case A)

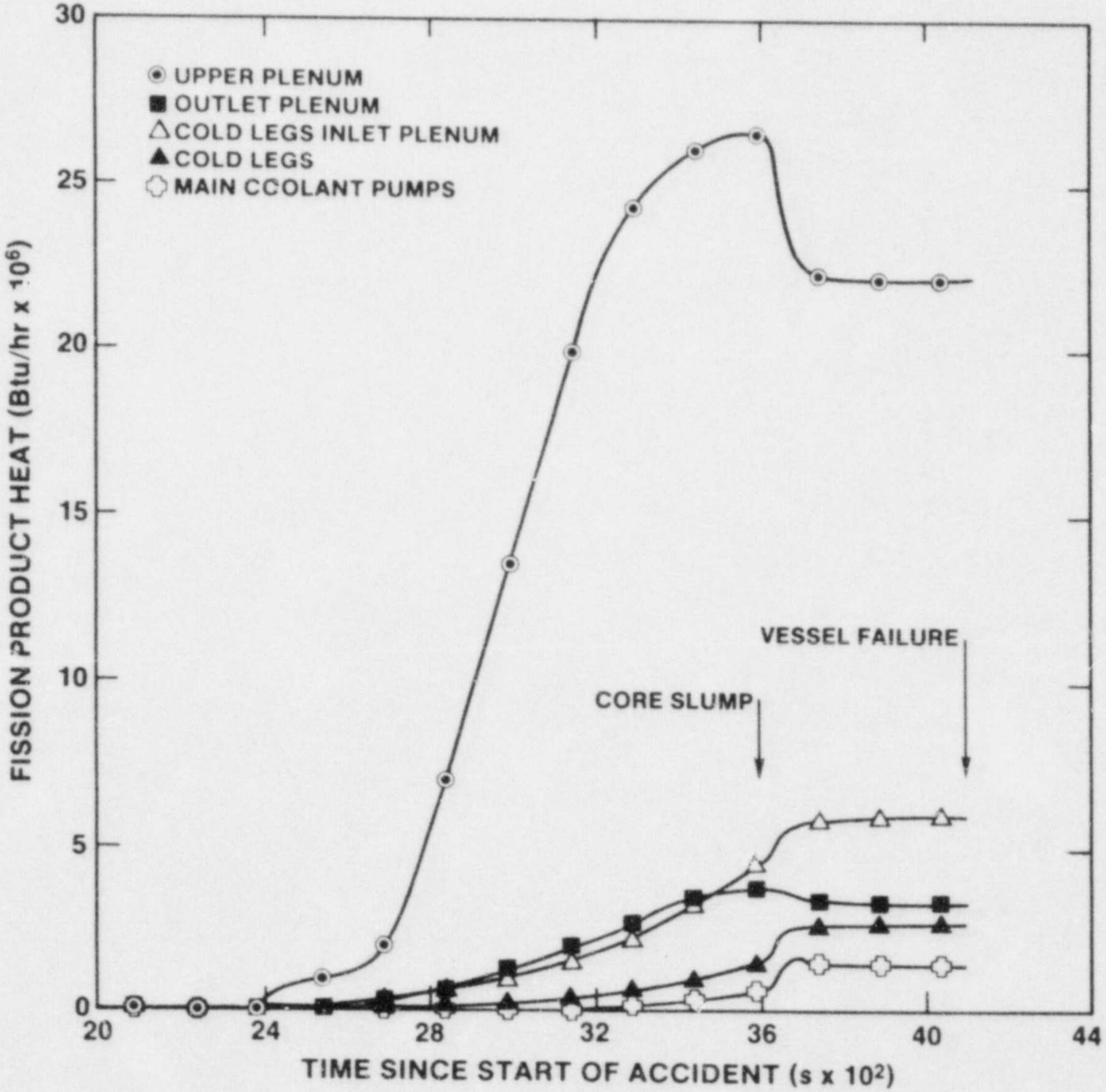

Figure 45. Fission Product Heating TMLB' Pump Seal LOCA (Case A)

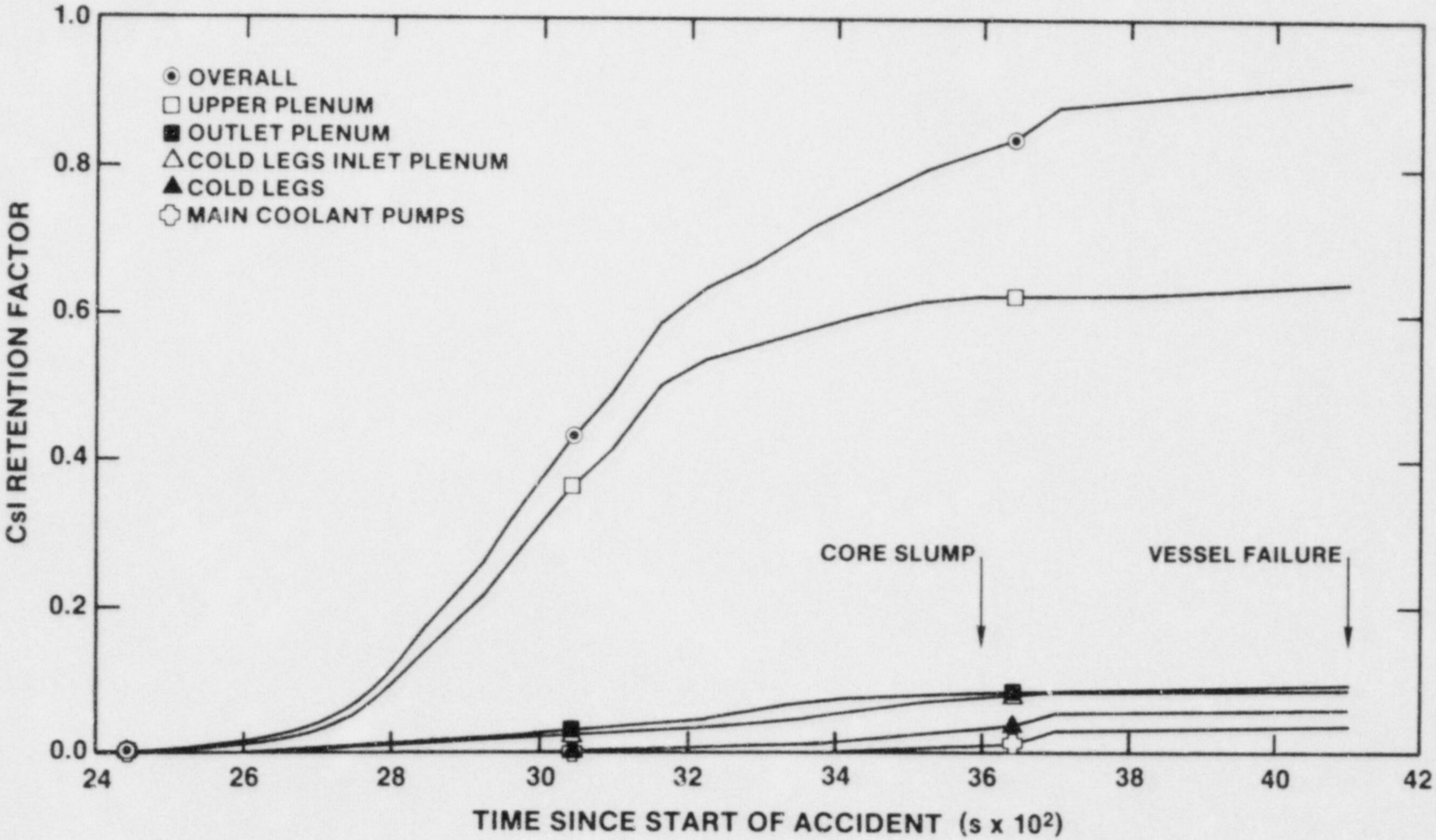

Figure 46. CsI Retention Factor TMLB' Pump Seal LOCA (Case A)

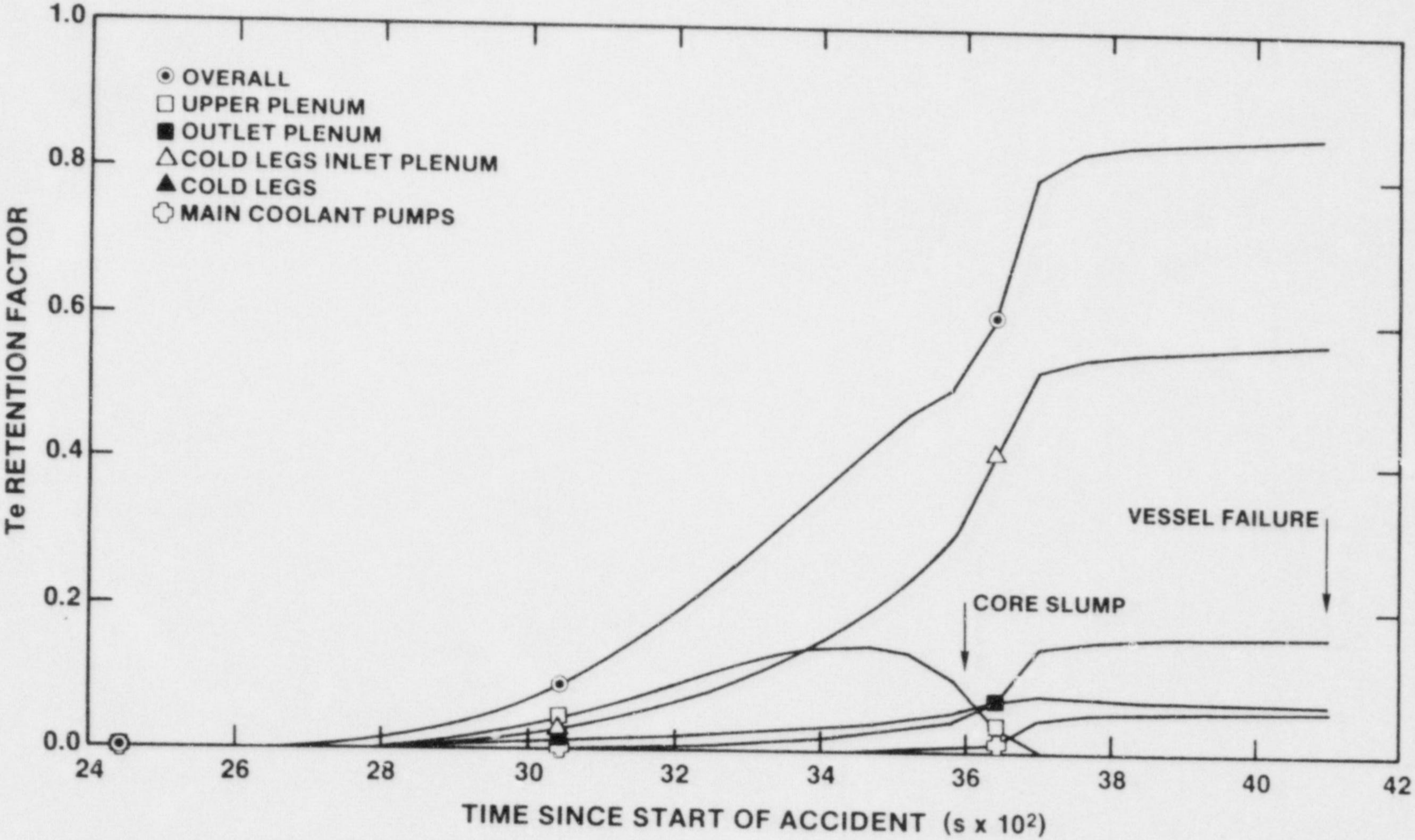

Figure 47. Te Retention Factor TMLB' Pump Seal LOCA (Case A)

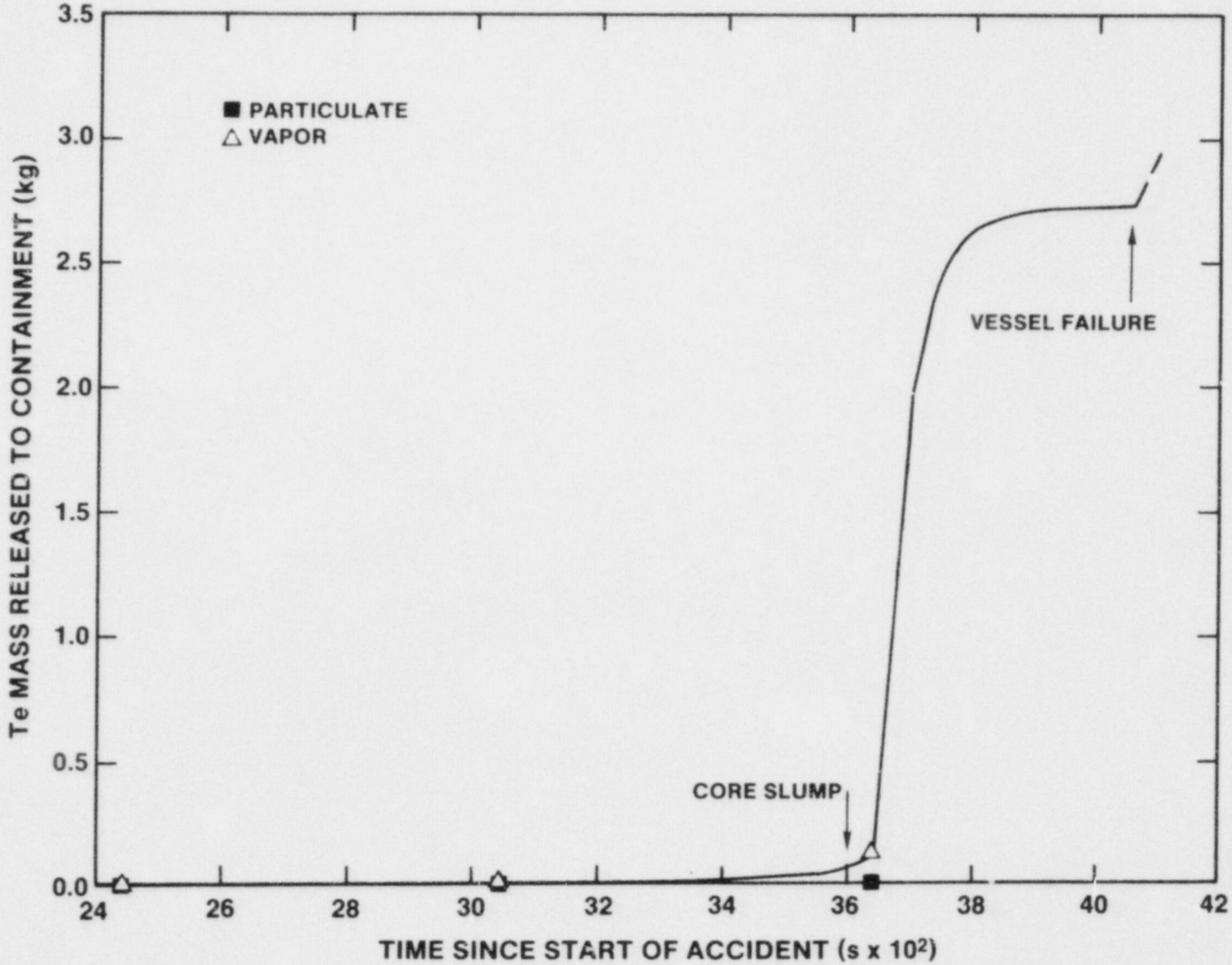

Figure 48. Te Mass Released TMLB' Pump Seal LOCA (Case A)

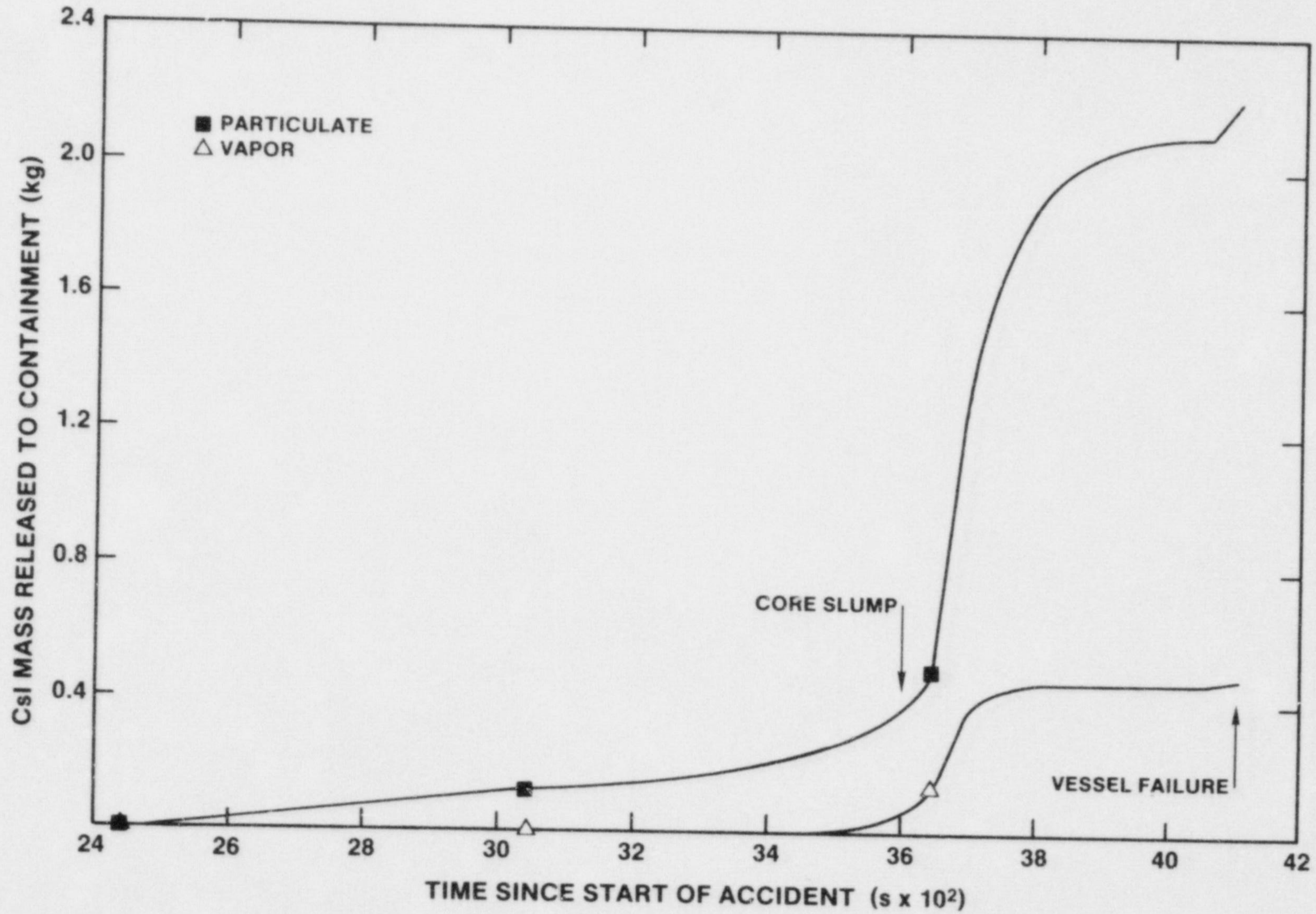

Figure 49. CsI Mass Released TMLB' Pump Seal LOCA (Case A)

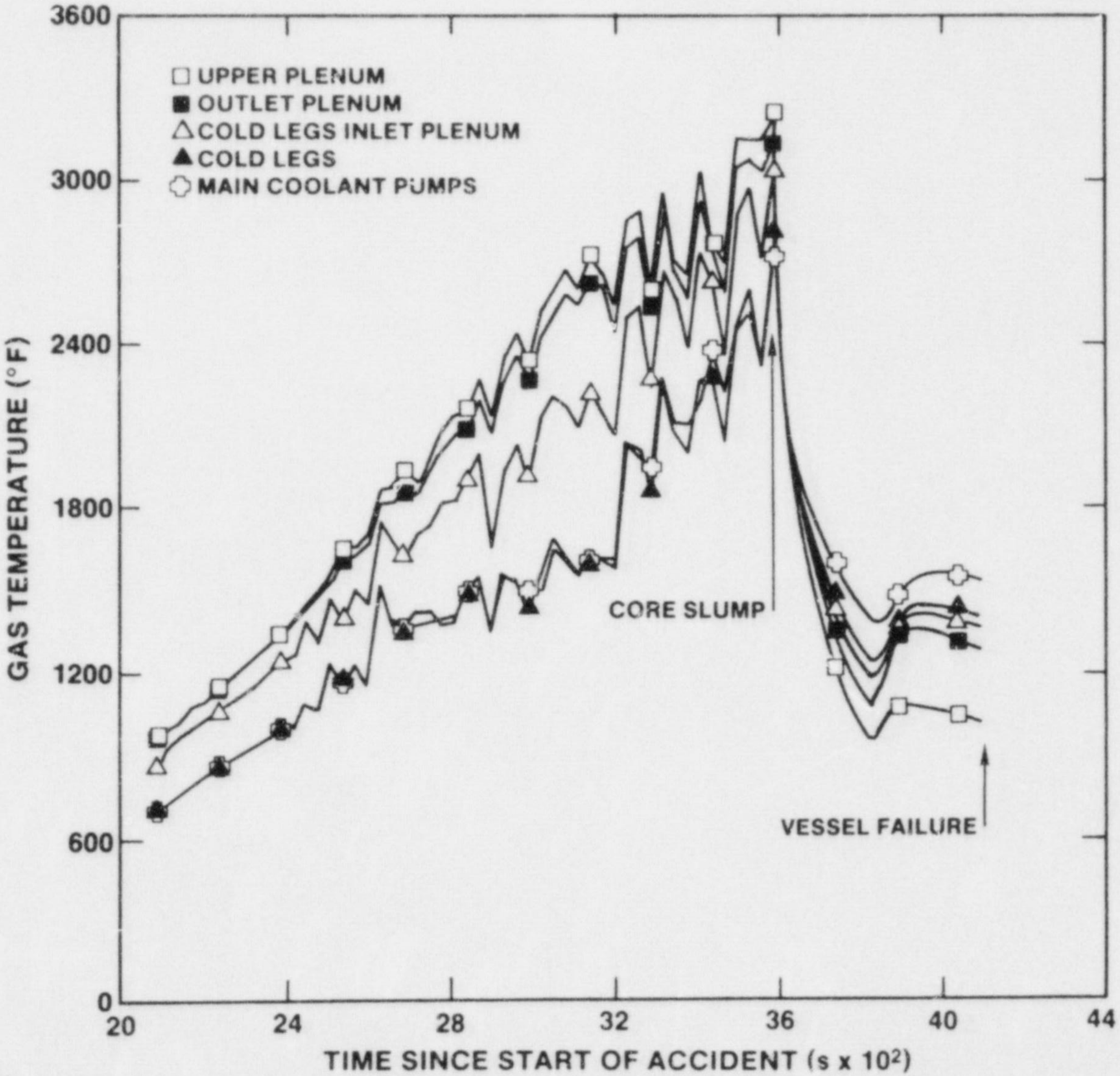

Figure 50. Primary System Gas Temperature TMLB' Pump Seal LOCA (Case B)

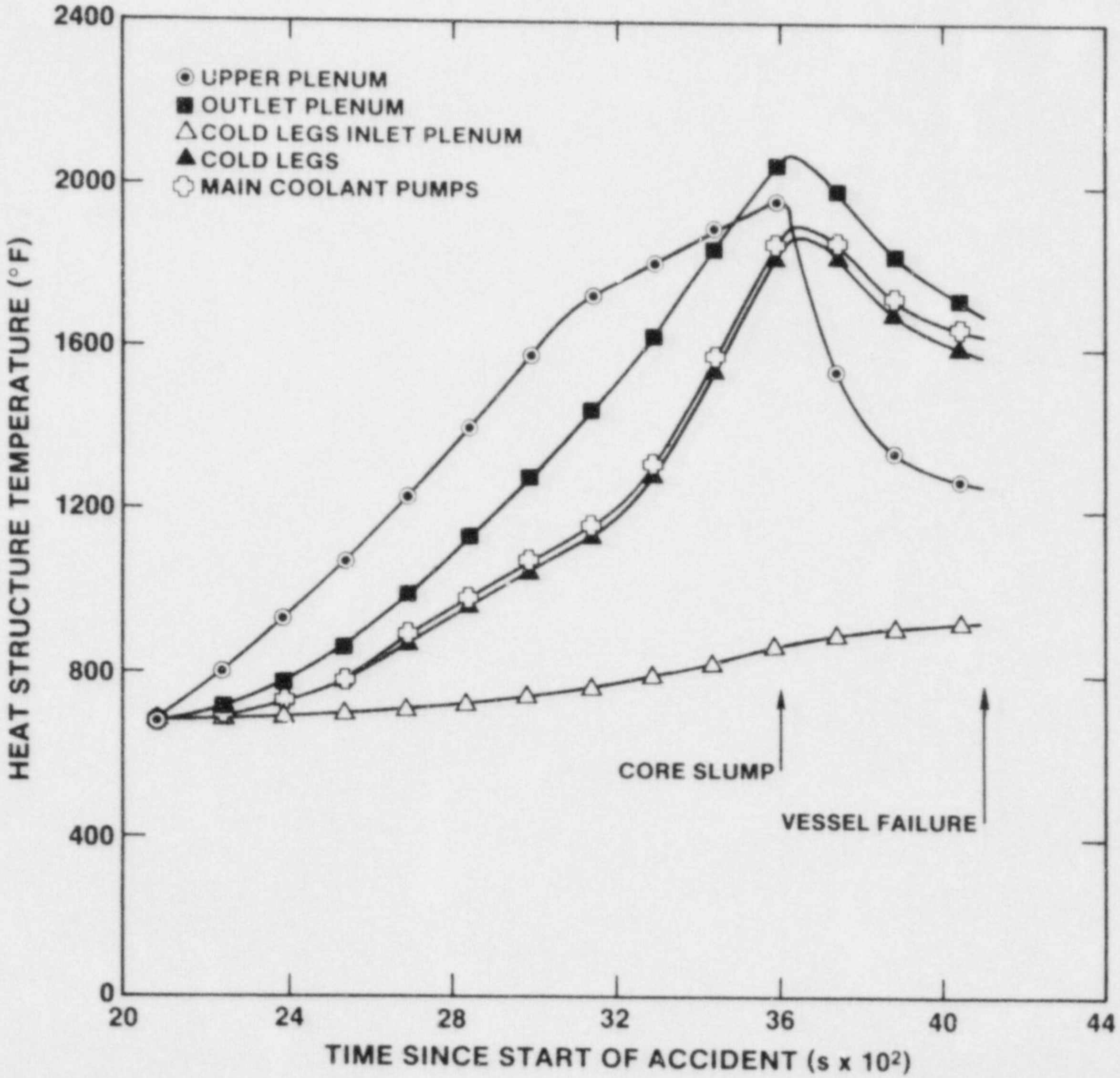

Figure 51. Primary System Structure Temperatures TMLB' Pump Seal LOCA (Case B)

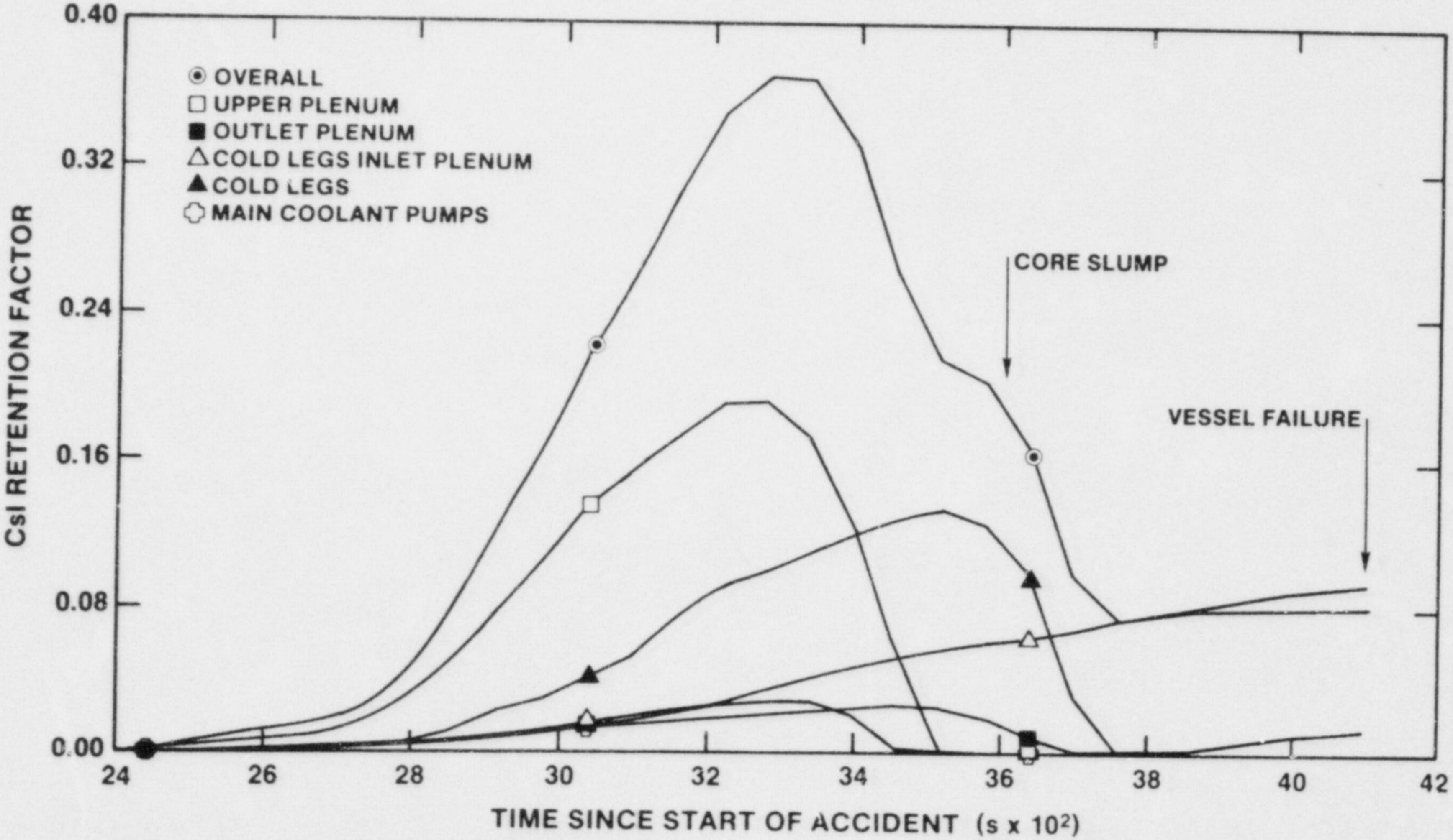

Figure 52. CsI Retention Factor TMLB' Pump Seal LOCA (Case B)

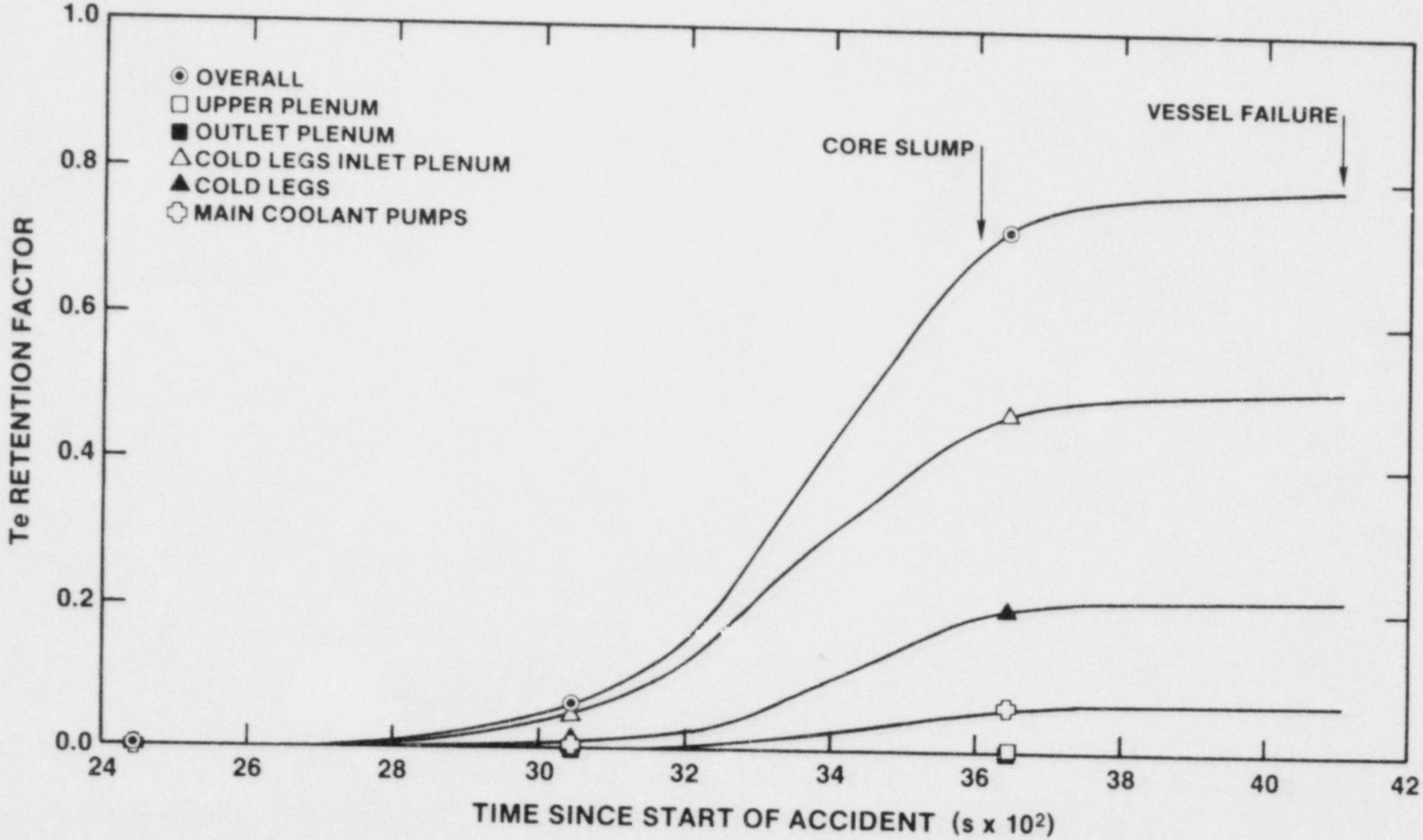

Figure 53. Te Retention Factor TMLB' Pump Seal LOCA (Case B)

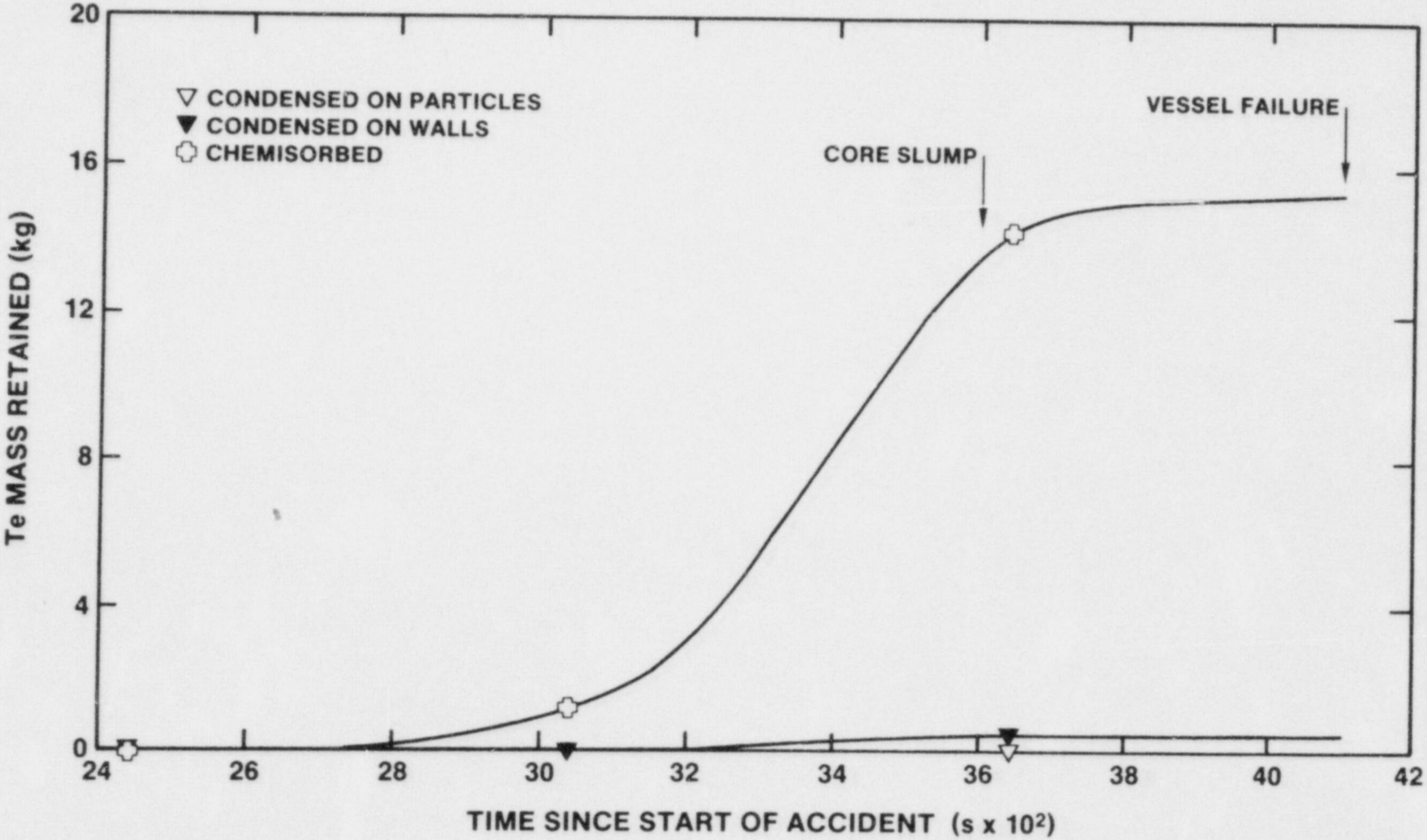

Figure 54. Te Mass Retained TMLB' Pump Seal LOCA (Case B)

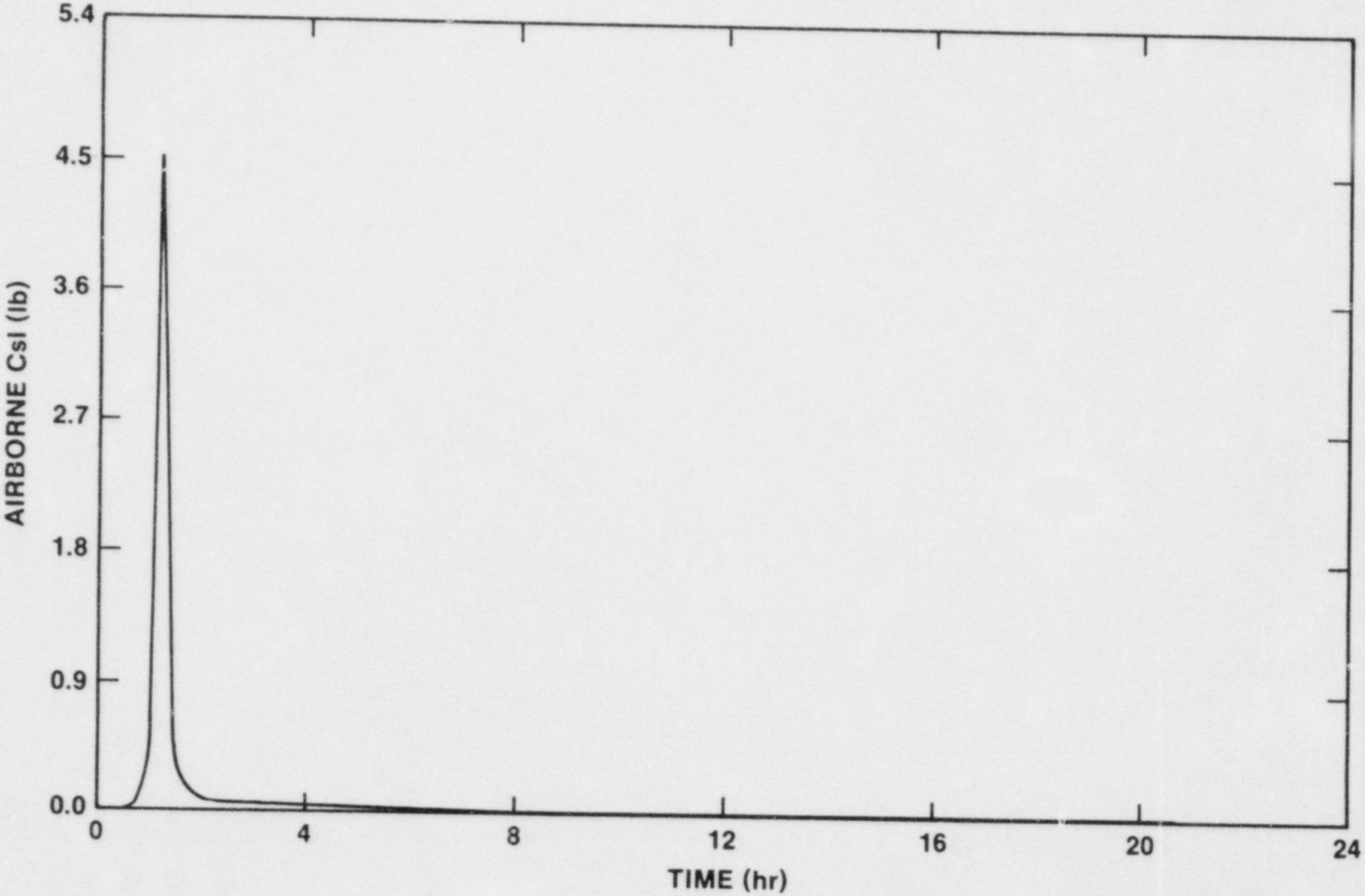

Figure 55. Airborne CsI TMLB' Pump Seal LOCA (Case-030)

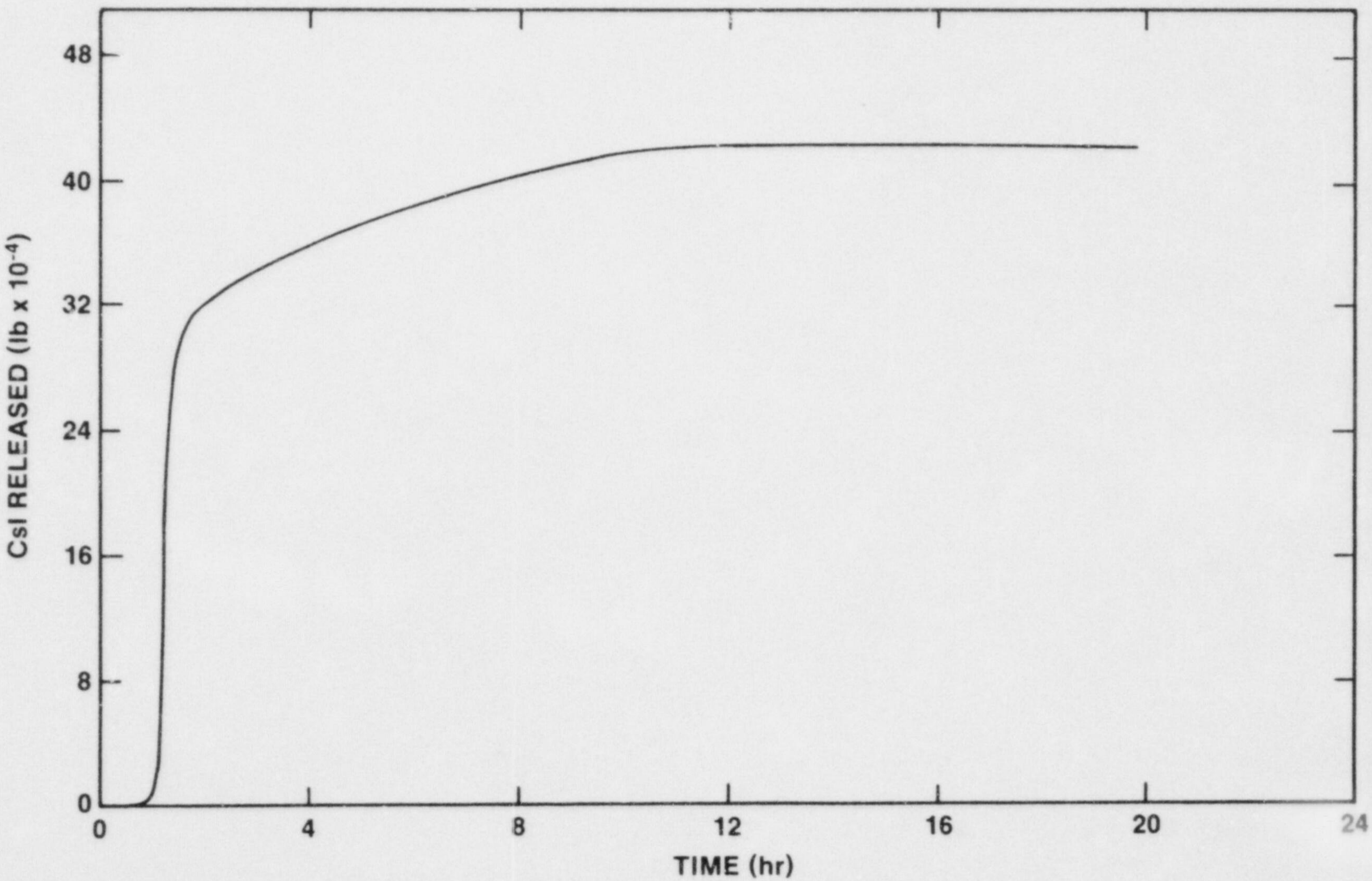

Figure 56. Leaked CsI TMLB' Pump Seal LOCA (Case-030)

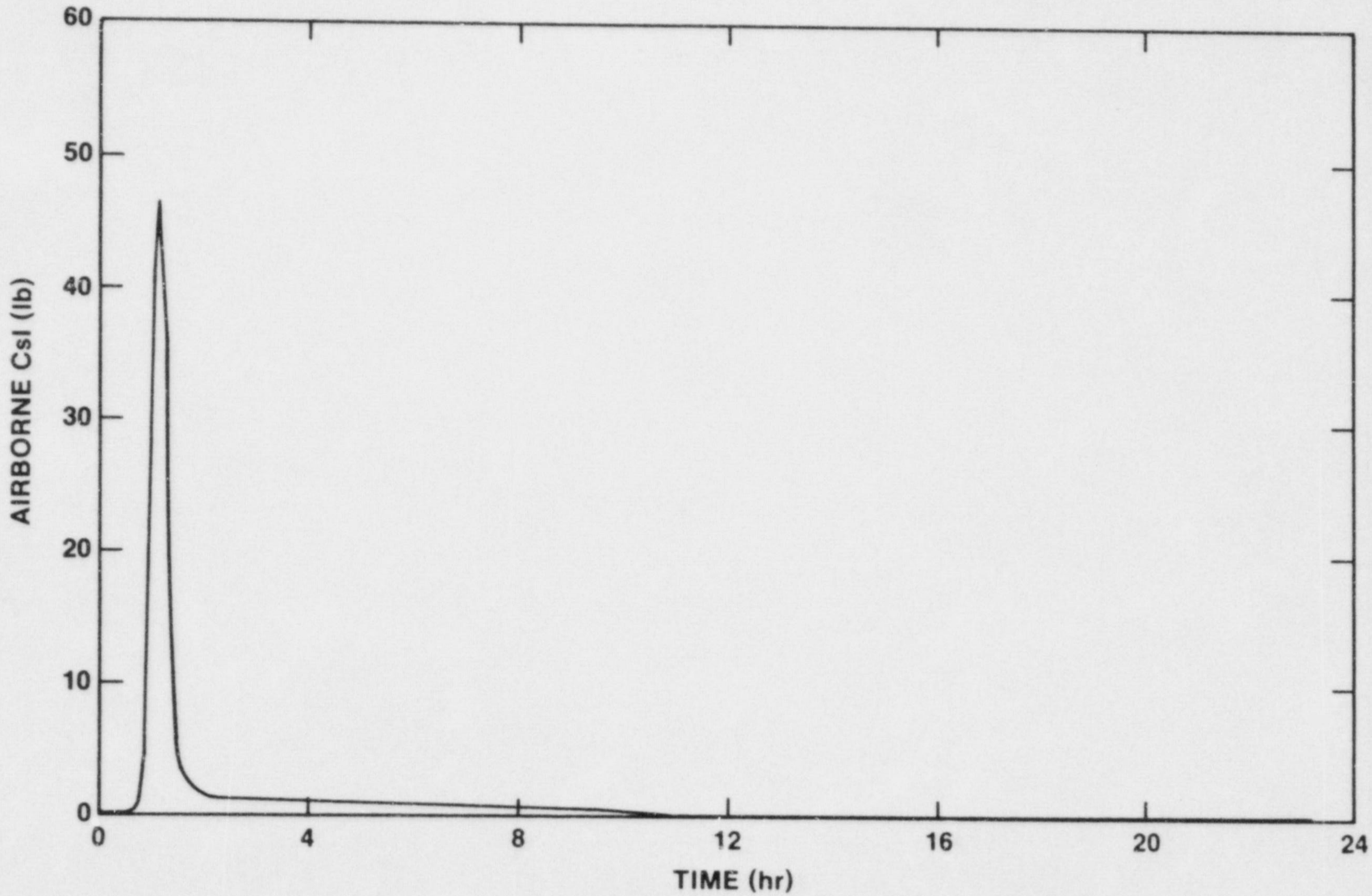

Figure 57. Airborne CsI TMLB' Pump Seal LOCA (Case-031)

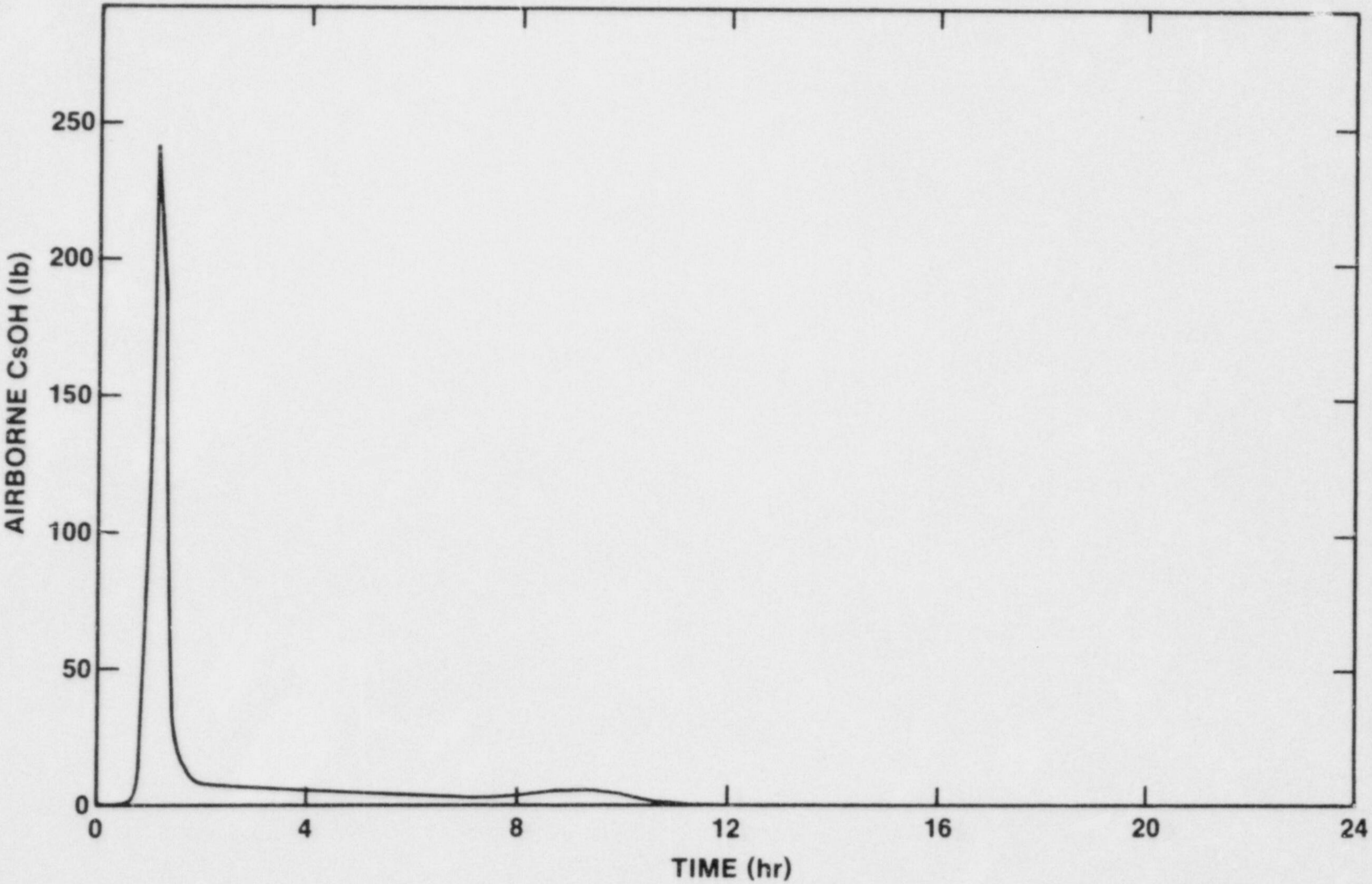

Figure 58. Airborne CsOH TMLB' Pump Seal LOCA (Case-031)

123/124

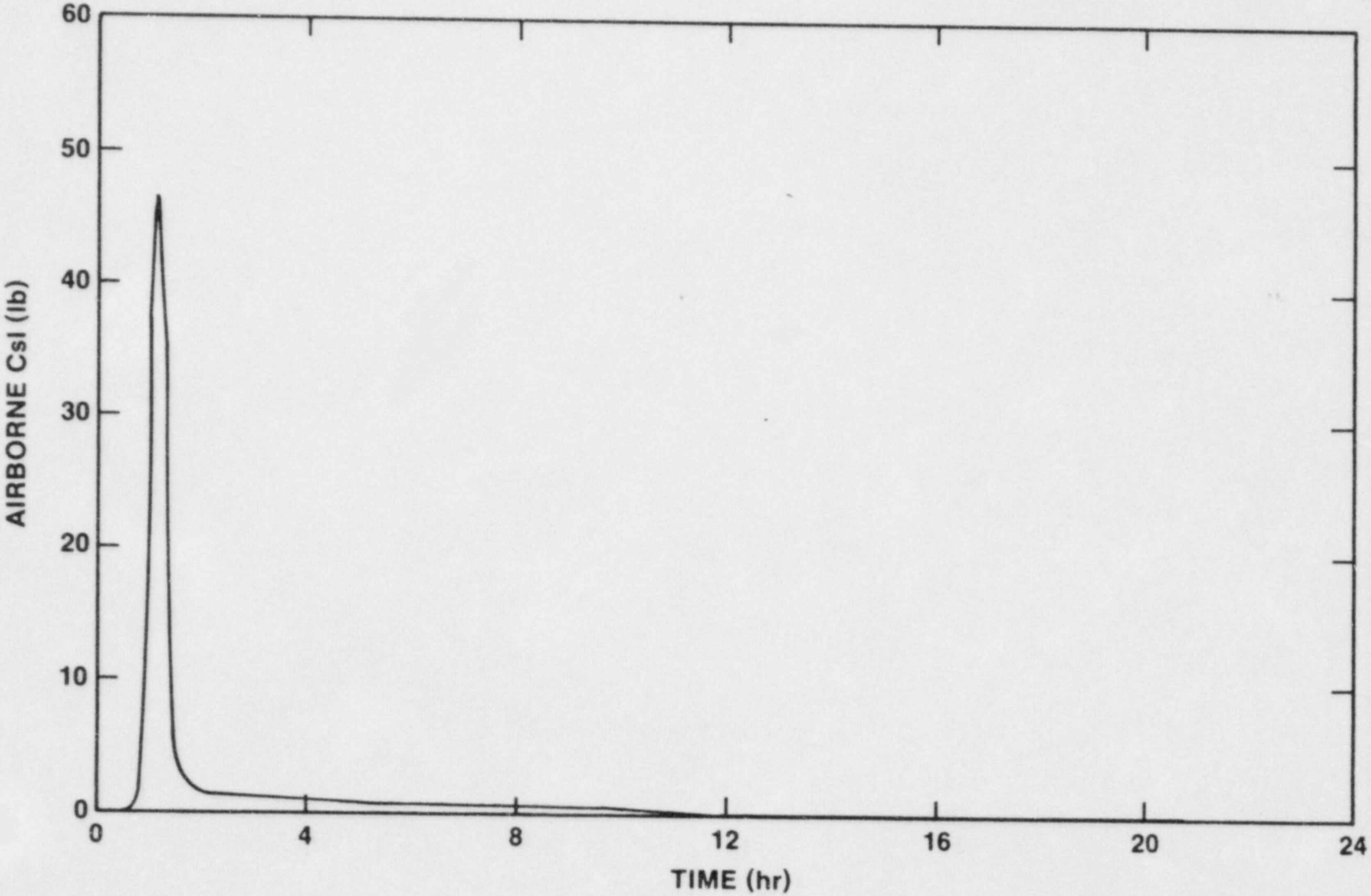

Figure 59. Airborne CsI TMLB' Pump Seal LOCA (Case-131)

DISTRIBUTION:

U.S. Government Printing Office
Receiving Branch (Attn: NRC Stock)
8610 Cherry Lane
Laurel, Maryland 20707
200 copies for RG

Mr. Thomas Walker (8)
Office of Nuclear Regulatory Research
U.S. Nuclear Regulatory Commission
Washington, D.C. 20555

Mr. Rich Denning
Battelle Columbus Laboratory
505 King Avenue
Columbus, Ohio 43201

Dr. W. T. Pratt
Brookhaven National Laboratory
Building 130, Brookhaven Lane
Upton, New York 11973

Mr. R. J. Dallman
EG&G Idaho
Willow Creek Building, W-3
Post Office Box 1625
Idaho Falls, Idaho 83415

Oak Ridge National Laboratory (2)
Building 9201-3, Station 59
Post Office Box Y
Oak Ridge, Tennessee 37830
Attn: Mr. S. A. Hodge
Mr. T. Kress

Mr. J. Travis
Los Alamos National Laboratory
Post Office Box 1663
Los Alamos, New Mexico 87545

Mr. Kenneth Keith
Tennessee Valley Authority
400 West Summit Hill Drive
W10d182 C-k
Knoxville, Tennessee 37902

Mr. Wang Lau
Tennessee Valley Authority
400 Commerce
W9C157-CD
Knoxville, Tennessee 37902

Mr. P. P. Bieniarz
Risk Management Associates
2309 Dietz Farm Road N.W.
Albuquerque, NM 87107

Mr. J. L. Tills
Jack Tills and Associates
209 Eubank, N.E.
Albuquerque, NM 87123

Sandia Distribution:

3141	S. A. Landenberger (5)
3151	W. L. Garner
6400	A. W. Snyder
6410	J. W. Hickman
6411	A. S. Benjamin (10)
6412	A. L. Camp
6415	F. E. Haskin
6420	J. V. Walker
6422	D. A. Powers
6425	W. J. Camp
6425	R. D. Gasser (15)

NRC FORM 335 (2-84) NRCM 1102, 3201, 3202 — U.S. NUCLEAR REGULATORY COMMISSION — **BIBLIOGRAPHIC DATA SHEET** — SEE INSTRUCTIONS ON THE REVERSE	1. REPORT NUMBER (Assigned by TIDC, add Vol. No., if any) NUREG/CR-4563 SAND86-0576
2. TITLE AND SUBTITLE: Analysis of Station Blackout Accidents for the Bellefonte Pressurized Water Reactor	3. LEAVE BLANK
	4. DATE REPORT COMPLETED — MONTH: April — YEAR: 1986
5. AUTHOR(S): R. D. Gasser, P. P. Bieniarz, J. L. Tills	6. DATE REPORT ISSUED — MONTH: Sept. — YEAR: 1986
7. PERFORMING ORGANIZATION NAME AND MAILING ADDRESS (Include Zip Code): Sandia National Laboratories, Post Office Box 5800, Albuquerque, New Mexico 87185	8. PROJECT/TASK/WORK UNIT NUMBER
	9. FIN OR GRANT NUMBER: FIN No. A-1258
10. SPONSORING ORGANIZATION NAME AND MAILING ADDRESS (Include Zip Code): Division of Accident Evaluation, Office of Nuclear Regulatory Research, US Nuclear Regulatory Commission, Washington, D.C. 20555	11a. TYPE OF REPORT: Technical
	b. PERIOD COVERED (Inclusive dates)
12. SUPPLEMENTARY NOTES	

13. ABSTRACT (200 words or less)

An analysis has been performed for the Bellefonte PWR Unit 1 to determine the containment loading and the radiological releases into the environment from a station blackout accident. A number of issues have been addressed in this analysis which include the effects of direct heating on containment loading, and the effects of fission product heating and natural convection on releases from the primary system. The results indicate that direct heating which involves more than about 50% of the core can fail the Bellefonte containment, but natural convection in the RCS may lead to overheating and failure of the primary system piping before core slump, thus, eliminating or mitigating direct heating. Releases from the primary system are significantly increased before vessel breach due to natural circulation and after vessel breach due to reevolution of retained fission products by fission product heating of RCS structures.

14. DOCUMENT ANALYSIS – a. KEYWORDS/DESCRIPTORS	15. AVAILABILITY STATEMENT: Unlimited
b. IDENTIFIERS/OPEN-ENDED TERMS	16. SECURITY CLASSIFICATION (This page) UNCLASSIFIED (This report) UNCLASSIFIED
	17. NUMBER OF PAGES
	18. PRICE

☆ U.S. GOVERNMENT PRINTING OFFICE: 1986—676-049/41012

120555078877 1 1AN1R3
US NRC
ADM-DIV OF PUB SVCS
POLICY & PUB MGT BR-PDR NUREG
W-501
WASHINGTON DC 20555